

Phosphoinositide 3-kinase γ controls LPS-induced myocardial depression via sequential cAMP- and iNOS- signaling

Dissertation

zur Erlangung des akademischen Grades Doctor of Philosophy (Ph.D.)

vorgelegt dem Rat der Medizinischen Fakultät

der Friedrich- Schiller- Universität Jena

von M.Sc. Bernadin Ndongson-Dongmo

geboren am 15.05.1977 in Dschang, Kamerun

Gutachter:

1. Prof. Dr. Reinhard Bauer

2. Prof. Dr. Reinhard Wetzker

3. PD. Dr. Sebastian Stehr

Summary

Sepsis-induced myocardial depression (SIMD) is an early and frequent event of infection-induced systemic inflammatory response syndrome (SIRS). SIMD is caused by disturbed myocardial contractility regardless of enhanced adrenergic stimulation. Pathogenesis of SIMD corresponds to the severity of sepsis, but is frequently associated with improved outcome of septic patients.

Phosphoinositide-3 kinase γ (PI3K γ) is known to coordinate by its scaffold function the coincident signaling of major cardiac phosphodiesterases in order to prevent pathological β -adrenergic overstimulation by appropriate cAMP degradation. However, the role of this enzyme in SIRS-induced SIMD is unknown. The objective of this study aimed to determine the specific role of lipid kinase-dependent and -independent function of PI3K γ in the pathogenesis of SIRS-induced SIMD.

PI3K γ wild-type (wt), knockout (PI3K $\gamma^{-/-}$), and kinase-dead (PI3K $\gamma^{KD/KD}$) mice were exposed to LPS-induced SIRS and assessed for survival, cardiac autonomic nervous system (ANS) function and left ventricular (LV) performance. Additionally, primary adult cardiomyocytes derived from the respective mouse genotypes were used for mechanistic analysis of PI3K γ effects on myocardial contractility and inflammatory response.

Contractility data exhibited under control conditions comparable myocardial functioning in all genotypes studied. After 3 and 24 hours of LPS administration, a marked and progressive reduction in contractility was verified in wt mice. In contrast, mice lacking the signaling protein PI3K γ (PI3K $\gamma^{-/-}$) showed a significant increase in contractility 3 h after LPS administration, but decreased thereafter, although remained elevated in comparison to wild type mice. Mice expressing a kinase-dead PI3K γ mutant (PI3K $\gamma^{KD/KD}$) showed a phenotype similar to wt mice, suggesting that the protein expression of PI3K γ and thus its scaffold function is responsible for specific regulation of cardiac contractility due to LPS-induced SIRS. The anticipated marked increase of sympathetic activation early after LPS administration as well as the increased myocardial catecholamine content and myocardial adrenoreceptor expression was shown to be quite similar in wildtype and PI3K γ -mutant mice used suggesting that the observed marked differences in contractile function are caused by difference in genotype-specific cardiomyocyte function.

At the cellular level, we confirmed that PI3K γ deficiency results in significant enhanced intracellular cAMP content compared PI3K $\gamma^{KD/KD}$ cells that display similar cAMP levels like cardiomyocytes derived from wildtype mice. Furthermore, we verified in cardiomyocytes

derived from PI3K γ ^{-/-} mice a significantly enhanced and prolonged cAMP-mediated signaling via protein kinase A (PKA) of calcium trafficking amplitude regarding the activation of ryanodine receptor (RyR) and phospholamban (PLN) phosphorylation, compared to wild type and PI3K γ ^{KD/KD} cardiomyocytes

We further screened for negative effects of inflammatory responses in myocardial performance and found a profound and long-lasting upregulation of inducible nitric oxide synthase (iNOS) expression and concomitant inflammation in PI3K γ ^{-/-} cardiomyocytes and heart tissue, whereas wildtype (and PI3K γ ^{KD/KD}) mice showed just a weak induction of iNOS expression. iNOS upregulation in PI3K γ ^{-/-} mice was mainly regulated by NFAT and was associated with drastic reduction in intact heart contractility and cardiomyocytes calcium trafficking verified by reduced phospholamban activation. This effect was rescued by iNOS and NFAT inhibition. While functional recovery was reached in all mice seven days after SIRS induction, only PI3K γ knockout mice exhibited sustained iNOS and MMP-9 content in cardiac tissue.

This study reveals the lipid kinase-independent scaffold function of PI3K γ as mediator of immediate adaptive SIMD. Stimulation of cardiac phosphodiesterases by PI3K γ is shown to constrain both, myocardial hypercontractility early after infection-induced SIRS and the subsequent inflammatory responses. The as yet undescribed PI3K γ 's scaffold function of NFAT control warrants an adaptive modulation of iNOS expression and myocardial inflammatory response suggesting that the scaffold function of PI3K γ is responsible for immediate adaptive SIMD preventing myocardial hypercontractility early after infection-induced SIRS and enhanced proinflammatory response to avoid likely harmful sequels.

Zusammenfassung

Sepsis-induzierte myokardiale Depression (engl. Sepsis-induced myocardial depression (SIMD)) ist eine frühe und häufige Komplikation des infektionsinduzierten systemischen Inflammations-Antwort-Syndroms (engl. systemic inflammatory response syndrome (SIRS)). SIMD wird durch eine Störung der myokardialen Kontraktilität hervorgerufen, die trotz vorherrschender verstärkter adrenerger Stimulation auftritt. Die Pathogenese der SIMD korrespondiert mit der Schwere einer Sepsis, ist aber häufig assoziiert mit verbesserter Prognose von Sepsis-Patienten.

Das Signalprotein Phosphoinositide-3 kinase γ (PI3K γ) koordiniert beim Schutz vor pathologischer β -adrenerger Überstimulation eine angepassten cAMP-Degradation durch seine Gerüstfunktion infolge abgestimmter Signaltransduktion wesentlicher kardialer Phosphodiesterasen. Jedoch ist bislang die Rolle von PI3K γ bei der SIRS-induzierten SIMD unbekannt.

Ziel der vorliegenden Untersuchung ist die Aufklärung der spezifischen Rolle der lipidkinase-abhängigen und –unabhängigen Funktionen von PI3K γ bei SIRS-induzierter SIMD.

Bei PI3K γ -Wildtyp (wt), Knockout (PI3K $\gamma^{-/-}$), und Kinase-dead (PI3K $\gamma^{KD/KD}$) Mäuse wurde eine LPS-induzierte SIRS induziert und deren Überleben, die Auswirkungen auf das kardiale autonome Nervensystem (ANS) und die linksventrikuläre (LV) kontraktile Funktion ermittelt. Darüber hinaus wurden an primären adulten Kardiomyozyten mechanistische Untersuchungen zu PI3K γ -abhängigen Auswirkungen auf die myokardiale Kontraktilität und die inflammatorische Antwort durchgeführt.

Unter Ausgangsbedingungen wiesen die untersuchten Mäuse unabhängig vom Genotyp übereinstimmende Werte in den ermittelten Kontraktilitätsparametern auf. Drei und 24 h nach LPS-Gabe war eine progressiv verminderte Verminderung bei wt-Mäusen nachweisbar. Dem gegenüber zeigten PI3K γ -defiziente Mäuse drei Stunden nach LPS-Gabe eine deutlich gesteigerte Kontraktilität, die nachfolgend drastisch abfiel, jedoch im Vergleich zu wt-Mäusen erhöht war. Mäuse mit exprimierter PI3K γ -kinase-dead Mutation (PI3K $\gamma^{KD/KD}$) wiesen einen den wt-Mäusen entsprechenden Phänotyp auf. Somit ist offensichtlich die Gerüstfunktion von PI3K γ für die spezifische Regulation der kardialen Kontraktilität bei SIRS nach LPS-Gabe verantwortlich. Die antizipierte nachhaltig gesteigerte sympathische Aktivierung, ein erhöhter myokardialer Katecholamingehalt und die myokardiale Adrenorezeptor-Expression waren in der frühen Phase nach LPS-Gabe bei wt-Mäusen und denen mit PI3K γ -Mutationen übereinstimmend. Diese Befunde legen nahe, dass die beobachteten deutlichen Kontraktilitätsdiffe-

renzen durch genotyp-spezifische Unterschiede in inhärenten Eigenschaften der Kardiomyozyten verursacht sind.

Wir konnten bestätigen, dass PI3K γ -Defizit einen erhöhten intrazellulären Gehalt von cAMP im Kardiomyozyten zur Folge hat. Demgegenüber weisen PI3K $\gamma^{KD/KD}$ -Kardiomyozyten einen den wt-Zellen entsprechenden cAMP-Gehalt auf. Darüber hinaus konnten wir nachweisen, dass Kardiomyozyten aus PI3K γ -defizienten Mäusen im Vergleich mit wt- und PI3K $\gamma^{KD/KD}$ -Kardiomyozyten eine verstärkte elektromechanische Kopplung durch verbesserte transiente Ca²⁺-Ein- und Austransporte (Ca²⁺-Trafficking) aufweisen. Dies wird durch beschleunigten Ca²⁺-Ein- und Austransport infolge Aktivierung des Ryanodinrezeptors (RyR) und erhöhter Phospholamban (PLN)-Phosphorylierung verursacht und durch verstärktes und länger andauerndes cAMP Signaling via Proteinkinase A (PKA) vermittelt.

Darüber hinaus überprüften wir, in wieweit negative Auswirkungen auf die myokardiale Leistungsfähigkeit durch dafür bekannte inflammatorische Antwortreaktionen nachweisbar waren. Wir konnten zeigen, dass eine ausgeprägte und lang anhaltende Hochregulation der induzierbaren NO-Synthase (iNOS) in PI3K $\gamma^{-/-}$ -Kardiomyozyten und -Herzgewebe auftraten, wo hingegen wt- und PI3K $\gamma^{KD/KD}$ -Mutanten lediglich eine geringgradige iNOS-Induktion zeigten. Die nachgewiesene starke iNOS- Hochregulation in PI3K $\gamma^{-/-}$ -Mäusen war hauptsächlich durch NFAT reguliert und war assoziiert mit drastischer Verminderung der myokardialer Kontraktilität und des Ca²⁺-Trafficking, die durch verminderte Phospholamban-Aktivierung verifiziert wurden. Letztere Befunde konnten durch Hemmung von iNOS und NFAT rückgängig gemacht werden. Eine weitgehend vollständige funktionelle Wiederherstellung konnte sieben Tage nach SIRS-Induktion bei allen untersuchten Genotypen nachgewiesen werden. Jedoch wiesen PI3K $\gamma^{-/-}$ -Mäuse noch zu diesem Zeitpunkt einen erhöhten iNOS- und MMP-9-Gehalt im Herzgewebe auf.

Die vorgelegte Untersuchung konnte nachweisen, dass die lipidkinase-unabhängige Gerüstfunktion von PI3K γ eine vermittelnde Funktion bei der adaptiven SIMD einnimmt. Die PI3K γ -abhängige Stimulation kardialer Phosphodiesterasen bewirkt sowohl eine Dämpfung der myokardialen Hyperkontraktilität in der frühen Phase der infektionsinduzierten SIRS als auch der nachfolgenden inflammatorischen Antwort. Die bisher nicht beschriebene, durch die Gerüstfunktion von PI3K γ vermittelte, Kontrolle der NFAT-Suppression gewährleistet eine adaptive Modulation von iNOS-Expression und myokardialer Entzündungsreaktion. Danach ist die Gerüstfunktion von PI3K γ offensichtlich für die adaptive SIMD verantwortlich, sodass eine myokardiale Hyperkontraktilität in der frühen Phase der infektionsinduzierten SIRS und

eine nachfolgende überschießende proinflammatorische Antwort des Herzgewebes mit potenziell schädlichen Folgen verhindert wird.

1. Introduction

1.1 Sepsis- brief overview

Sepsis is one of the oldest and most elusive syndromes in medicine. With the confirmation of germ theory by Semmelweis, Pasteur, and others, sepsis was recast as a systemic infection, often described as “blood poisoning,” and assumed to be the result of the host's invasion by pathogenic organisms that then spread in the bloodstream. Before that, Hippocrates firstly claimed that sepsis (σηΰρις) was the process by which flesh rots, swamps generate foul airs, and wounds fester and Galen later considered sepsis a laudable event, necessary for wound healing (Funk et al. 2009, Majno 1991). However, even with the advent of modern antibiotics consequently to the discovery of pathogenic organism's involvement; germ theory did not fully explain the pathogenesis of sepsis: many patients with sepsis died despite successful eradication of the inciting pathogen. Thus, researchers suggested that it was mainly the host response, not just the germ violence that drove the pathogenesis of sepsis (Cerra 1985). In 1992, an international consensus panel defined sepsis as a systemic inflammatory response to infection, noting that sepsis could arise in response to multiple infectious causes and that septicemia was neither a necessary condition nor a helpful term (Bone et al. 1992). Instead, the panel proposed the term “severe sepsis” to describe instances in which sepsis is complicated by acute organ dysfunction, and they codified “septic shock” as sepsis complicated by either hypotension that is refractory to fluid resuscitation or by hyperlactatemia. In 2003, a second consensus panel endorsed most of these concepts, with the caveat that signs of a systemic inflammatory response, such as tachycardia or an elevated white-cell count, occur in many infectious and noninfectious conditions and therefore are not helpful in distinguishing sepsis from other conditions (Levy et al. 2003). Ongoing advances in molecular biology have provided keen insight into the complexity of pathogen and alarm recognition by the human host and important clues to a host response that has gone awry (Angus und van der Poll 2013). Progress in clinical and translational sepsis research is meanwhile continuously reviewed and consecutively transferred into guidelines in order to improve sepsis diagnosis and therapy (Dellinger et al. 2013).

However, the complex pathogenesis of sepsis remains insufficiently explored and resulting therapeutic concepts are hitherto frequently unable to treat curatively patient suffered from severe sepsis and septic shock. A complex and dynamic interaction exists between pathogens and host immune-defence mechanisms during the course of invasive infection. It is now widely thought that the host response to sepsis involves many, concomitant, integrated, and

often antagonistic processes that involve both exaggerated inflammation and immune suppression. It has become apparent that infection triggers a complex, variable, and prolonged host response, in which both proinflammatory and anti-inflammatory mechanisms can contribute to clearance of infection and tissue recovery on the one hand and organ injury and secondary infections on the other. Several novel mediators resulting from disturbed host tissue and pathways have been shown to play a part. Moreover, evidence is accumulating that microbial virulence and bacterial load contribute to the host response and the outcome of severe infections (van der Poll und Opal 2008). Improved integrative understanding is needed to distinguish the hierarchy of the various mechanisms underlying multi-organ failure as a key consequence of severe sepsis often causative for fatal outcome (Rudiger et al. 2008a).

Severe sepsis remains a major challenge in medicine. Its mortality rate is high and its incidence is increasing worldwide (Angus und van der Poll 2013). Recent data from Germany revealed a sustained high number of 88,000 patients with severe sepsis or septic shock in 2011 in German hospitals, with associated hospital mortality rates of 43% for severe sepsis and 60% for septic shock, respectively (Heublein et al. 2013).

There are many well-known risk factors for systemic infections that most commonly precipitate severe sepsis and septic shock, including chronic diseases (e.g., the acquired immunodeficiency syndrome, chronic obstructive pulmonary disease, and many cancers) and the use of immunosuppressive agents (Angus et al. 2001, Angus und van der Poll 2013). Among patients with such infections, however, the risk factors for organ dysfunction are less well studied but probably include the causative organism and the patient's genetic composition, underlying health status, and preexisting organ function, along with the timeliness of therapeutic intervention (Angus et al. 2001, Angus und van der Poll 2013). Age, sex, and race or ethnic group characteristics are identified to influence the incidence of severe sepsis (Angus et al. 2001, Angus und van der Poll 2013, Mayr et al. 2010).

The clinical process usually begins with infection, which potentially leads to sepsis and organ dysfunction following a continuum of severity from sepsis to septic shock finally to the multiple organ dysfunction syndrome (MODS) and death (Gustot 2011). Organ dysfunction or organ failure may be the first clinical sign of sepsis, and no organ system is immune from the consequences of the inflammatory excesses of sepsis. The incidence of severe sepsis depends on how acute organ dysfunction is defined and on whether that dysfunction is attributed to an underlying infection (Angus und van der Poll 2013, Vincent et al. 2009). Indeed, before the introduction of modern intensive care with the ability to provide vital organ support, se-

vere sepsis and septic shock were typically lethal. Even with intensive care, rates of in-hospital death from septic shock were often in excess of 80% as recently as 30 years ago (Friedman et al. 1998). With advances in training, better surveillance and monitoring, and prompt initiation of therapy to treat the underlying infection and support failing organs, mortality has been reduced to 20 to 30% (Derek C. Angus et al 2013). However, the mechanisms that underlie organ failure in sepsis have been only partially elucidated.

1.2 Sepsis-associated impairment of the cardiovascular system and the multiple organ dysfunction syndrome

At least half of the high mortality rates (30%-80%) of severe sepsis, sepsis, and MODS has been attributed to the impairment of the cardiovascular system which is identified as a major organ dysfunction (Parrillo 1989). As an important organ system frequently affected by sepsis and always affected by septic shock, the cardiovascular system and its dysfunction during sepsis have been studied in clinical and basic research for more than 5 decades. In 1951, Waisbren was the first to describe cardiovascular dysfunction due to sepsis (Merx und Weber 2007, Waisbren 1951). He recognized a hyperdynamic state with full bounding pulses, flushing, fever, oliguria, and hypotension. In addition, he described a second smaller patient group who showed the symptoms of clammy and pale skin were hypotensive with low volume pulses and appeared more severely ill. With hindsight, the latter group might have been insufficiently volume-resuscitated, and indeed, timely and adequate volume therapy has been demonstrated to be one of the most effective supportive treatments in sepsis therapy (Rivers et al. 2001).

Under conditions of adequate volume resuscitation, the profoundly reduced systemic vascular resistance typically encountered in sepsis (Bone 1991, Werdan et al. 2009) leads to a concomitant elevation in cardiac index that obscures the myocardial dysfunction that also occurs. However, as early as the mid-1980s, significant reductions in both stroke volume and ejection fraction in septic patients were observed despite normal or even increased cardiac output (Parker et al. 1984). Importantly, the presence of cardiovascular dysfunction in sepsis was associated with a significantly increased mortality rate of 70% to 90% compared with 20% in septic patients without cardiovascular impairment (Parrillo et al. 1990).

Development of septic shock and concomitant microcirculatory disturbances characterize the state of sepsis disease in the most severe cases. Shock develops as a result of decreased vascular tone by mediator-dependent vasoparalysis, enhanced vascular permeability, sepsis-induced coagulation abnormalities and sepsis-induced cardiomyopathy, leading to low stroke

volume, low arterial blood pressure and, finally, impaired organ perfusion (Angus und van der Poll 2013, Rivers et al. 2001).

Sepsis impacts the entire organism in a time-dependent manner (Hotchkiss und Karl 2003). This syndrome can affect all organ systems including the cardiovascular system (Dyson et al. 2011), autonomic nervous system (Schmidt et al. 2005), endocrine system (Rudiger et al. 2008b), metabolism (Singer 2005) and bioenergetics (Brealey et al. 2002). During septic shock, circulatory compromise and mitochondrial damage (Suliman et al. 2004, Brealey et al. 2004) reduce intra-cellular ATP production and place the cells at risk of bio-energetic failure and cell death. In order to reduce the risk of cell death, adaptive changes may be activated (Singer et al. 2004). Cellular functions are reduced, perhaps in order to limit energy expenditure, thereby creating a new equilibrium between energy supply and consumption (Rudiger 2010). As a result, the organ like heart may survive in a state of functional downregulation. Consequently, extensive tissue necrosis is not a characteristic of sepsis-induced organ dysfunction (Rossi et al. 2007). When the inflammatory process is overcome, cellular energy generation can improve, leading to resumption of normal cell processes and functional recovery (Carre et al. 2010, Rudiger und Singer 2013).

1.3 Sepsis-induced cardiomyopathy

Clinical evidence of sepsis-induced cardiomyopathy is well-recognized as an early organ manifestation during sepsis and septic shock (Rudiger und Singer 2007). The involvement of the heart varies according to the timing and severity of the sepsis syndrome. During the very early phase of the disease, a left-ventricular (LV) ejection fraction (EF) >55% is indicative of sepsis, as demonstrated in a retrospective evaluation of shock patients in the emergency room (Jones et al. 2005). This might be explained by increased cardiac contractility due to adrenergic stimulation. Importantly, despite this high LVEF, stroke volume at this time point is low because of insufficient cardiac preload due to a high vascular permeability and low vascular tone. The compensatory rise in heart rate is often insufficient to maintain adequate cardiac output during this very early phase of sepsis. Vieillard-Baron and co-workers found that 60% of septic shock patients developed a LVEF <45% during the first 3 days of hemodynamic support. It can be concluded that LV systolic dysfunction is common in septic patients and potentially reversible in survivors (Vieillard-Baron et al. 2008). Myocardial depression in patients with septic shock was initially described as biventricular dilatation associated with a depressed left ventricular ejection fraction (LVEF), which was transient and reversible with a

gradual return toward a normal ventricular volume and normal ejection fraction in 7 to 10 days after onset of sepsis in survivors.

While some studies suggest that the presence of cardiac dysfunction is a risk factor for adverse outcomes (Landesberg et al. 2012), other reported more cardiac depression in sepsis survivors compared to non-survivors (Jardin et al. 1999, Parker et al. 1984). How can such conflicting results be explained? Clearly, the development of cardiac dysfunction requires some degree of inflammation. Hence, mild to moderate cardiac dysfunction might result from mild or short-lasting systemic inflammation, and therefore be a good prognostic sign. In very sick septic patients the presence of profound myocardial depression defined by a low LVEF may represent preload optimization and good adaptation, while a normal LVEF could be caused by persistent preload deficiency (Jardin et al. 1999) and/or ongoing harmful adrenergic over-stimulation.

1.3.1 Mechanisms of septic cardiomyopathy

Numerous mechanisms have been suspected to be responsible for the sepsis-induced cardiac dysfunction. Early sepsis is characterized by high levels of circulating catecholamines (Boldt et al. 1995, Dyson et al. 2011) that derive from the autonomous nervous system as well as activated immune-competent cells (Bergquist et al. 1994, Flierl et al. 2007). A major mechanism of sepsis-induced cardiac dysfunction is the attenuation of the adrenergic response at the cardiomyocyte level due to down-regulation of β -adrenergic receptors (Tang und Liu 1996, Tang et al. 1998) and depression of post-receptor signaling pathways (Bernardin et al. 1998, Matsuda et al. 2000). These changes are mediated by cytokines (Chung et al. 1990) and nitric oxide (Barth et al. 2006). Blunting of the adrenergic response is probably enhanced by neuronal apoptosis in the cardiovascular autonomic centres (Sharshar et al. 2003), and by inactivation of catecholamines by reactive oxygen species (Macarthur et al. 2000). The interaction of relevant mechanisms causative for septic cardiomyopathy is shown in the following scheme (Fig.1):

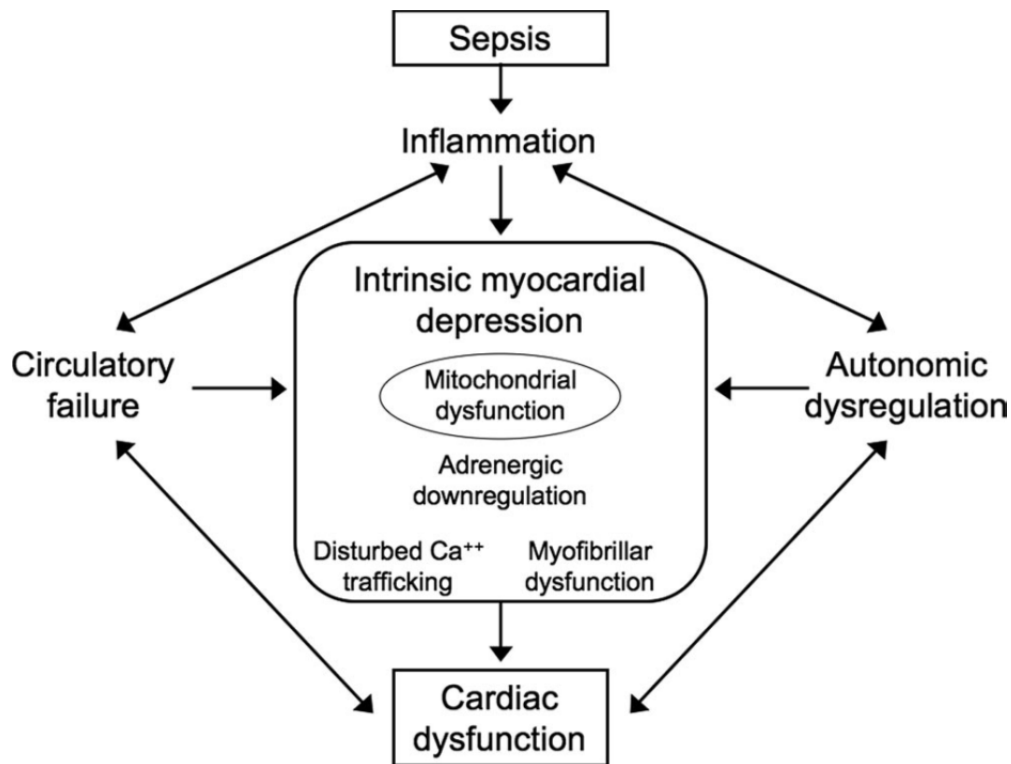


Figure 1. Schematic representation of different factors involved in sepsis-induced cardiac dysfunction. Cardiac performance during sepsis is impaired due to changes in the macro- and microcirculation, autonomic dysfunction, and inflammation-induced intrinsic myocardial depression. The mechanisms of intrinsic myocardial depression include down-regulation of adrenergic pathways, disturbed intracellular Ca^{2+} trafficking and impaired electromechanical coupling at the myofibrillar level. Mitochondrial dysfunction seems to play a central role in this sepsis-induced organ dysfunction (adopted from (Rudiger und Singer 2007)).

In order to specify proposed mechanisms in more detail the impact of relevant extramyocardial and inherent myocardial mechanisms causative for septic cardiomyopathy should be now outlined.

a. Extramyocardial mechanisms

i. Circulatory and Microvascular Changes

Early sepsis and septic shock are characterized by circulatory abnormalities that usually relate to intravascular volume depletion and vasodilation. Consequent underfilling of the heart leads to a reduced cardiac output. This potentially causes an oxygen supply-demand imbalance in various organ beds (Hotchkiss und Karl 1992) that is often reversed by fluid resuscitation (Rivers et al. 2001). Consequently, insufficiently resuscitated animal models are therefore likely to demonstrate reduced cardiac performance (Chagnon et al. 2006). Myocardial edema due to inflammation induced vascular leakage may also influence cardiac compliance and function (Yu et al. 1997). In addition, ventricular function is influenced by changes in after-

load. Pulmonary hypertension will worsen right heart function (Cohen et al. 1998), whereas right heart dilation will impair left heart function (Moore et al. 2001).

Macrocirculatory coronary blood flow is increased in patients with established septic shock (Cunnion et al. 1986). Concerning microcirculatory, although debate still ongoing, Hotchkiss and coworkers found no cellular hypoxia in septic rat hearts (Hotchkiss et al. 1991). In addition, it was reported that ischemic phenomena do not play a major role in sepsis-induced cardiac dysfunction. Nevertheless, if diastolic arterial pressure is very low because of a marked decrease in vascular tone, myocardial ischemia could ensue because diastolic blood pressure is the driving pressure for the left ventricular coronary blood flow (Lamia et al. 2005).

ii. Autonomic dysregulation

There is compelling evidence that dysregulation within the autonomic nervous system may influence cardiac dysfunction during pathogenesis of SIRS and sepsis. Some authors argue that severe sepsis is characterized by an autonomic failure, perhaps related to apoptosis in cardiovascular autonomic centers that can precede the onset of circulatory shock (Annane et al. 1999, Schmidt et al. 2001). Tachycardia, a typical sepsis feature, is viewed as a response to cardiac underfilling, adrenergic stimulation, and fever. Sepsis-related tachycardia has several adverse effects on the heart, including restricted diastolic ventricular filling, increased oxygen requirements, and, potentially, a tachycardia-induced cardiomyopathy.

Indeed, heart rate on presentation predicted survival in septic shock patients (Azimi und Vincent 1986).

Increasing evidence suggests that autonomic dysfunction contributes substantially to the development of the multiple organ dysfunction syndrome (MODS) (Werdan et al. 2009). The cardiac autonomic dysfunction in sepsis and MODS can be measured by parameters of the heart rate variability (HRV), which shows a strong impairment in both the sympathetically and the vagally mediated nervous signals. HRV measurement describes cerebral control of the heart. Cardiac autonomic function is severely impaired in patients with sepsis, SIRS, and MODS and shows prognostic implications (Schmidt et al. 2005). Autonomic impairment is most likely due to the action of bacterial toxins and sepsis and SIRS mediators, which interfere with autonomic nerve signals in the brain, with neuronal transmission, and with the target cell (e.g., cardiomyocyte pacemaker and ventricular cells). In the target cell, this interference can, in principle, be found at the level of receptors, signal transduction pathways, or ion channels (Werdan et al. 2009).

iii. Role of circulating myocardial depressant factors

The concept of a circulating myocardial depressant factor in sepsis was first proposed in the 1970s (Lefer 1970) and then confirmed by Parrillo and coworkers. They showed that serum obtained from patients during the acute phase of septic shock was able to decrease the extent and the velocity of rat cardiomyocytes shortening measured in vitro, whereas serum obtained from nonseptic patients immediately restored the contractile force. Importantly, this phenomenon no longer persisted in the recovery phase (Parrillo et al. 1985).

In extension of these findings, ultrafiltrates from patients with severe sepsis and simultaneously reduced left ventricular stroke work index displayed cardiotoxic effects and contained significantly increased concentrations of interleukin (IL)-1, IL-8, and C3a (Hoffmann et al. 1999). Additional potential candidates for myocardial depressant substance include other cytokines including TNF α , prostanoids, and nitric oxide (NO) (Merx und Weber 2007).

However, studies using isolated cardiomyocytes harvested from endotoxin-induced septic animals and studied ex vivo, reported contractile depression similar to in vivo measurements in spite of the absence of a direct contact with plasma (Tavernier et al. 2001). Therefore, it has been concluded that intramyocardial mechanisms must be involved in the sepsis-induced cardiac dysfunction irrespective of the presence of circulating depressing substances. It is noteworthy that cardiomyocytes are able to generate TNF- α , IL-1 β , IL-6, cytokine-induced neutrophil chemoattractant (CINC)-1, macrophage migration inhibitory factor (MIF), and high-mobility group box (HMGB)-1 during endotoxemia, sepsis, and burn injury (Flierl et al. 2008).

b. Intramyocardial mechanisms

i. Role of β -adrenergic receptor hypo-responsiveness

The physiological pathway of β -receptor agonists leads to the formation of cyclic adenosine monophosphate (cAMP) through adenylate cyclase. This triggers intracellular transduction signals, which lead to the release of calcium ions from the sarcoplasmic reticulum into the cytosol and eventually to the contraction of myocardial cells (Fig. 2). Hence, short-term β -adrenergic stimulation with catecholamines increases cardiac contractility and heart rate. However, prolonged and excess stimulation can lead to myocardial damage by calcium overload and consequent cell necrosis (Opie 2004). During sepsis, various studies have documented elevated catecholamine levels in patients (Annane et al. 1999, Bernardin et al. 1998) and animals (Hahn et al. 1995, Iwase et al. 2001). Circulating catecholamines may be autooxidized by superoxide and thus inactivated (Macarthur et al. 2000).

During septic shock, a decrease in the number of β -receptors and in the adenylyl cyclase activity was reported (Reithmann et al. 1993). Others found a blunted contractile response in rat cardiomyocytes after cytokine stimulation despite a normal receptor density (Gulick et al. 1989). Notably, responses to increased extracellular calcium ion concentrations were normal. The underlying mechanism was identified to be a disruption of signal transduction across the cell membrane (Chung et al. 1990). In endotoxemic rabbits, stimulatory G-proteins were decreased (Matsuda et al. 2000), whereas in both nonsurvivors of septic shock (Bohm et al. 1995) and septic animals (Wu et al. 2003), inhibitory G-proteins were increased. These changes result in decreased activity of adenylyl cyclase and reduced levels of cyclic adenosine monophosphate. In summary, β -adrenergic stimulation during sepsis is blunted by alterations occurring at different levels of the signaling cascade. However, it remains to be determined how these effects on calcium signaling are linked to time-dependent changes in the β -adrenergic response, and any protective effects on the myocardium during prolonged sepsis (Rudiger und Singer 2007).

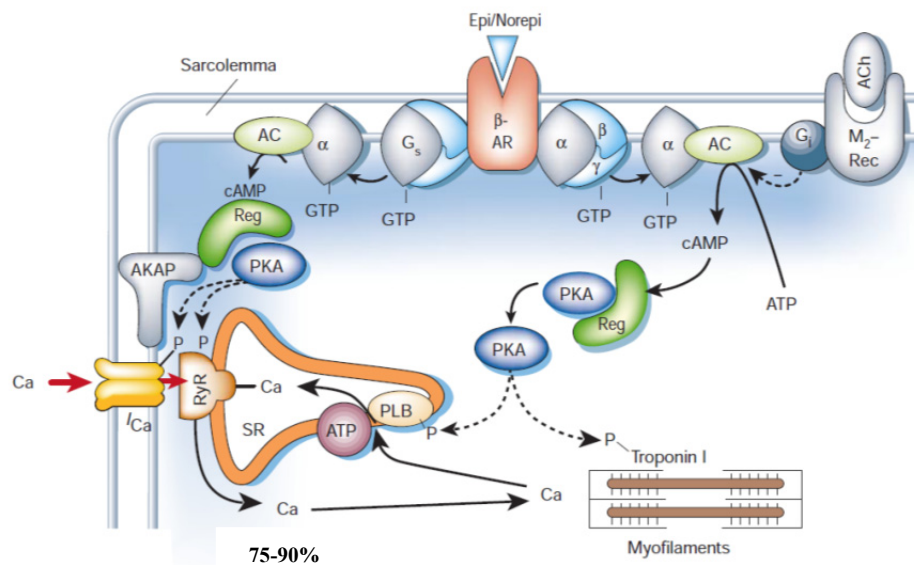


Figure 2: Schematic illustration of adrenergic receptor activation and phosphorylation targets relevant to excitation–contraction coupling. AC, adenylyl cyclase; ACh, acetylcholine; AKAP, A kinase anchoring protein; b-AR, b-adrenergic receptor; M2-Rec, M2-muscarinic receptor; RyR, ryanodine receptor; PLB, phospholamban; Reg, PKA regulatory subunit; SR, sarcoplasmic reticulum (adopted from (Bers 2002)).

ii. *Role of altered intracellular calcium trafficking*

Cardiac contraction requires that calcium ions combine with the troponin complex, especially with the troponin C. Interaction of calcium ion with the troponin C leads to a spatial

conformation change of troponin I, which releases actin, allows formation of actin and myosin bridges resulting in cardiac contraction (Bers 2002).

Sepsis-induced myocardial dysfunction is characterized by altered intracellular calcium trafficking. Suppression of L-type calcium currents (Liu und Schreur 1995, Stengl et al. 2010), decreases in ryanodine receptor density and activity (Dong et al. 2001, Wu und Liu 1992), and changes of calcium re-uptake into the sarcoplasmic reticulum (Wu et al. 2002, Wu et al. 2001) have all been demonstrated in sepsis models. On a myofibrillar level, sepsis affects the calcium sensitivity of contractile proteins (Takeuchi et al. 1999, Wu et al. 2001). These changes will impair both systolic and diastolic function, but it remains to be determined how they relate to blunted β -adrenergic signaling and defective enzyme phosphorylation.

iii. Role of nitric oxide (NO) and the peroxynitrite pathways

NO exerts a plethora of biological effects in the cardiovascular system (Schulz et al. 2005). In healthy volunteers, low-dose NO increases LV function, whereas inhibition of endogenous NO release by intravenous infusion of the NO synthase (NOS) inhibition reduced heart performance (Rassaf et al. 2006). Higher doses of NO have been shown to induce contractile dysfunction by depressing myocardial energy generation (Fig. 3) (Kelm et al. 1997).

In the past two decades, it has become clear that nitric oxide (NO) may have direct and indirect as well as beneficial and deleterious effects in the pathogenesis of sepsis and septic shock (Hotchkiss und Karl 1992, Hotchkiss et al. 1999). Sepsis leads to the expression of inducible NOS (iNOS) in the myocardium (Khadour et al. 2002), followed by high-level NO production, which in turn importantly contributes to myocardial dysfunction, in part through the generation of cytotoxic peroxynitrite, a product of NO and superoxide (Pacher et al. 2007).

Excessive NO production is an important player during hypotension and catecholamine resistance in septic shock (Boyle et al. 2000). However, its role and impact on septic cardiomyopathy is still a matter of debate. Whereas disproportionate levels of NO sustain the ability of the left ventricle to fill during diastole, and thereby crucially support adequate myocardial perfusion (Belcher et al. 2002, Cotton et al. 2002), cardiodepressant activity of proinflammatory cytokines also seems to involve NO: exposure of rat cardiomyocytes to septic sera depressed contractility (see below), but NOS inhibition restored contractility to control levels (Kumar et al. 1999). Moreover, deficiency or selective blockade of inducible NOS (iNOS) protected against the development of cardiac dysfunction in endotoxemic mice (Ichinose et al. 2003, Ullrich et al. 2000).

There is compelling evidence that NO plays also an indirect role in myocardial contractility regulation and its disturbance via the production of free radicals, especially peroxynitrite (Kohr et al. 2012). Peroxynitrite is emerging as a crucial modulator of myocardial function during health and disease. Under physiological conditions, low levels of peroxynitrite serve to maintain and/or increase basal and β -AR-stimulated contraction in the myocardium. This occurs via RyR and PLB phosphorylation through direct PKA activation and SERCA activation via S-nitrosylation (Shan et al. 2010). Conversely, supra-physiological levels of peroxynitrite (due to iNOS expression and increased ROS levels via NADPH oxidase and xanthine oxidase) are detrimental to myocardial function and decrease β -AR-stimulated cardiomyocyte contraction. This occurs via PLB dephosphorylation through PP2a activation, decreased RyR activity, mitochondrial dysfunction, and myofilament protein cleavage (Kohr et al. 2012). Specifically, peroxynitrite, rather than NO per se, has been shown to impair muscle contractility during sepsis by its ability to denature proteins, perturb calcium flux, and depress mitochondrial respiration during experimental sepsis (Ishida et al. 1996, Xie et al. 1998). In contrast, neutralization of peroxynitrite improved cardiac dysfunction in a rodent model of sepsis (Lancel et al. 2004).

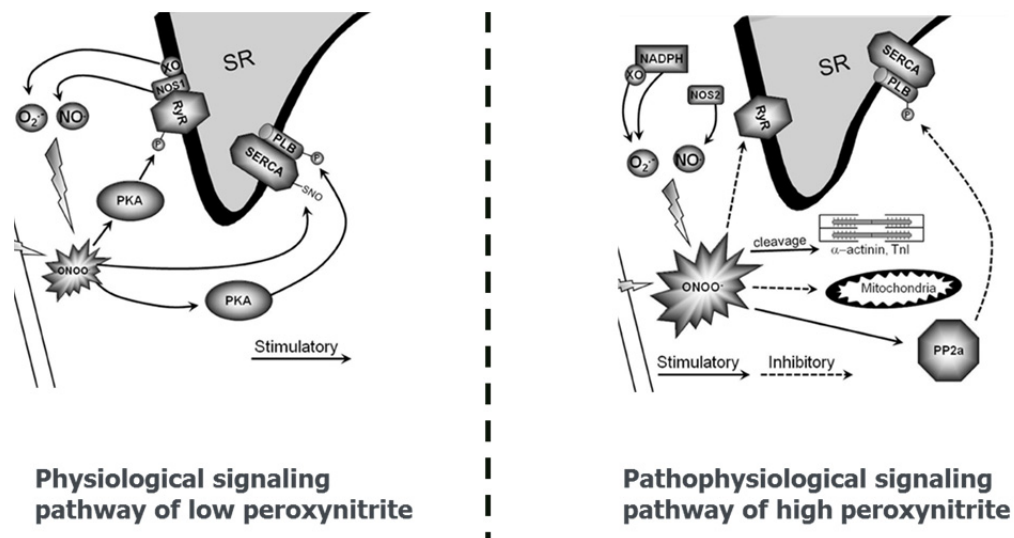


Figure 3: Schematic illustration of detrimental effect of supra-physiological level of peroxynitrite on myocardial function. (RyR, ryanodine receptor; PLB, phospholamban; ONOO-, peroxynitrite; PP2a, protein phosphatase 2a; NOS2, inducible nitric oxide synthase (iNOS) (adopted from (Kohr et al. 2012))).

Furthermore, NO, produced in large amounts during sepsis, can bind to complex IV of the respiratory chain and then compete with oxygen, inhibiting this complex and increasing production of reactive oxygen species (ROS) (Rabuel und Mebazaa 2006).

Given the existence of different NOS isoforms and their various modulating interactions, dose-dependent NO effects, and the precise balance of NO, superoxide, and thus peroxynitrite

generated in subcellular compartments, further mechanistic approaches are necessary to improve our understanding of the complex NO biology and its derived reactive nitrogen species in pathogenesis of septic cardiomyopathy.

iv. Role of Matrix metalloproteinases

Matrix metalloproteinases (MMPs) are zinc-dependent endopeptidases that degrade components of extracellular matrix and modulate inflammatory proteins. They can be classified broadly by substrate specificity into collagenases (MMP-1, -8, and -13), gelatinases (MMP-2 and -9), stroma-lysins (MMP-3, -10, -11), elastases (MMP-7 and -12), and membrane-type (MT-MMPs-14 and -17). The regulation of MMPs is modulated by tissue-specific MMPs inhibitors (Brinckerhoff und Matrisian 2002). In sepsis, inflammatory cytokines (such as IL-1, TNF- α) and peroxynitrites activate the release of MMPs, which leads to matrix degradation, coagulopathy, and organ damage (Khadour et al. 2002). The role of different MMPs has been investigated in both animal and human models of sepsis with conflicting results. In a rat model of sepsis (Lalu et al. 2004), lipopolysaccharide-induced myocardial depression was associated with decreased activity of MMP-2 and increased circulating levels of MMP-9, which suggests that MMP-9 may contribute to endotoxin-induced myocardial depression. In another rat model of early sepsis, MMP-9 was found to correlate with the severity of sepsis and histologic tissue damage (Teng et al. 2012). Consistent with these observations, MMP inhibitors were found to be protective against sepsis-induced cardiomyopathy in a rat model of sepsis (Lalu et al. 2003). In contrast to animal models of sepsis, several human studies reported a correlation between MMP-9 and sepsis severity and mortality (Hoffmann et al. 2006), whereas others reported an inverse correlation with sepsis severity and mortality (Lorente et al. 2009). Based on these findings, a definitive and exclusive role of MMPs is unclear in human sepsis. These contrasting findings might be the result of multiple (and potentially conflicting) factors modulate the release of MMPs and their inhibitors at different time points and severity stages of sepsis (Zaky et al. 2014).

1.3.2 Appropriateness of research approaches to study septic cardiomyopathy

The complexity of sepsis makes the clinical study of sepsis and sepsis therapeutics difficult. Animal models have been developed in an effort to create reproducible systems for studying sepsis pathogenesis, preliminary testing of potential therapeutic agents and different

components of this multi-faceted life-threatening disease. It is obvious that myocardial dysfunction in sepsis has been the focus of intense research activity.

Meanwhile it is recognized that for translational and therapy-targeted approaches appropriate infection models are indispensable (Buras et al. 2005, Dyson und Singer 2009, Rittirsch et al. 2007). Several well-standardized experimental approaches are described in order to perform an infection which develops a clinical picture associated with many prototypical features of sepsis culminating in sepsis associated multi-organ dysfunction. In principle, they can be divided into two categories: exogenous administration of a viable pathogen (such as bacteria); or alteration of the animal's endogenous protective barrier (inducing colonic permeability, allowing bacterial translocation) (Buras et al. 2005). However, despite its clinical relevance and widespread use in sepsis research, one of the major concerns of infection models is consistency (Rittirsch et al. 2009).

Consequently, for mechanistic approaches with time-critical requirements and attempt to verify definable components of sepsis, like the initial infection-induced SIRS, other elaborated approaches with high-grade standardized animal response are more appropriate. Therefore, we used the LPS model where a defined amount of endotoxin is given as systemic administration via instillation into the abdominal cavity leading to an uniform response of the host (i.e. mice mutants) with development of the full picture of infection-induced SIRS. Clearly, this approach is based on model of sepsis underlies the notion that it is the host response that causes the clinical features of sepsis and not the intact pathogen per se. Endotoxin is part of the outer membrane of the cell envelope of gram-negative bacteria. The term endotoxin is often used exchangeably with LPS, as LPS represents the main biologically active component of endotoxin. The i.v. infusion of LPS as well as its instillation into the abdominal cavity causes sepsis-like symptoms, accompanied by similarities to pathophysiological responses in patients with sepsis, such as hematological alterations (Remick et al. 2000). Furthermore, LPS infusion induces an increase of proinflammatory cytokines in serum (Remick et al. 1990), another parallel to septic patients, whose elevated cytokine levels correlate with severity of the disease (Waage et al. 1987). However, the LPS experimental model and sepsis in humans differ in several key points, especially in profile and time course of cytokine release. Cytokine levels (TNF- α , IL-6, CXC chemokines) peaked much later and occurred at much lower levels in human patients with sepsis as well as infection models of sepsis when compared with effects of LPS infusion (Cavaillon et al. 2003, Remick et al. 2000, Gonnert et al. 2011). Nevertheless, when molecular mechanisms of organ-specific alterations during infection-induced SIRS are target of basic science studies - especially when SIRS is known to initiate early dis-

turbances of organ function in sepsis - the LPS model in mouse mutants remain one of the most appropriate approaches in order to investigate organ-specific effect in intact animals. Of note, this approach enables cell-targeted approaches under comparable experimental conditions, e.g. cell-culture studies on primary cells (obtained from the same mouse mutants and stimulated with LPS in cell culture) for mechanistic investigations.

Therefore, we decide to use the LPS model to investigate the role of PI3K γ in infection-induced SIRS in order to explore whether or not PI3K γ is causally involved in pronounced suppression myocardial contractility.

1.4 Brief overview on PI3Ks

Phosphoinositide 3-kinases (PI 3-kinases; PI3Ks) represent a family of lipid kinases whose members affect several aspects of cellular signal transduction. The PI3K family comprises three classes of enzymes (class I, Class II and Class III) that can be distinguished and grouped on the basis of their sequence similarity, substrate specificity, and mode of activation. PI3K family is characterized by distinct biochemical properties and activation mechanisms allowing their involvement in signal transduction that control variety of cellular events, including cell survival, proliferation, migration, metabolism, NO production, Ca²⁺ fluxes, and more (Hawkins et al. 2006).

The class III PI3K Vps34 (vacuolar protein-sorting defective 34) is the only PI3K that is present in all eukaryotes including yeast and plants, thus representing the most ancient PI3K variant. Both in vivo and in vitro, class III phosphorylates phosphatidylinositol (PtdIns; PI) to phosphatidylinositol 3-phosphate (PI(3)P). The function of class II PI3Ks is less well understood. Although they are able to phosphorylate both PI and phosphatidylinositol 4-phosphate (PI(4)P) in vitro, they are thought to use PI as their predominant in vivo substrate. In contrast to the other PI3Ks, class II PI3Ks are monomeric (Lindmo und Stenmark 2006, Engelman et al. 2006). Like the class III PI3K, class I PI3Ks are heterodimeric enzymes composed of a p110 catalytic subunit and a regulatory subunit.

Class I PI3Ks transduce signals from two major classes of cell surface receptors - receptor tyrosine kinases (RTKs) and G protein coupled receptors (GPCRs) - to a set of common effectors, which regulate a plethora of cellular events. All class I PI3Ks preferentially phosphorylate phosphatidylinositol 4,5-bisphosphate (PI(4,5)P₂) in vivo, although their in vitro set of substrates includes PI and PI(4)P as well. Their lipid product phosphatidylinositol 3,4,5-trisphosphate (PIP₃) is recognized by certain PH (pleckstrin homology) domains. PH domains are characterized by a common fold rather than a specific sequence motif and are one of the

most prominent protein (Lemmon 2004). Although a generic function for PH domains has not been identified so far, some of them are able to bind PI lipids with high affinity and specificity (Hurley und Misra 2000). Such PH domains feature basic residues at certain positions that make up a loose consensus sequence (Vanhaesebroeck et al. 2001). The class I PI3K effectors bear PH domains that bind PIP3 or phosphatidylinositol 3,4-bisphosphate (PI(3,4)P2). The latter is generated by the SH2-containing inositol 5-phosphatase (SHIP). SHIP1 is predominantly expressed in hematopoietic cells, where it functions as a negative regulator of immune signaling (Krystal 2000, Huber et al. 1998). In contrast, the SHIP2 isoform is broadly expressed (Rohrschneider et al. 2000), but appears to lack a significant physiological role, because SHIP2 knockout mice display only a very mild phenotype (Sleeman et al. 2005). PI3K signals are terminated by the 3' phosphatase PTEN (phosphatase and tensin homolog deleted on chromosome 10, which dephosphorylates both PIP3 and PI(3,4)P2 (Leslie und Downes 2002). Depending on the nature of the regulatory subunit, class I PI3Ks are further subdivided into classes IA and IB. The class IA PI3Ks p110 α (Hiles et al. 1992, Klippel et al. 1993, Shoelson et al. 1993), p110 β (Hu et al. 1993), and p110 δ (Vanhaesebroeck et al. 1997) associate with regulatory subunits of the p85 family, which mediate activation downstream of RTKs. The class IA regulatory subunits are encoded by three genes, giving rise to at least five different isoforms by alternative splicing (Vanhaesebroeck et al. 2001), of which p85a is most abundant (Koyasu 2003).

Because the catalytic subunits do not display apparent preferences towards certain regulatory subunits (Hawkins et al. 2006), class IA PI3K holoenzymes are referred to as the catalytic subunits. Whereas p110 α and p110 β are ubiquitously expressed, expression of p110 δ is largely confined to leukocytes (Vanhaesebroeck et al. 2001). p110 γ represents the only class IB PI3K (Stoyanov et al. 1995) which, in contrast to the class IA PI3Ks, is activated exclusively by GPCRs via heterotrimeric G proteins. PI3K γ is composed of p110 γ and the regulatory p101 or the novel p87^{PIKAP} (p87, also called p84) subunit (Voigt et al. 2006, Suire et al. 2005, Voigt et al. 2005, Stephens et al. 1997).

1.4.1 Brief introduction on PI3K γ structure and function

As mention above, phosphatidylinositol 3-kinase γ (PI3K γ) is the only member of the Class IB of the lipid kinases superfamily that catalyze the phosphorylation of phosphatidylinositol-4,5-bisphosphate (PtdIns(4,5)P₂) at the 3'-OH group, giving rise to the second messenger phosphatidylinositol-3,4,5-trisphosphate (PtdIns(3,4,5)P₃;). PI3K γ associates with two

regulatory subunits, p101 and p84, that control its expression, activation and subcellular location (Fig. 4).

PI3K γ activation is driven by activation of pertussis-toxin-sensitive G α_i -coupled G-protein-coupled receptors (GPCRs), and is mediated by direct association of its catalytic domain with the $\beta\gamma$ -subunits of G proteins and Ras. Several proteins, such as Ras, mitogen-activated protein kinase (MAPK) kinase (MEK), phosphodiesterases (PDE), p101 and p84, can bind to PI3K γ , indicating a protein-scaffold function in addition to its enzymatic activity. PI3K γ was also shown to directly phosphorylate and activate MEK (further detail, see Fig. 4). Although monomeric p110 γ can be stimulated to some extent by G $\beta\gamma$ dimers in vitro, p101 appears to be necessary for optimal stimulation of PI3K γ by G $\beta\gamma$ (Brock et al. 2003). Accordingly, G $\beta\gamma$ subunits released upon stimulation of Gi-coupled GPCRs are bound by p101,

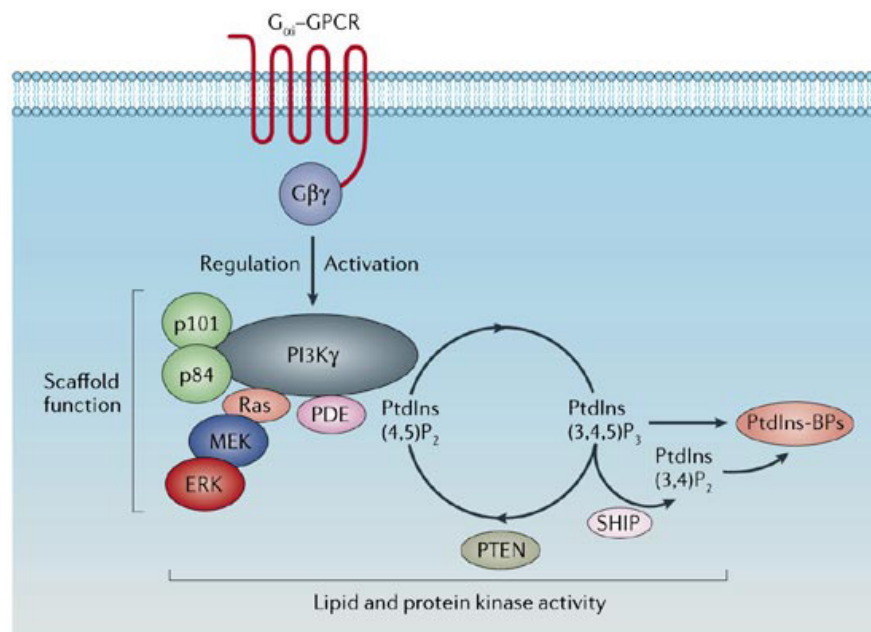


Figure 4: Schematic representation of PI3K γ 's different molecular functions. (Detailed description is referred in the text; GPCR, G protein coupled-receptor; PDE, Phosphodiesterase; MEK, mitogen-activated protein kinase (MAP) kinase; ERK, extracellular-signal-regulated kinase; PTEN, phosphatase and tensin homolog; SHIP, SH2-containing inositol 5-phosphatase (adopted from (Ruckle et al. 2006))).

whereby the p110 γ /p101 heterodimer translocates to the plasma membrane. Therefore, p110 γ has access to its substrate PI(4,5)P₂, and G $\beta\gamma$ further enhances its catalytic activity by an allosteric mechanism via a binding site on p110 γ itself. As is the case for class IA PI3Ks, Ras proteins can further activate p110 γ at the site of the membrane (Suire et al. 2002, Pacold et al. 2000). PI3K γ is mainly expressed in leukocytes and other immune-competent cells, but also in cardiomyocytes (Crackower et al. 2002), hepatocytes (Recknagel et al. 2012) and sensory

neurons (Konig et al. 2010). Knowledge concerning the physiological functions of PI3K γ largely stems from three independent lines of p110 γ knockout (p110 $\gamma^{-/-}$) mice that have been generated and characterized in recent years (Hirsch et al. 2000, Li et al. 2000, Sasaki et al. 2000). p110 $\gamma^{-/-}$ mice are viable, fertile, but exhibit alterations in various physiological and pathophysiological contexts. According to its expression pattern, p110 γ performs functions mainly in the hematopoietic system, but also in heart and certain others tissues

1.4.2 Brief introduction on PI3K γ and myocardial contractility

Recent works have established an important role for PI3K γ in cardiomyocytes. Despite the low expression levels of p110 γ in the heart, this lipid kinase appears to be a key regulator of cardiac pathophysiology (Ghigo et al. 2011, Damilano et al. 2010). Several groups have demonstrated the involvement of p110 γ in the modulation of β -adrenergic receptor (β -AR) signaling. Indeed, p110 γ cooperates with β -AR kinase 1 (also known as GRK-2) and with the

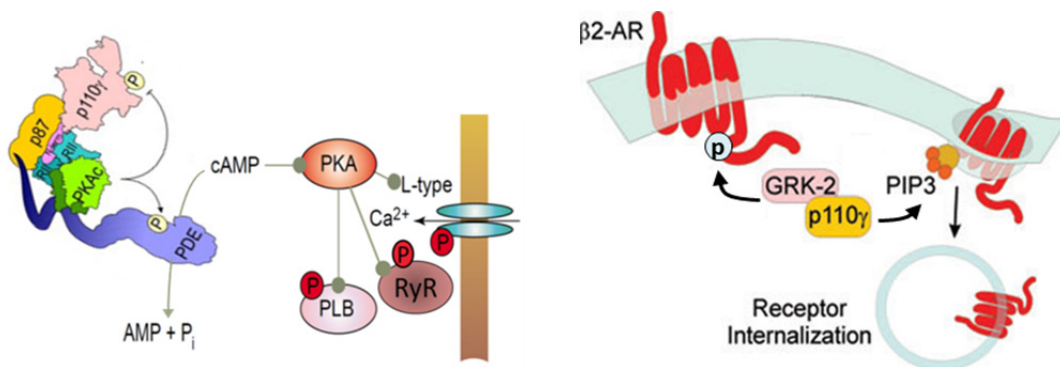


Figure 5. Involvement of PI3K γ in the down-regulation of the β -adrenergic pathway. (A): Contributions of PI3K γ 's scaffold function in the degradation of cAMP via activation of PDEs (adopted from(Perino et al. 2011)). (B): Contribution of PI3K γ to β -adrenergic receptor desensitization via scaffold function for Gs uncoupling by GRK2-mediated receptor phosphorylation and via kinase function in receptor internalization by PIP3 (adopted from (Damilano et al. 2010)).

clathrin-dependent endocytic machinery to dampen the cAMP signaling by promoting desensitization (Gs uncoupling and internalization) and downregulation of β -ARs (Naga Prasad et al. 2001, Naga Prasad et al. 2003). In addition to the control of β -AR response, p110 γ also affects downstream events of β -AR signaling through a kinase-independent mechanism (Hirsch et al. 2009). By activating the phosphodiesterases PDE3B and PDE4, which hydrolyze cAMP to 5'-AMP (Conti und Beavo 2007, Kerfant et al. 2007, Patrucco et al. 2004), p110 γ restricts cardiac cAMP levels, eventually limiting PKA-mediated events. In concord-

ance, hearts from $p110\gamma^{-/-}$ mice do not show obvious structural abnormalities, but they exhibit a marked enhancement in basal contractility due to increased levels of myocardial cAMP (Crackower et al. 2002, Patrucco et al. 2004).

Mice expressing a kinase-dead $p110\gamma$ ($p110^{KD/KD}$) show normal cAMP levels as well as unchanged contractile function (Patrucco et al. 2004). This indicates that in addition to lipid kinase activity that contributes to β -AR density and function, $p110\gamma$ has an important role as a scaffold protein, regulating cAMP levels and myocardial contractility (Fig 5). The molecular mechanism through which $p110\gamma$ acts as a cAMP modulator was recently unraveled in a report indicating that $p110\gamma$ functions as an A-kinase anchoring protein (AKAP). Indeed, $p110\gamma$ directly and selectively binds the regulatory subunit II of PKA and tethers PKA to the proximity of PDE3B (Perino et al. 2011). In this way, PKA can phosphorylate and activate PDE leading to enhanced intracellular cAMP degradation.

1.5 Objectives and aim of this study

Sepsis-induced myocardial depression (SIMD) is a frequent event that corresponds to the severity of sepsis and is reversible in survivors (Rudiger und Singer 2013). SIMD occurs early since a considerable part of septic patients express features of myocardial dysfunction already at admission (Vieillard-Baron et al. 2008, Werdan et al. 2011). The consequences of an already exaggerated systemic host response to infection may be further impaired by a reduced myocardial performance and finally lead to sepsis-induced cardiocirculatory shock (Angus und van der Poll 2013, Krishnagopalan et al. 2002). SIMD is frequently associated with improved outcome of septic patients (Vieillard Baron et al. 2001, Etchecopar-Chevreuril et al. 2008) indicating the relevance of adaptive myocardial hypocontractility to maintain cell viability by down-regulating oxygen consumption, energy requirements and ATP demand (Levy et al. 2005).

Infection-associated SIMD is the result of complex host-pathogen interactions, called systemic inflammatory response syndrome (SIRS) that causes intrinsic myocardial dysfunction via activation of pathophysiological signaling pathways (Rudiger und Singer 2007, Zaky et al. 2014). Initiation of SIMD is mainly caused by microbial toxins and proinflammatory mediators that are excessively released during the innate immune response. As a consequence, β -adrenergic receptor (β -AR) responsiveness and signaling are attenuated despite enhanced catecholamine access, which leads to reduced myocardial contractility (Rudiger und Singer 2007). Among a plethora of exogenous and endogenous mediators that may interfere with myocardial function agonists of the toll-like receptor 4 (TLR4) are known to activate the phosphatidylinositol 3-kinase (PI3K γ) pathway and to provoke depression of myocardial contractility (Boyd et al. 2006, Fallach et al. 2010, Xu et al. 2010).

In cardiomyocytes, catecholamine-induced stimulation of the G protein-coupled β -ARs utilizes the second messenger cyclic AMP (cAMP) to regulate cardiac contraction via cAMP/protein kinase A (PKA) activation and phosphorylation of effectors of the cardiac excitation-contraction coupling such as the L-type Ca²⁺ channel (LTCC), the ryanodine receptor (RyR), phospholamban, and troponin I. PI3K γ coordinates via its scaffold function the stimulation of the major cardiac phosphodiesterase (PDE) 3 and PDE4 isoforms, thus creating a feedback loop to prevent pathological overstimulation by appropriate cAMP degradation (Perino et al. 2011). Therefore, although multiple PI3K isoforms are expressed in the heart, PI3K γ is particularly involved in controlling heart contractility (Crackower et al. 2002, Damilano et al. 2010, Patrucco et al. 2004). In sepsis-induced SIRS, the PI3K γ pathway is

involved in decreased myocardial contraction (Fallach et al. 2010, Xu et al. 2010). Nonetheless, the molecular role of PI3K γ in SIMD remains unclear.

Hitherto, just one study has been published which showed that PI3K γ is involved in SIRS-induced cardiac dysfunction, mediated by enhanced myocardial alarmin release early after onset of systemic inflammation (Xu et al. 2010). However, the molecular mechanism(s) of PI3K γ -dependent as well as alarmin-mediated myocardial depression remain elusive.

Aim of this thesis is to explore whether or not PI3K γ is causally involved in pronounced suppression myocardial contractility early after lipopolysaccharide (LPS)-induced inflammation.

We hypothesize that sustained β -adrenergic stimulation during the early period of SIRS may negatively influenced by PI3K γ .

In addition, it should be clarified if PI3K γ lipid-kinase independent mechanisms are able to mediate sustained suppression of cardiomyocyte inflammatory response induced by LPS and/or autocrine cytokines.

Furthermore, it should be investigated if additional inflammatory reactions may be involved in the longer lasting development of suppressed myocardial contractility. It is suggested that iNOS activity may be involved in disturbed myocardial contractility in consequence of acute infection-induced SIRS. We ask for a PI3K γ involvement.

For that purpose, a well-characterized mouse model of infection-induced SIRS by intraperitoneal endotoxin/LPS injection was used, which is suited for mechanistic studies with time-critical requirements (Buras et al. 2005). PI3K γ wild-type, knockout, and kinase-dead mice were exposed to LPS-induced SIRS and assessed for survival, cardiac autonomic nervous system (ANS) function and left ventricular performance. Additionally, primary adult cardiomyocytes derived from the respective mouse genotypes were used for mechanistic analysis of PI3K γ effects on myocardial contractility and inflammatory response.

2. Materials and methods

2.1 Materials

2.1.1 Mice

i. Animals and LPS-induced SIRS

PI3K γ knockout (PI3K $\gamma^{-/-}$) (Hirsch et al. 2000) and PI3K γ kinase-dead (PI3K $\gamma^{KD/KD}$) mice (Patrucco et al. 2004) were on the C57BL/6J background for more than 10 generations. Consequently, age-matched C57BL/6 mice were used as controls. The animals were maintained with 12 h light and dark cycles with free access to food and water. Ambient temperature was 29±1 °C during the whole experimental period. Experiments were approved by the committee of the Thuringian State Government on Animal Research. Mice received LPS (10 mg/kg, intraperitoneal, from Escherichia coli serotype 055:B5, Sigma–Aldrich, St. Louis, USA, Lot #032M4082V) as a single intraperitoneal injection. Additionally 500 μ l saline was injected subcutaneously immediately after LPS administration as well as after 24h and 48h to ensure appropriate fluid resuscitation. Mice developed SIRS with tachycardia and decline of the clinical status (Gonnert et al. 2011) with a maximum 24 h after administration. Mortality rate remained less than 10 per cent irrespective of the genetic background.

2.1.2 Lists of chemicals, substances for stimulation, inhibitors, antibodies, kits, catheter/transmitter and software for data acquisition

i. Chemicals

Table 1: Chemicals

Products	Application	Source
Collagenase II	Cell isolation	Worthington Biochemicals
Taurine	Cell isolation	Sigma
Glucose	Cell isolation	MERCK
NaCl	Cell isolation	ROTH
KCl	Cell isolation	ROTH
KH ₂ PO ₄	Cell isolation	ROTH
Na ₂ HPO ₄	Cell isolation	ROTH
MgSO ₄ ·7H ₂ O	Cell isolation	MERCK
Na-HEPESb	Cell isolation	AppliChem
CaCl ₂	Cell isolation	AppliChem GmbH
Fetal calf serum	Cell isolation	Cambrex Bio Science

Laminin	Cell culture	Sigma
MEM Earle's w 0.85 g/l NaHCO ₃	Cell culture	Biochrom
2,3-Butanedione monoxime (BDM)	Cell culture	Sigma
BSA FFA free	Cell culture	Sigma
Glutamine	Cell culture	Sigma
Pen/strep	Cell culture	Cambrex Bio Science
Natriumdiphosphat tetrabasisch (Na ₄ P ₂ O ₇)	Cell lysate	Sigma
Natriumorthovanadat (Na ₃ VO ₄)	Cell lysate	Sigma
DL-Dithioereitol (DTT)	Cell lysate	Sigma
Deoxycholic acid	Cell lysate	Sigma
Dimethylsulfoxid (DMSO)	Cell lysate	Sigma
2-Mercaptoethanol (ME)	Cell lysate	Sigma
Phenylmethylsulfonylfluorid (PMSF)	Cell lysate	Sigma
Complete, EDTA-free Protease inhibitor cocktail tablets (PIC)	Cell lysate	Roche
Bio-Rad DC Protein Assay	Cell lysate	Bio-Rad Laboratories Inc
Glycin	Western Blot	AppliChem
Tris(hydroxymethyl) aminomethan (Tris)	Western Blot	AppliChem
Acrylamid 4K-Lösung 30 % Mix 29:1	Western Blot	AppliChem
Spectra™ Multicolor Broad Range Protein Ladder (10-260 kDa)	Western Blot	Fermentas life science
N,N,N,N-Tetraethylethylendiamin (TEMED)	Western Blot	AppliChem
Tween® 20	Western Blot	SERVA Electrophoresis
Amersham™ ECL™ Western Blotting Reagents	Western Blot	GE Healthcare UK
PFA	IHC	Sigma
Ethanol	IHC	Nordbrand Nordhausse
Paraffin	IHC	MERCK
Citrate	IHC	FLUKA
Xylene	IHC	VWR international
Heparin-Natrium	Mice	Hoffmann-La Roche AG
Isoflurane	Mice	Abbvie Deutschland
Pancuronium	Mice	Cura MED Pharma GmbH

ii. *Substances for Stimulation:*

Table 2: Substances for stimulation

Products	Target	Use	Source
LPS	Mice	10mg/kg bw	Sigma
LPS	Cells	1µg/ml	Sigma
TNFα	Cells	50ng/ml	Immunotools
IL-1β	Cells	50ng/ml	Thermo Scientific
Norepinephrine	Mice	0.1mg/kg bw	Sigma
Norepinephrine	Cells	30µM	Sigma

iii. *Inhibitors:*

Table 3: Inhibitors

Inhibitor	Target	Use	Source
Rolipram	PDE4	1µM	Sigma
Cilostazol	PDE3	1µM	Sigma
1400w	iNOS (Mice)	10mg/kg bw	Sigma
1400w	iNOS (Cells)	40µM	Sigma
Cyclosporin A	NFAT	1 µM	Sigma
PD09859	ERK	50 µM	Sigma

iv. *Antibodies:*

Table 4: Antibodies

Antigen	Type (IgG)	Use	Source
P110γ (PI3Kγ)	Rabbit	1:1000	Cell signaling
alpha actinin	Mouse	1:500	Invitrogen
ryanodine (phospho)	Rabbit	1:8000	Abcam
phospholamban (phospho)	Rabbit	1:8000	Cell signaling
iNOS	Rabbit	1:500 (WB)	Abcam
iNOS	Rabbit	1:250 (IHC)	Abcam
NFAT (phospho)	Rabbit	1:1000	Sigma
vinculin	Rabbit	1:2000	Cell signaling

NFkB (Phospho)	Rabbit	1:1000	Cell signaling
JNK (phospho)	Mouse	1:1000	
ERK1/2 (phospho)	Mouse	1:1000	Cell signaling
P38 (Phospho)	Rabbit	1:1000	Cell signaling
beta2 adrenergic re- ceptor	Rabbit	1:1000	Abcam
beta2 adrenergic re- ceptor (phospho)	Rabbit	1:1000	Abcam
mmp9	Rabbit	1:1000	Cell signaling

v. *Kits:*

Table 5: Kits

Kits	Application	Source
Catecholamine (CA) ELISA Kit	Cardiac tissue	Blue Gene
cAMP ELISA Kit	cardiomyocytes	Promega
Tunel Kit	Paraffin-embedded cardiac tissue	Roche
H&E Kit	Paraffin-embedded cardiac tissue	Sigma
Sirus-Red kit	Paraffin-embedded cardiac tissue	
Masson-Goldner kit	Paraffin-embedded cardiac tissue	

vi. *Data acquisition: Catheter/transmitter and software*

Table 6: Data acquisition: Catheter/Transmitter and software

catheter/transmitter	Software	Application	Company
Millar catheter	PowerLab sys- tem	Left ventricular performances	ADInstruments
Radiofrequency transmitter	Ponemah Soft- ware 5.20	ECG/Temperature	Data Science International (DSI)

2.1.3 Experimental procedures

i. *Endotoxemia challenge model*

Inflammation was induced by intraperitoneal injection of 0.5 ml of normal saline (NS) containing LPS (10 µg/g bw) for 3h, 24h, 3 days or 1 week to 3-mo-old mice. This dosing regimen is in accord with previous studies assessing LPS-induced cardiac dysfunction (Xu et

al. 2010, Boyd et al. 2008). Control mice received saline. As an in vitro correlate of inflammation, cardiomyocytes were exposed to norepinephrine (30 μ M) or a mixture of norepinephrine (30 μ M), LPS (1 μ g/ml) and cytokines (TNF α , 50ng/ml and IL1- β , 50ng/ml).

2.1.3.1 Measurement of left ventricular performance

i. *General procedure*

Mice were anesthetized by isoflurane (2% in oxygen), intubated, and ventilated with a respirator (MiniVent Model 845, Hugo Sachs Elektronik-Harvard Apparatus GmbH, March-Hugstetten, Germany). A 1.4F microconductance pressure-volume catheter (model SPR-839; Millar Instruments Inc) was positioned in the left ventricle (LV) via the right carotid artery for continuous registration of LV pressure-volume loops in closed chest animals (Pacher et al. 2008, Houser et al. 2012) (Fig. 6). Pressure-volume loops were generated using a PowerLab system (ADInstruments Ltd., Oxford, UK) connected to the Millar catheter. Calibration of the recorded volume signal was obtained by hypertonic (7.5%) saline wash-in technique (Steendijk und Baan 2000). All measurements were performed while ventilation was turned off momentarily. Indices of systolic and diastolic cardiac performance were derived from LV pressure-volume data obtained at steady state. LV end systolic elastance (E_{es}) was considered to be an appropriate parameter to determine of myocardial contractile state (Kass et al. 1989, Pacher et al. 2008).

Myocardial responsiveness was assessed by calculation of percentage change of dP/dtmax induced by bolus injection of norepinephrine (100pg/kg) into the jugular vein.

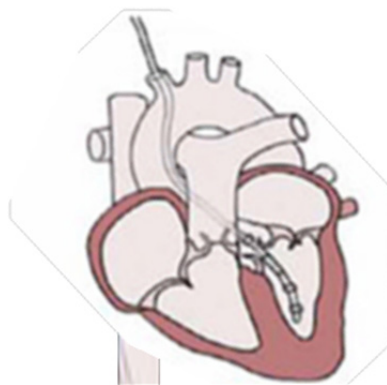


Figure 6: Schematic representation of measuring catheter placement within the cavity of the left ventricle, introduced via right carotid artery and ascending aorta (adopted from (Pacher et al. 2008)).

ii. *Establishment of adequate mechanical ventilation in mice*

Appropriate experimental conditions for *in vivo* measurement of myocardial contractility requires the establishment of standardized conditions including appropriate anesthesia, muscular relaxation, fluid substitution, body temperature control, and adequate artificial ventilation for the mice strains used under the given experimental prerequisites. Therefore, a pilot study was performed in order to verify appropriate experimental conditions for reproducible experimental performance in healthy and compromised mice for at least 3 hours. Inhalation anesthesia with isoflurane (1,5%) in oxygen was used as recommended (Zuurbier et al. 2002). Muscular relaxation (pancuronium bromide, 0.2 mg kg⁻¹ body weight h⁻¹, i.p.), was performed after tracheotomy and endotracheal tube insertion. Appropriate mechanical ventilation (MiniVent Model 845, Hugo Sachs Elektronik-Harvard Apparatus GmbH, March-Hugstetten, Germany) was adjusted to maintain normoxic and normocapnic blood gas values (blood gas analyser, model ABL50, Radiometer, Copenhagen, Denmark). In addition, arterial hemoglobin content and oxygen saturation were measured using a haemoximeter (model OSM2, Radiometer). Blood was collected from left common carotid artery. The samples were collected at different settings of ventilator stroke rate and tidal volume in order to determine the optimal setting that keep measuring parameters at the normal ranges for at least 3h (arterial pCO₂: 35-40 mmHg; Hb:10-11mmol/l; pH 7.35-7.45).

Established setting is recorded according to the body weight of mice in Table 7.

Table 7: Ventilatory parameters in accordance to body weight.

Weight (g)	tidal volume (µl)	Respiratory rate (Stroke min⁻¹)	Isoflurane (%)	Oxygen (%)
18-19	105	135	1.5	100
19-20	110	135	1.5	100
20-21	115	135	1.5	100
21-22	120	135	1.5	100
22-23	125	135	1.5	100
23-24	130	135	1.5	100
24-25	135	132.5	1.5	100
25-26	140	132.5	1.5	100
26-27	145	132.5	1.5	100
27-28	150	132.5	1.5	100
28-29	155	132.5	1.5	100
29-30	160	132.5	1.5	100
30-31	165	130	1.5	100
31-32	170	130	1.5	100
32-33	175	130	1.5	100
33-35	180	130	1.5	100

iii. Catheter calibration for microconductance pressure-volume measurements

The calibration cuvette approach was used. Blood sample from a donor animal was used to enable the exact calibration factor of the given microconductance catheter for accurate assessment of left ventricular (LV) blood volume measurement, i.e. in order to convert the rough volume data (given in arbitrary unit) into volume units (μl). Therefore, a mouse insulator-type calibration cuvette was used (provided by the manufacturer), was placed into a pre-warmed water bath ($37\text{ }^{\circ}\text{C}$) and after temperature equilibration quickly filled with freshly taken blood from heparinized animals in a series of six holes with gradually increasing known volume. The catheter tip was positioned central of the respective hole, gently introduced so that all 4 electrodes are submerged for 10–20 s. Conductance changes were recorded for calibration. Volume calculation was performed and the calibration factor was calculated using the last square principle for calibration curve determination.

Calibration was performed before every series of experiment.

iv. Surgical procedure for pressure-volume (PV) catheter placement and data acquisition

Initially, the animal was transferred into a chamber containing anesthetic gas (isoflurane 3% for induction). When the animal is anesthetized (not responding to tail or ear pinch), the spontaneously breathing animal was continuously narcotized via funnel with mixture of 100% oxygen and 2% isoflurane. Body temperature was monitored by a rectal temperature probe, and was maintained throughout the experiment at $37\pm 0.3^{\circ}\text{C}$ using a warmed pad and a feedback-controlling device. After shaving a midline neck incision was performed, and via tracheostomy an endotracheal cannula of appropriate size was inserted and fixed by suture. Afterwards, mechanical ventilation was performed by connection of the tracheotomy cannula to the respirator (isoflurane was decreased to 1.5%) and muscular relaxation. Corresponding ventilation settings were performed according to the pre-established values for frequency and tidal volume.

Next, via inverted T-shaped middle-neck incision from mandible to the sternum the right common carotid artery (RCC) was prepared, while the vagal nerve was preserved. The cranial RCC branch was closed by suture, and the catheter was introduced via small incision and advanced in caudal direction. The pressure-volume catheter was connected to a commercial conductance system (Millar MPVS/ Power Lab, ADInstruments Ltd., Oxford, UK) producing a constant current of 30 mA at a frequency of 2 kHz. Pressure trace was continuously recorded and first measure was performed when catheter tip has reached the ascending aorta. Catheter

ter was continuously advanced until the tip was placed in the cavity of the left heart, fixed in place by tightened surgical knots, and verified by typical pressure trace recordings (Fig 7).

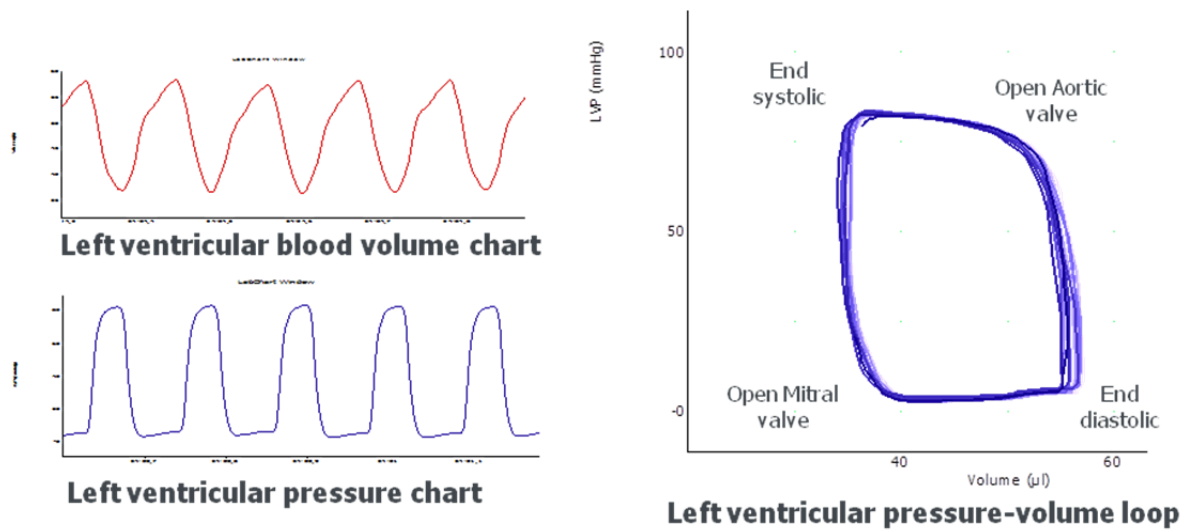


Figure 7: Representative normal traces of mouse left ventricular pressure and blood volume recordings (left panel) and resulting PV loops (right panel) representing different steps of heart function.

After stabilization for 10–15 min, baseline recordings of PV loops at steady state conditions were performed.

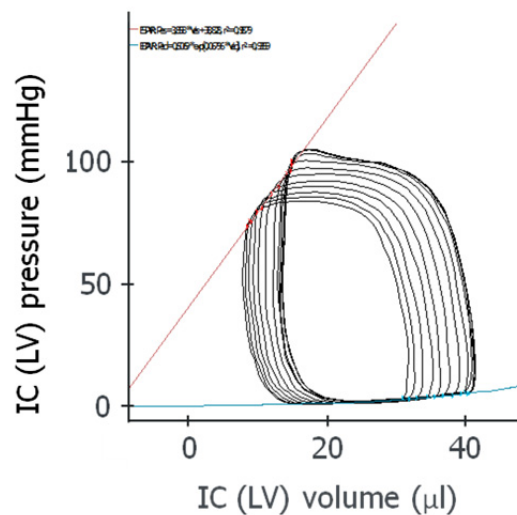


Figure 8: Representative normal mouse PV loops during gradual preload reduction (ICV occlusion) and resulting connecting line of end-systolic (red line) and end-diastolic (blue curve) loop points, extrapolated to the y-intercept. Slope of the end-systolic maxima connecting line gives end-systolic elastance, which defines chamber end-systolic stiffness, is generally accepted as an index of ventricular contractile state insensitive to load and is prone to particularly assess acute changes (Kass et al. 1989, Pacher et al. 2008).

After baseline recording, the inferior cava vein (ICV) occlusions were performed while ventilation was turned off momentarily. For that purpose, the upper abdominal cavity was opened by an incision just below the costal arch on the right side; the inferior caval vein was then gently exposed and temporarily closed for transient preload decline (Fig. 8). Using this procedure, the changes of end-systolic pressure-volume relations (amount of its gradual decline) delivers a valuable measure of myocardial contractility which is not confounded by influences of pre- and/or afterload changes (Kass et al. 1989, Pacher et al. 2008).

Finally, a 10- to 20- μ l bolus of 15% saline was rapidly injected into the right jugular vein to yield an estimate of the parallel conductance (V_p) as a prerequisite to perform absolute volume calibration in every single animal (see below).

In vivo assessment of myocardial response on β -adrenergic stimulation was performed by bolus injection of norepinephrine (NE; 100 ng/g BW) into the jugular vein. The percentage change of dp/dt_{max} due to stimulation was used as index of myocardial responsiveness (Fig. 9).

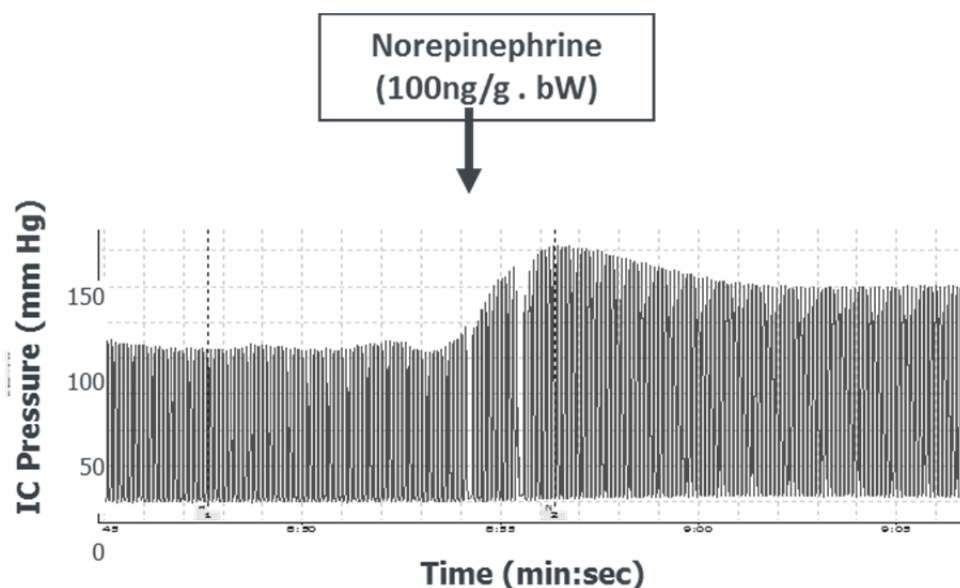


Figure 9: Representative example of left ventricular pressure response due to NE bolus administration for assessment of myocardial responsiveness.

v. *Data analysis*

Volume signal calibration: Simultaneous, continuous measurement of intraventricular pressure and volume represents the gold standard for *in vivo* heart contractility estimation (Burkhoff et al. 2005, Pacher et al. 2008). Whereas pressure measurement by miniaturized tip catheters delivers nearly unbiased data with neglectable shift transients, ventricle volume estimation by instantaneous left ventricular conductance measurement using a multielectrode

catheter (Baan et al. 1984) requires careful calibration since the total signal combines left ventricular cavity conductance with conductance of the ventricular wall and other structures outside the ventricle (Kass et al. 1986). Ideally, the current which is passed between the both exterior electrodes should go through the blood only, but in reality, some of the applied current flows through the surrounding tissues (mainly heart muscle), which are conductors, too. Therefore, frequently an overestimation of the intraventricular blood volume occurred. As the heart muscle acts as a shunt to the applied current, this effect is referred to as parallel conductance or, for volume calculations, as parallel volume (V_p). Consequently, absolute volume determination requires assessment of parallel conductance (V_p) offset because of conductivity of structures external to the blood pool. Therefore, in every single experiment V_p has to be measured.

For individual V_p estimation a saline bolus calibration with hypertonic saline bolus injection was performed. Therefore, in each animal at the end of the experiment an injection of 5–10 μ l hypertonic (7.5% saline solution) i.v. (jugular vein) was performed in order to induce a visible shift of instantaneously recorded PV loops to the right (change in conductance) without significant decrease in the pressure signal amplitude.

2.1.3.2 Assessment of cardiac autonomous nervous system (ANS) functions

i. *Surgical procedure for transmitter implantation*

Mice were quickly anesthetized in a chamber with 3% isoflurane and installed on the operating path with the head into a conical cylinder connected to gas anesthesia providing mixture of 100% oxygen and 2% isoflurane. After carefully shaving the abdominal area with an electric shaver and depilation with a commercially available hair-removal cream, a midline incision was made on the abdomen and the intraperitoneal cavity was gently opened. An implantable 1.6-g wireless radiofrequency transmitter (ETA-F10, Data Sciences International, St. Paul, MN) was inserted under sterile conditions; the leads were transferred through the abdominal wall and the intra-abdominal cavity was closed by a surgical suture. The cathodal lead was looped forward subcutaneously to an area overlying the scapula and anchored in place with a permanent suture. The anodal lead was brought subcutaneously to place it near the heart apex. Thereafter skin incision was sutured. A heating lamp was used to maintain body temperature between 36 and 37°C. Experiments (LPS administration) were initiated 10 days after surgical procedure.

ii. *Data acquisition and processing*

Continuous data recording was performed for 7 days. For simultaneous ECG, body temperature and motor activity recording, analog signals were digitalized by the telemetric receiver (model RPC-1, Data Sciences International, St. Paul, MN) and transferred via DSI Data Exchange Matrix at a sampling rate of 2 kHz with 12-bit precision (acquisition software: Ponemah Software 5.20) without signal filtering, and stored on PC for off-line data analysis. Instantaneous heart rate (HR) was derived from the reciprocal RR interval time series. Therefore, the individual R-waves, with the R-wave peak as the trigger point, were sequentially recognized (ATISApr®[®], GJB Datentechnik GmbH, Langewiesen, Germany). Accurate R-wave peak detection was verified by visual inspection. The distance of consecutive R wave peaks was measured by a precision of 0.5 milliseconds (ms). The series of R-R intervals (T1, T2, T3 Tn) was stored as a function of the beat number. This series constitutes the RR interval time series (measured in ms). The reciprocal of this series represents the instantaneous HR (in beats per minute).

HRV indices were derived from RR interval time series obtained from predetermined time periods (last hour prior LPS administration, 3rd to 4th h after LPS administration, 24th to 25th h after LPS administration, 72th to 73th h after LPS administration and 168th to 169th h after LPS administration), characterized by resting behavior of the investigated animals (polygraphic features: lack of motor activity, uniform ECG recordings). Extracted RR interval time series were transferred to MATLAB (The MathWorks GmbH, Ismaning, Germany) for pre-processing and data analysis (Hoyer et al. 2013). First, we excluded extreme values of the R-R intervals (<70 ms, >400 ms) and other outliers on the basis of the median and quartile of nearby R-R values (number of excluded R-R intervals was always < 1%). The remaining R-R intervals are considered normal-to-normal (NN) intervals. Time and frequency domain measures were calculated for each 2-min segment of normal R-R interval data and summarized for each time period selected. In the time domain, (i) mean HR (reciprocal of R-R intervals, measured in beats per minute (bpm)), (ii) standard deviation of all normal R–R intervals (SDNN, in ms), reflecting total autonomic variability, (iii) square root of the mean square successive differences between successive normal intervals (RMSSD, in ms), reflecting short-term variations in HR; (iv) skewness as a measure of the amount of asymmetry in a data set probability distribution reflecting the asymmetric contribution of vagal and sympathetic activity with their different time constants and pattern formation (Hoyer et al. 2013) were calculated for each segment of data. HRV complexity was assessed using the multiscale entropy (MSE) method as described in detail elsewhere (Costa et al. 2005, Hoyer et al. 2013). In the

frequency domain, the power spectral density (PSD) of the R-R interval time series was computed using Fast Fourier transform. Two different frequency domain measures of HRV were calculated, low-frequency range (LF) 0.15 –1.5 Hz reflecting contributions of vagal and sympathetic rhythms and high-frequency range (HF) 1.5–5 Hz indicating vagal activities. HF and LF were also used to determine the LF/HF ratio, which is indicative of sympatho-vagal balance.

2.1.3.3 Cell culture studies

i. Primary adult cardiomyocyte preparation

The protocol used for isolation and culture of adult mouse cardiomyocytes was modified according to previous reports (O'Connell et al. 2006, Louch et al. 2011)

Heart excision and cannulation: When the animal has been successfully anesthetized, the chest cavity was opened and the heart rapidly excised. Following excision, the heart was rapidly immersed in Ca^{2+} -free perfusion buffer (in mM: NaCl: 120.4; KCl: 14.7; KH_2PO_4 : 0.6; Na_2HPO_4 : 0.6; $\text{MgSO}_4\cdot 7\text{H}_2\text{O}$: 1.2; Na-HEPESb: 10; NaHCO_3 : 4.6; Taurine: 30; BDM: 10; Glucose: 5.5; pH 7.0, room temperature). The aorta was then positioned onto the cannula and secured with a silk suture. Immediately afterwards, the heart was mounted directly on a perfusion system. This procedure ensures that the coronary arteries, which are distal to the aortic valve, and therefore the coronary circulation is perfused with the enzyme solution. Therefore the solution penetrates heart, promoting uniform digestion.

Perfusion and digestion: Perfusion was started by using perfusion buffer in order to remove blood from coronary circulation to prevent clotting or blood digestion. After 4 min washing, the perfusion buffer was replaced by an enzyme solution (1mg/ml collagenase type 2: Worthington; 310u/mg, prepared in perfusion buffer and supplemented with Ca^{2+} at 12.5 μM). After perfusion with the enzyme solution (12min), the heart appeared soft, flaccid and pale.

Trituration, enrichment and restoration of Ca^{2+} : After digestion was completed, the heart was isolated from other connecting tissue, dissected in 2.5 ml enzyme solution into small pieces and gently triturated with a plastic transfer pipette (3min). To allow cells to gradually return to normal cytosolic Ca^{2+} levels without becoming Ca^{2+} overloaded and depolarized, extracellular Ca^{2+} content was gradually increased in 5 steps (12,5 μM ; 50 μM ; 200 μM ; 600 μM and 1.2mM) to a final concentration of 1.2 mM in perfusion buffer supplemented with fetal bovine serum (3 first steps) and nonfat bovine serum albumin (2 last steps). The above calcium reintroduction steps were conducted at the same time as an enrichment of cell suspension with viable cardiac myocytes was induced by allowing cells to sediment via gravity (5min for each

steps) and gentle centrifugation (17g for 3 min). After the last centrifugation, the pellet constituted essentially of rod-shaped cardiomyocytes (more than 90%) and 100% cardiomyocytes (Fig. 10).

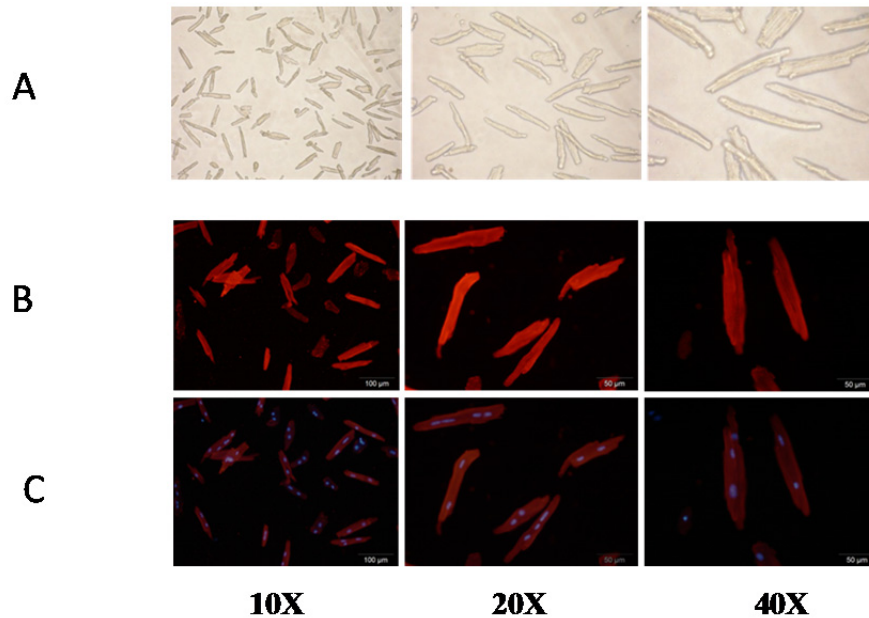


Figure 10: (A): Light microscopic image of adult mouse cardiomyocytes in petri dish (35mm) at 10X, 20X and 40X; note the high percentage (> 90%) of rod-shaped cardiomyocytes. (B): Fluorescence image of adult mouse cardiomyocytes in coverslips at 10X, 20X and 40X stained with α -actinin. (C): α -actinin staining merged with DAPI; note the 100% of cardiomyocytes.

Culture and stimulation: After the last centrifugation, the pellet (constituted essentially by rod-shaped cardiomyocytes) was re-suspended in plating medium (MEM 0,85g/l NaHCO₃, BSA, penicillin/strep, glutamine and BDM) and seeded in culture dishes, precoated for 1,5h at room temperature with laminin. After storage in an incubator (1,5h, 5% CO₂, 37°C), plating medium was replaced with BDM free culture medium (MEM 0,85g/l NaHCO₃, BSA, penicillin/strep and glutamine), cells were washed (1x) with the same medium and kept in this medium for 15h before stimulation.

ii. Heart tissue catecholamine content assessment

The heart tissue content of catecholamines (epinephrine (E) and norepinephrine (NE)) was determined using a competitive enzyme-linked immunosorbent assay (antibodies-online GmbH, Aachen, Germany). At the end of the desired LPS treatment time, animals were anesthetized, the hearts were excised and the heart tissue was roughly washed in PBS after exci-

sion, homogenized and centrifuged at 1500 g for 15 min at 4°C. Supernatant was immediately frozen at -80°C until measurement. Catecholamine measurement was performed following the manufacturer's protocol.

iii. cAMP assay

The cAMP levels in isolated adult ventricular cardiomyocytes and myocardial tissue were measured using the cAMP competitive enzyme immunoassay system (GE Healthcare Amersham Biosciences) or the cAMP GloAssayKit (Promega, Mannheim, Germany) following the manufacturer's protocol.

iv. SDS-PAGE and Western Blotting

Protein expression and activation were analyzed by western blotting and immunodetection. Cells were lysed and the proteins were separated by sodium dodecyl sulfate - polyacrylamide gel electrophoresis (SDS-PAGE).

Protein preparation for Western blot analysis: At the end of indicated stimulation time for cell in vitro or freshly isolated cells after mice injection (time indicated), proteins were extracted after incubation of cells using RIPA lysis buffer (50 mM Tris (pH 7.4), 2 mM EDTA, 1 mM EGTA, 50 mM NaF, 1 mM DTT, 10 mM Na₄P₂O₇, 1 mM Na₃VO₄, 1 % Triton X-100, 0,1 % SDS , 0,5 % Deoxycholat, 5 µl/ml PMSF, 10 µl/ml PIC) on ice for 15 min. Lysate were centrifuged at 13000 rpm for 15 min, the supernatant was transferred into new tubes and used for protein concentration by Lowry procedure (Reagents, Bio-Rad Laboratories Inc, detection at a wavelength of 750 nm using a spectrophotometer). Samples were denatured by heating at 95°C for 5 min in Laemmli's buffer and were stored at -20°C until usage for SDS-PAGE.

Immunoblotting: For immunoblotting, protein was separated by reducing SDS 6%, 7.5% or 10% polyacrylamide gel electrophoresis and transferred to nitrocellulose membranes (Mini Trans-Blot Cell, Biorad, USA) in the blotting tank at 1.5 A for 100 min. After transfer, membrane was blocked with 5 % non-fat dry milk in Tris-buffered solution added with tween 20 (Sigma-Aldrich; TBST) for 1h at room temperature, blots were incubated after washing with the respective primary antibodies (overnight, 4°C). Detection was achieved using peroxidase-coupled secondary antibodies (1 h, room temperature). To visualize protein bands, the signals were characterized with an enhanced chemiluminescence ((GE Healthcare Amersham TM ECL TM Western Blotting Detection Reagents (ECL) or Amersham TM ECL TM PLUS Western Blotting Detection Reagents (ECL plus) and autoradiography films (AGFA, Medical X-Ray films, Germany)).

Densitometric evaluation of Western Blots: Signal quantify from western blots was performed using ImageJ (National Institutes of Health, Bethesda, Maryland, USA). After development, the films were scanned and intensity was measured. During the measurement, intensities of the background were subtracted from the values of the different bands. The resulting intensities were normalized to loading control (vinculin) and indicated as arbitrary units.

v. *Histopathology and immunohistochemistry*

Hearts were in situ fixated with 4 % paraformaldehyde in phosphate buffer (5min) after rinsing with PBS (3min). Fixed heart was removed immediately and post-fixated in 4 % paraformaldehyde at 4 °C for 1 day, embedded in paraffin and cut into 6- μ m-thick sections. For immunohistochemistry, each deparaffinized, slide-mounted tissue section was incubated, after blockade of non-specific binding sites and antigen retrieval (microwave, 750 W, 11 min, 0.01 mol/l citrate buffer, pH 6), with the desired primary antibody in phosphate-buffered saline (PBS) at 4 °C overnight, followed with the associated secondary antibody at 4 °C for 1 h, and visualized by fluorescence imaging. Control sections were incubated with goat serum in absence of the primary antibody. The following primary antibodies were used: goat polyclonal anti-iNOS (1:250) antibody (Abcam, Cambridge, UK) for iNOS staining and anti-myeloperoxidase (MPO, dianova, Hamburg, Germany) for neutrophils staining. For visualization, the secondary fluorescent goat anti-mouse isotype-specific antibodies Alexa Fluor® 488 (Molecular Probes, Inc., Eugene, USA) were used. To determine the degree of apoptosis-like cell death, sections were deparaffinized, pretreated with 20 mg/ml proteinase K, and washed in PBS prior to TUNEL staining. Terminal deoxynucleotidyl transferase-mediated dUTP end-labeling (TUNEL) staining (In Situ Cell Death Detection Kit, POD; Roche, Germany) were used according to the manufacturer's protocol. Furthermore, mounted sections of heart tissue were stained with hematoxylin and eosin (H&E) for routine histology. Masson-Goldner method for collagen staining was used according to the manufacturer's protocol.

2.1.3.4 Statistics

Data are reported as mean \pm standard deviation (SD). Comparisons between groups were made with one-way or two-way analysis of variance, if appropriate. If normality test failed, Kruskal–Wallis one-way analysis of variance on ranks was used. In case of repeated measurements, one-way or two-way analysis of variance with repeated measures was used. Post hoc comparisons were made with the Holm–Sidak test or the Dunn's method was used, if appropriate. Differences were considered significant when $p < 0.05$.

3. Results

3.1 PI3K γ deficient mice display a delayed myocardial depression after LPS induces SIRS

To investigate the role of PI3K γ in LPS-induced myocardial depression, we used PI3K γ -deficient mice (PI3K $\gamma^{-/-}$) and mice carrying a targeted mutation in the PI3K γ gene causing loss of lipid kinase activity (PI3K $\gamma^{KD/KD}$). As shown in our previous studies, these genotypes allow assigning the phenotype of the mouse model to either PI3K γ lipid kinase activity (Stoyanov et al. 1995) or kinase-independent “scaffold” function such as stimulation of phosphodiesterases and cellular cAMP control (Patrucco et al. 2004, Perino et al. 2011). SIRS provoked by LPS induced a pronounced and longer lasting PI3K γ upregulation (Fig. 21).

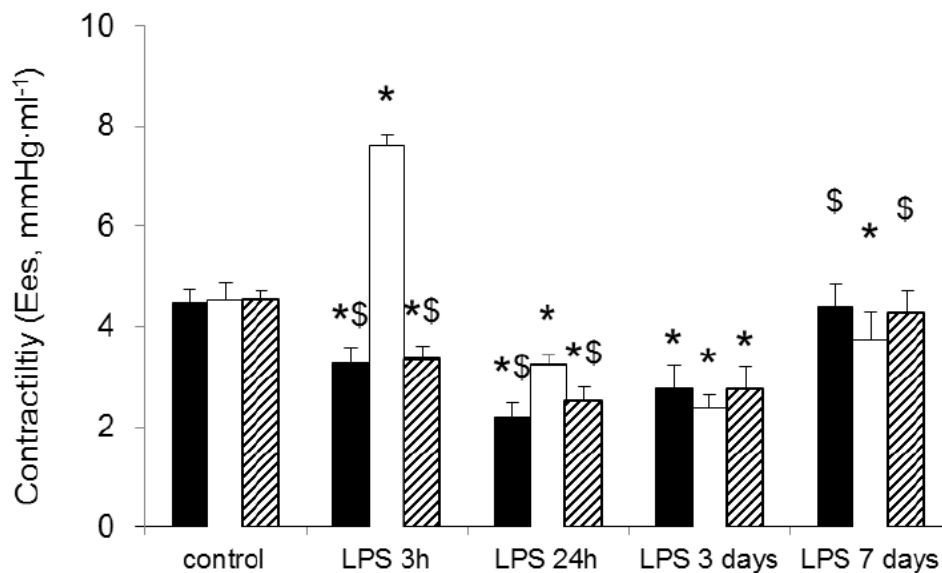


Figure 11: PI3K γ -deficient mice (PI3K $\gamma^{-/-}$, open columns) display early myocardial hypercontractility followed by delayed myocardial depression after LPS induces SIRS. In contrast, wild-type (black columns) and PI3K γ -kinase-dead (hatched columns) mice developed early after LPS administration myocardial depression characterized by reduced myocardial contractility that remained up to 3 days.

Values are mean + SD, n=10-15 per group and time point. *^{\$} p < 0.05, * significant difference between the control and LPS-stimulated state within each group, ^{\$} significant differences to PI3K $\gamma^{-/-}$ mice (two-way ANOVA, followed by Holm–Sidak test for post hoc multiple comparisons).

Figure 11 shows a strongly enhanced increase of myocardial contractility in PI3K γ -knockout mice (PI3K $\gamma^{-/-}$) 3 h after LPS, while wild type mice exhibited a marked reduction of myocardial contractility. In line with this, hemodynamic consequences have been verified since alterations in cardiac output reflect the opposing myocardial reactions in wild type and PI3K $\gamma^{-/-}$ mice (Table. 8). In order to verify the importance of lipid kinase-dependent or -

independent signaling reactions for the observed hypercontractility in PI3K γ ^{-/-} mice we studied the response to LPS in lipid PI3K γ ^{KD/KD} mice. In these mice, LPS-induced myocardial depression was comparable to wild-type mice indicating that the scaffold protein activity of PI3K γ was able to compensate the disturbed myocardial function early in the development of SIRS-induced SIMD.

Consequently, we asked for possible PI3K γ dependent differences in β -adrenergic signaling mainly responsible for myocardial contractility control. Comparative investigations of PI3K γ ^{-/-} and PI3K γ ^{KD/KD} mice clearly indicate lipid kinase independence of the opposing effects on myocardial contractility early after LPS administration and suggest the known PI3K γ 's scaffold function and potentially concomitant effects on cAMP signaling as a major cause for increased myocardial contractility in PI3K γ deficiency (Fig. 5).

At 24h, although the contractility in PI3K γ ^{-/-} was still higher than in WT and PI3K γ ^{KD/KD}, a drastic reduction in PI3K γ ^{-/-} was intriguingly observed. More intriguingly, the depression inexistent in PI3K γ ^{-/-} mice (hypercontractility) after 3h LPS appears from 3h to 24h and even higher than WT and PI3K γ ^{KD/KD} mice. These observations in PI3K γ ^{-/-} mice clearly suggest additional mechanism(s) able to negatively control the contractility that could be extra- or intra-cardially. However, the evaluation of hemodynamics parameters including cardiac output (CO) and arterial blood pressure (ABP) (Table 8) revealed that the reduced contractility did not markedly compromise systemic hemodynamics. Therefore, disturbed myocardial perfusion can be excluded, thus, intrinsic myocardial factors and/or autonomic nervous system (ANS) de-regulatory effects are suggested.

Three days after LPS, the observed myocardial depression, detected in PI3K γ ^{-/-} mice 24h after LPS administration, was more pronounced while WT and PI3K γ ^{KD/KD} displayed at this time point an increase contractility compared to 24h. More interestingly, the contractility was completely rescued in WT and PI3K γ ^{KD/KD} mice 1 week after LPS administration, while PI3K γ ^{-/-} mice still display a slightly but significant reduction in contractility compare to control (Fig. 11).

Table 8: Hemodynamic parameters and indices of systolic and diastolic function

		Control		LPS 3h		LPS 24h		LPS 3 days		LPS 7 days	
		WT	PI3K γ ^{-/-}	WT	PI3K γ ^{-/-}	WT	PI3K γ ^{-/-}	WT	PI3K γ ^{-/-}	WT	PI3K γ ^{-/-}
Blood pressure _{sys} (mmHg)	WT	93 ± 6	94 ± 6	94 ± 6	94 ± 8	83 ± 8*	82 ± 5*				
	PI3K γ ^{-/-}	90 ± 4	94 ± 5	88 ± 7 [§]	70 ± 8*						
	PI3K γ ^{KD/KD}	85 ± 5	93 ± 4	86 ± 8* [§]	79 ± 9*	82 ± 6					
Cardiac output (μL/min)	WT	15.0 ± 3.1	12.5 ± 3.1	8.7 ± 2.0*	16.9 ± 1.0	16.4 ± 2.6					
	PI3K γ ^{-/-}	15.0 ± 3.2	12.3 ± 3.2	8.9 ± 2.0*	17.0 ± 1.2	16.8 ± 2.7					
	PI3K γ ^{KD/KD}	14.8 ± 3.4	13.2 ± 4.9	9.0 ± 2.1*	15.8 ± 3.4	16.3 ± 2.5					
Ejection fraction (%)	WT	64 ± 8	48 ± 7* [§]	39 ± 7*	64 ± 6	66 ± 9					
	PI3K γ ^{-/-}	63 ± 11	60 ± 8	46 ± 4*	58 ± 6	64 ± 4					
	PI3K γ ^{KD/KD}	63 ± 7	46 ± 6* [§]	39 ± 11*	63 ± 6	65 ± 6					
Tau (ms)	WT	5.2 ± 1.1	7.7 ± 2.6*	12.5 ± 2.7*	6.9 ± 1.7	5.5 ± 0.5					
	PI3K γ ^{-/-}	5.8 ± 0.6	5.6 ± 2.1 [§]	5.7 ± 1.3 [§]	8.3 ± 1.6*	7.0 ± 1.3					
	PI3K γ ^{KD/KD}	4.8 ± 0.4	6.7 ± 2.3	7.4 ± 2.0* [§]	7.7 ± 2.0*	6.3 ± 1.5					

(Values are given as means ± SD, * $P < 0.05$, § significant difference vs. control; § significant difference vs. wild type (WT) mice; § significant difference vs. PI3K γ ^{-/-} mice, respectively.)

3.2 Effect of LPS-induced SIRS on cardiac ANS regulation and catecholamine release

In order to verify PI3K γ dependent effects of LPS-induced SIRS on cardiac ANS regulation heart rate and indices of heart rate variability as well as cardiac catecholamine content was evaluated by telemetric data recording and heart tissue analysis.

As shown in Figure 12 early enhanced activation of the cardiac sympathetic tone with increased tachycardia (A), reduced heart rate variability (B), and elevated catecholamine release (D), as well as shifted sympathico-vagal balance (C) indicate fast SIRS response after intraperitoneal LPS administration (10 mg/kg). Alteration of telemetric parameters persisted for at least 3 days, but the PI3K γ dependent reverse myocardial and hemodynamic response early after intraperitoneal LPS challenge was clearly caused by different intrinsic myocardial factor. Furthermore, the anticipated marked increase of sympathetic activation early after LPS administration was quite similar in wildtype and PI3K γ -mutant mice used.

The extent of tachycardia as well as the alteration of the obtained HVR indices demonstrates a similar enhancement of sympathetic input to the heart in all genotypes. In addition, the increased myocardial catecholamine content as well as myocardial β 2-adrenoreceptor expression and trafficking (Fig. 12E, Fig. 14) early after intraperitoneal LPS challenge were largely comparable. As shown in Figure 12D, PI3K γ ^{-/-} mice displayed enhanced myocardial contractile responsiveness on intravasal NE stimulation indicating upregulation of β -adrenergic signaling.

Together, the comparison of PI3K γ ^{-/-} and PI3K γ ^{KD/KD} mice regarding myocardial responsiveness clearly indicates lipid kinase independence of the observed effect on myocardial contractility early after LPS administration and suggest the known PI3K γ scaffold function and potentially concomitant effects on cAMP signaling as a major cause for increased myocardial contractility in PI3K γ deficiency.

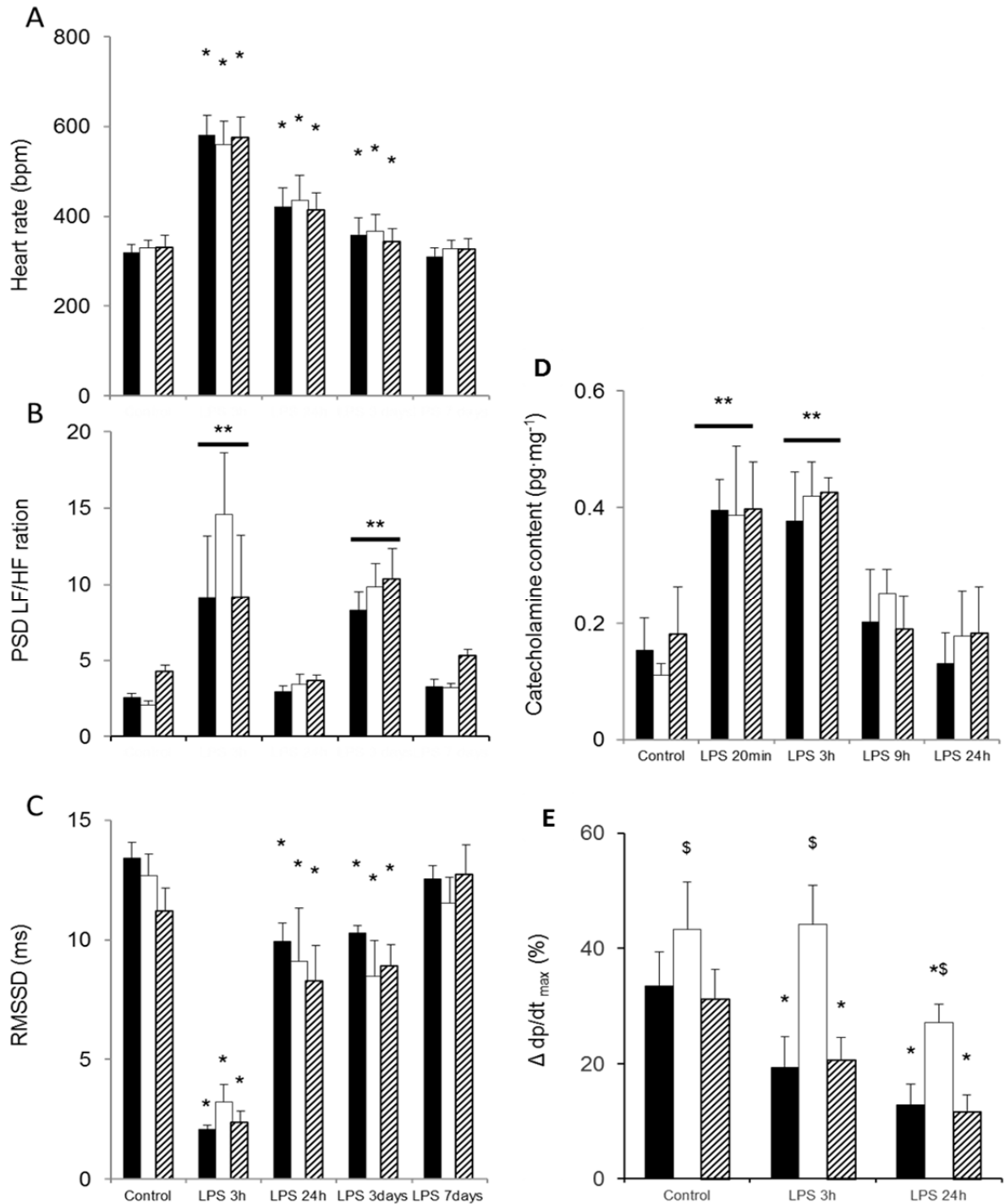


Figure 12: ANS control on heart function measured by telemetric assessment (A-C, n=8-10 per group and time point), heart tissue analysis of catecholamine content (D, n=3-4 per group and time point) and myocardial contractile responsiveness (E, n=4 per group and time point) in wild-type (black columns), PI3K $\gamma^{-/-}$ (open columns) and PI3K $\gamma^{KD/KD}$ mice. Values are mean + SD. *[§] p < 0.05, * significant difference between the control and LPS stimulation, [§] significant differences to wild-type mice (two-way ANOVA, followed by Holm-Sidak test for post hoc multiple comparisons).

3.3 Loss of PI3K γ scaffold function activates myocardial Ca²⁺ trafficking by increased intracellular cAMP

Cyclic adenosine monophosphate (cAMP), the key second messengers or effector involved in regulation of β -adrenergic pathway is generated upon engagement of β -AR/Gs-triggered stimulation of adenylyl cyclase, leading to the activation of protein kinase A (PKA), which in turn controls myocardial contractility (Kerfant et al. 2006, Xiang und Kobilka 2003). In order to verify mechanisms underlying the lipid kinase-independent effects of PI3K γ on myocardial contractility, we used primary cardiomyocytes derived from wild type (PI3K $\gamma^{+/+}$),

PI3K $\gamma^{-/-}$ and PI3K $\gamma^{KD/KD}$ mice and asked for PI3K γ -dependent effects of enhanced β -adrenergic stimulation that occurs in SIRS.

Therefore, first the level of cAMP was quantified after stimulation (NE) of cardiomyocytes obtained from wildtype (PI3K $\gamma^{+/+}$), PI3K $\gamma^{-/-}$ and PI3K $\gamma^{KD/KD}$ mice.

Since the beta-adrenergic pathway is the main pathway driving myocardial inotropic function (Bers 2002, Katz und Lorell 2000), we investigate the β 2-adrenergic pathway regarding the availability of cAMP, the expression of β 2--adrenergic receptor, the activity of phosphodiesterase and the Ca²⁺ trafficking fluxes.

3.3.1 PI3K γ dependent cAMP availability

Cycle adenosine monophosphate (cAMP), as the main effector of the beta-adrenergic pathway, was quantified in primary adult cardiomyocytes. We confirmed in this cell culture approach previous findings from heart tissue extracts that PI3K γ deficiency results in enhanced intracellular cAMP content, whereas loss of lipid kinase activity of PI3K γ displays similar cAMP levels like cardiomyocytes derived from wildtype mice (Fig. 13). Furthermore, NE stimulation provoked a rather long-lasting (up to 3h in our setting) increase of cAMP in PI3K γ deficient cardiomyocytes, whereas β -adrenergic stimulation failed to enhance cAMP levels in PI3K $\gamma^{+/+}$ and PI3K $\gamma^{KD/KD}$ cardiomyocytes.

These data confirm the role of PI3K γ 's scaffold function in the down-regulation of the beta-adrenergic pathway. Intriguingly, LPS-induced upregulation of PI3K γ expression (Fig. 21) suggests an enhanced contribution of PI3K γ -mediated control of cellular cAMP under the condition of SIRS.

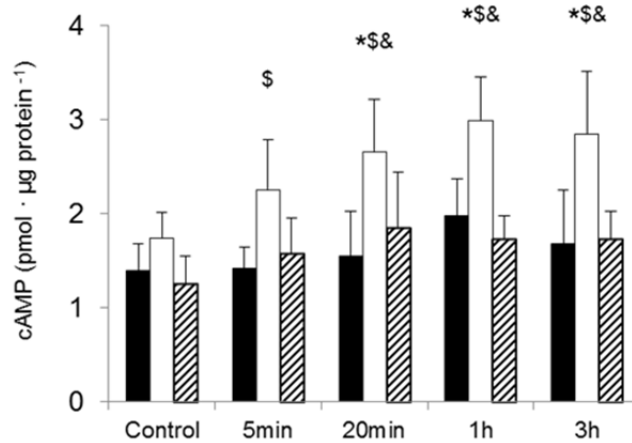


Figure 13: cAMP availability in cardiomyocytes (n=5 per group and time point) in wild-type (black columns), PI3K γ ^{-/-} (open columns) and PI3K γ ^{KD/KD}. Cardiomyocytes derived from PI3K γ ^{-/-} mice display during β -adrenergic activation an enhanced and prolonged cAMP-mediated signaling.

Values are mean + SD. * $\$&$ p < 0.05, * significant difference vs. control, \$ significant difference to wild-type cardiomyocytes, & significant difference to PI3K γ ^{KD/KD} cardiomyocytes, (two-way ANOVA, followed by Holm–Sidak test for post hoc multiple comparisons).

3.3.2 PI3K γ dependent β -adrenergic receptor desensitization

Desensitization of plasma membrane β -adrenergic receptors (β AR) has been reported to be associated with the cAMP levels. The molecular mechanisms underlying rapid β AR desensitization do not require just internalization of the receptors, but also initial interruption of β AR-functioning by receptor uncoupling from the stimulatory G protein (G_s). Phosphorylation of β AR by at least two kinases, PKA and the GRK kinase (G protein-coupled receptor kinase) at serine-355 and -356 are pivotal to GRK-mediated desensitization, β -arrestin binding, and internalization of β ARs (Vaughan et al. 2006, Hausdorff et al. 1990) Therefore, both PI3K γ dependent phosphorylation and total expression of β 2-adrenergic receptor was evaluated by Western blot.

We found that, β 2-AR phosphorylation (Ser 355, 356) indicating receptor desensitization was enhanced early after NE+Cyt stimulation onset (up to 3h) in wt cardiomyocytes while PI3K γ ^{-/-} cardiomyocytes showed attenuated receptor phosphorylation (Fig. 14A). PI3K γ ^{KD/KD} cardiomyocytes displayed similar behavior as wt cardiomyocytes indicating the scaffold function of PI3K γ in the receptor desensitization is relevant. These findings are in line with a previous report on the role of scaffold proteins in organizing receptor-initiated signaling pathways involving GRK leading to the receptor phosphorylation (Hall und Lefkowitz 2002). Furthermore, data support the suggested role of PI3K γ (as well as other PI3Ks) as a main contributor via protein-protein interaction to the activity of GRK (Nienaber et al. 2003). Total β 2-

AR expression remained constant after NE+Cyt stimulation in PI3K γ ^{-/-} cardiomyocytes for up to 24 h, whereas WT and PI3K γ ^{KD/KD} displayed gradual downregulation (Fig. 14B). These finding indicates the consequence of the verified receptor phosphorylation as a regulator for internalization (with possible deterioration). The better conservation of the receptor level in PI3K γ ^{KD/KD} cardiomyocytes (compared to wt) indicates the contribution of PIP₃ to the internalization process (deterioration) as previously reported (Perino et al. 2011).

Figure 14: Expression and phosphorylation of β 2-adrenergic receptor (β 2-AR) on cardiomyocytes derived from wild-type (wt, black columns), PI3K γ ^{-/-} (open columns) and PI3K γ ^{KD/KD} cells under baseline conditions (Control) and after stimulation with norepinephrine (30 μ M) and a mixture of TNF α and IL β 1 (Cyt). (A): quantification (n=3 per group and time point) and representative blot of Phospho β 2-AR at serine 355 and 356 in cardiomyocytes. (B): quantification (n=3 per group and time point) and representative blots of total β 2-AR expression in cardiomyocytes.

Values are mean + SD. *^s p < 0.05, * significant difference between the control and NE+Cyt stimulation, ^s significant difference to wild-type cardiomyocytes (two-way ANOVA, followed by Holm–Sidak test for post hoc multiple comparisons).

Together, these findings showed the contribution of PI3K γ in the regulation of the receptor-initiated step of the β 2-AR signaling pathway via desensitization and downregulation of β 2-AR.

3.3.3 PI3K γ dependent control of myocardial phosphodiesterase activity and control of the contractility pathway.

Cyclic nucleotide phosphodiesterases (PDEs) are enzymes that regulate intracellular cAMP levels. Studies using transgenic mice in combination with family-specific PDE inhibitors have demonstrated that PDE3 and PDE4 isoforms regulate cardiac contractility by modulating cAMP levels in various subcellular compartments (Beca et al. 2011). Therefore, we verify using a pharmacological approach the influence of these PDEs on β -AR mediated phospholamban phosphorylation as a verified readout for enhanced β -AR signaling resulting in improved myocardial contractility.

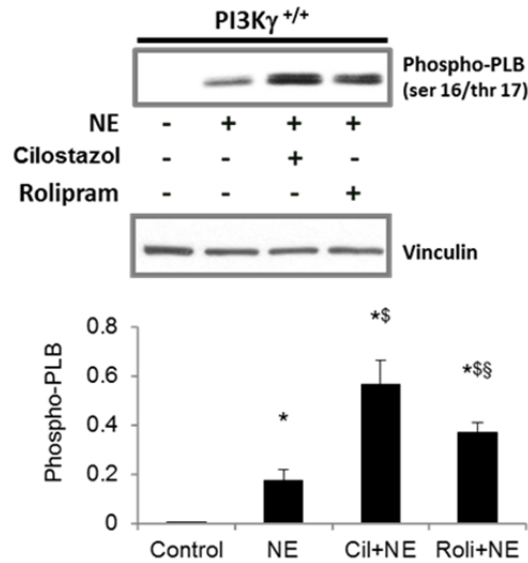


Figure 15: Influence of PDE3 and PDE4 on β -AR signaling in wild-type cardiomyocytes. Note the effect on phospholamban phosphorylation (Phospho-PLB) by stimulation with norepinephrine ($30\mu\text{M}$) alone or with pharmacological PDE3 (cilostazol, Cil, $1\mu\text{M}$, administration 1h before NE stimulation) and PDE4 (rolipram, Roli, $1\mu\text{M}$, administration 1h before NE stimulation), respectively.

Values are mean + SD. *^{§§} $p < 0.05$, * significant difference compared to control, § significant difference to NE stimulation, § significant difference compared to NE+Cil. (Two-way ANOVA followed by Holm–Sidak test for post hoc multiple comparisons).

Pharmacological PDE3 inhibition induced in primary adult cardiomyocytes a marked enhancement of the stimulated β -AR pathway by a factor of about 3 whereas PDE4 inhibition was slightly less effective (Fig. 15). These data verified previous findings (Kerfant et al. 2006, Perino et al. 2011) that PI3K γ controls during enhanced β -adrenergic activation the extent of myocardial excitation–contraction coupling via Ca^{2+} trafficking by appropriated cAMP degradation.

3.3.4 PI3K γ dependent control of intra cardiomyocytes Ca^{2+} trafficking Cardiac contraction results from calcium-dependent interaction of myosin and actin myofilaments. Decisive prerequisite for effective cardiac excitation–contraction coupling resulting in appropriate contraction force exhibits a fast and nearly complete cytosolic Ca^{2+} removal during diastole and in turn a fast Ca^{2+} entry from sarcoplasmic reticulum (SR) and extracellular space. Cyclic storage/release of Ca^{2+} via SR represents a main part of total Ca^{2+} flux (75-90%) throughout cardiac contraction/relaxation cycle and is controlled by the phosphorylation

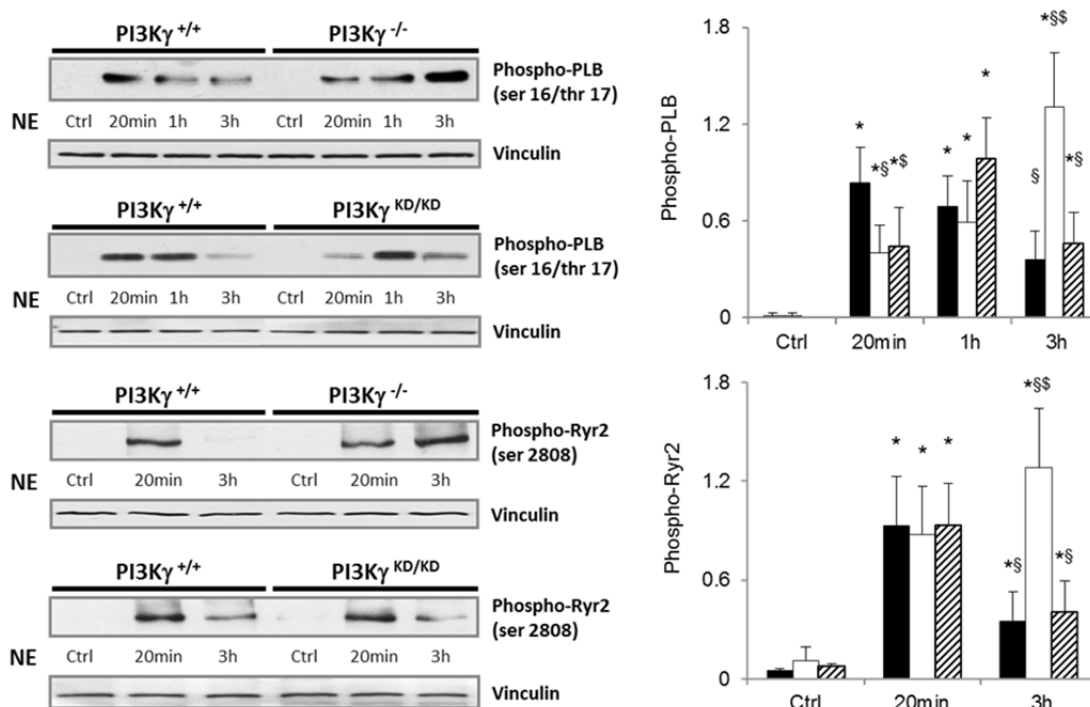


Figure 16: Cardiomyocytes derived from PI3K γ ^{-/-} mice displayed during β -adrenergic activation a pronounced ryanodine receptor (Ryr) and phospholamban (PLB) phosphorylation early after LPS-induced SIRS (right panel). Norepinephrine (NE, 30 μ M) stimulation led in PI3K γ ^{-/-} cardiomyocytes to sustained and enhanced sarcoplasmic reticulum calcium trafficking indicated by reinforced ryanodine receptor phosphorylation (Phospho-Ryr2) and phospholamban phosphorylation (Phospho-PLB). In contrast, wild-type (PI3K γ ^{+/+}) and lipid-kinase dead (PI3K γ ^{KD/KD}) cardiomyocytes responded with restraint β -adrenergic signaling leading to Phospho-Ryr2/ Phospho-PLB downregulation after short-time activation (left panel). Values are mean + SD. * $\&$ $\&$ p < 0.05, * significant difference vs. control, $\&$ significant difference to wild-type cardiomyocytes, $\&$ significant difference to PI3K γ ^{KD/KD} cardiomyocytes, $\&$ significant difference to “20 min” (two-way ANOVA, followed by Holm–Sidak test for post hoc multiple comparisons).

status of both the ryanodine receptor (Ryr, Ca²⁺ release channel) and phospholamban (PLB, modulate Ca²⁺ reuptake via sarco/endoplasmic reticulum Ca²⁺-ATPase (SERCA) into SR) (Bers 2002). Ryr and PLB are both downstream targets of cAMP/PKA (at serine 2808 for Ryr and serine 9 for PLB) (Braunwald 2013, Katz und Lorell 2000). Therefore, the phosphorylation status of Ryr and PLB represent suitable marker for Ca²⁺ trafficking fluxes. Thus, PI3K γ dependent Ryr and PLB activation by β -AR stimulation was investigated.

As anticipated we verified in cardiomyocytes derived from PI3K γ ^{-/-} mice an enhanced and prolonged cAMP-mediated signaling via protein kinase A (PKA) activation with pronounced ryanodine receptor (RyR) and phospholamban (PLB) phosphorylation (Fig. 16), indicative for

accelerated intracellular Ca^{2+} trafficking leading to improved myocardial excitation–contraction coupling (Bers 2002).

3.4 Delayed myocardial depression after LPS administration in PI3K γ deficiency is iNOS mediated

Measurements of LV contractile function in the intact heart revealed PI3K γ -dependent effects on dynamics and time course of LPS-induced myocardial response. Specifically, contractility of PI3K γ -deficient mice showed a markedly increased LV contractility early after LPS administration. Furthermore, LV contractility was progressively compromised up to marked myocardial depression at 24 hours prolonged to three days with a decline percentage from 3h higher than in wild type and PI3K $\gamma^{\text{KD/KD}}$ mice (Fig. 11). Because LPS-induced myocardial depression can be mediated by a multitude of factors including ANS disturbances and circulatory dysregulation, which were obviously not responsible for amount and genotype-specific response in our studies (Fig. 12), other influences has to be considered. Therefore, we checked for apoptosis and necrosis, signs for fibrosis and leukocyte invasion as well as other indicators for enhanced myocardial inflammation (Konstantinidis et al. 2012). Microscopic evaluation of cardiac tissue provided just distinct histological effects over time of observation including a slightly enhanced number of apoptotic cells, no signs for necrosis or fibrosis and a temporarily increased number of leukocytes three days after LPS injection (Table 9). However, data did not explain pronounced and prolonged cardiac depression. Therefore, we asked for reasons inherent in cardiomyocytes which may be responsible for compromised myocardial function. We screened for known inflammatory responses in heart tissue accompanied by compromised myocardial performance and cytokines/iNOS pathway was suspected giving the frequent reported involvement of this route in the myocardial depression and it high negative inotropic effect.

Table 9: Cell death, Inflammatory cells infiltration, morphological and structural changes

Groups	Tunel	Necrosis	Contracture ligaments	Myophago-cytosis	Leukocytes	Endothelial swelling	Fibrosis
Control	PI3K ^y ^{+/+}	No	No	No	No	No	No
	PI3K ^y ^{-/-}	No	No	No	No	No	No
	PI3K ^y ^{KD/KD}	No	No	No	No	No	No
LPS 24 hours	PI3K ^y ^{+/+}	Moderate	No	No	Low	Yes	No
	PI3K ^y ^{-/-}	Moderate	No	No	Low	Yes	No
	PI3K ^y ^{KD/KD}	Moderate	No	No	Low	Yes	No
LPS 3 days	PI3K ^y ^{+/+}	low	No	No	Moderate	Yes	No
	PI3K ^y ^{-/-}	low	No	No	Stronger	Yes	No
	PI3K ^y ^{KD/KD}	low	No	No	Moderate	Yes	No
LPS 1 week	PI3K ^y ^{+/+}	No	No	No	No	Yes	No
	PI3K ^y ^{-/-}	No	No	No	No	Yes	No
	PI3K ^y ^{KD/KD}	No	No	No	No	Yes	No

3.4.1 PI3K γ dependent iNOS expression in cardiac depression

iNOS is recognized as one of the most important depressing factor produced during inflammation in cardiac tissue (Kohr et al. 2012). We therefore investigated the expression of iNOS in cardiac tissue after LPS treatment by immunohistochemistry.

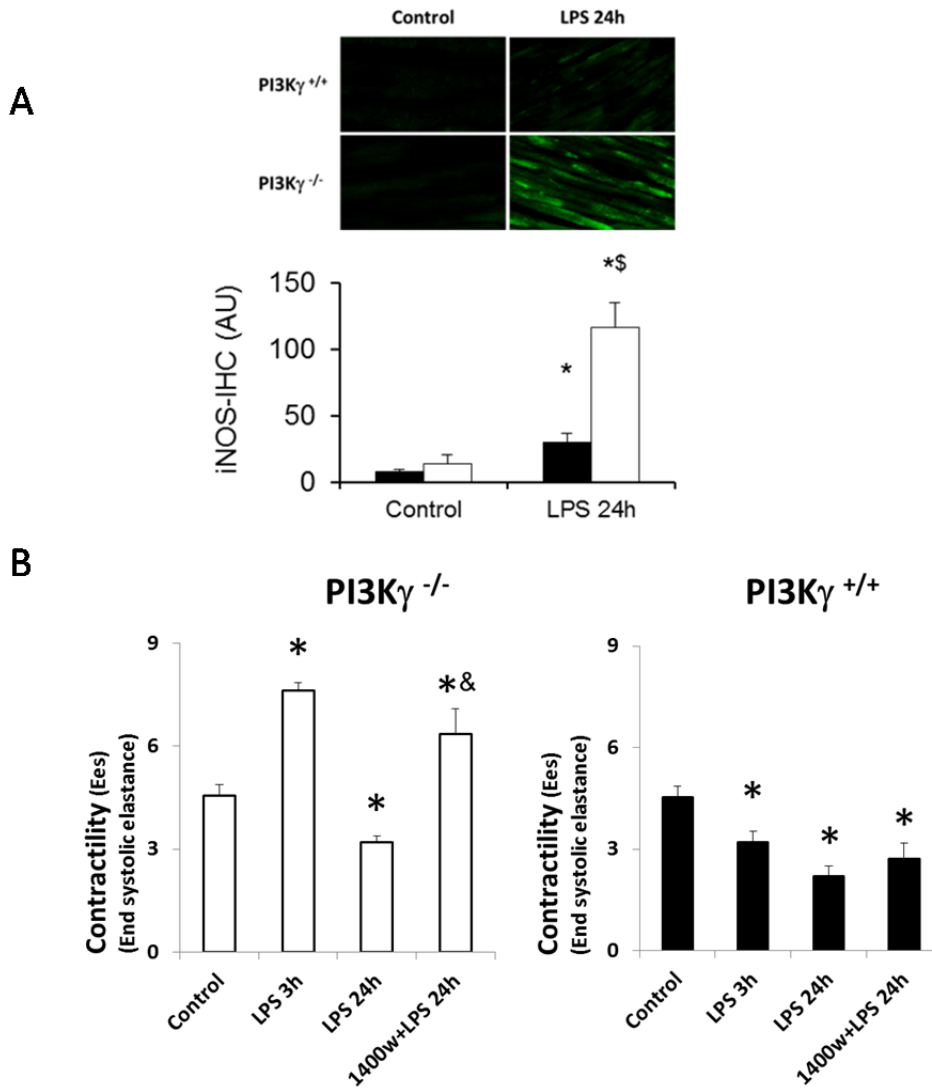


Figure 17: Loss of PI3K γ results in enhanced iNOS expression in cardiac tissue in consequence of sustained proinflammatory stimuli after LPS administration and appears to be responsible for delayed myocardial depression. (A): Top panel: Representative image of iNOS expression in paraffin-embedded cardiac tissue of wild-type (black columns) and PI3K γ ^{-/-} (open columns) mice after intraperitoneal injection of LPS (10mg/kg bw). Bottom panel: Fluorescence intensity of iNOS expression (n=4 at each group and time point). (B): myocardial contractility (Ees) in wild-type (black columns) and PI3K γ ^{-/-} (opens columns) mice 3h and 24 h after intraperitoneal injection of LPS alone or 24h after LPS in addition with 1400w (selective inhibitor of iNOS) at 10mg/kg bw (n=6 at each group and time point).

Values are mean + SD. *^{s&} p < 0.05, * significant difference vs. control, ^s significant difference to wild-type cardiomyocytes, & significant difference to “LPS 24h” (two-way ANOVA, one-way ANOVA, followed by Holm–Sidak test for post hoc multiple comparisons).

In the cardiac tissue, the expression of iNOS after LPS treatment was markedly increased in PI3K γ ^{-/-} mice while wild type showed a weak increase (Fig. 17A). Furthermore, the observed genotype-specific difference in iNOS expression was in accordance with the observed genotype-specific depression differences in heart contractility (Fig. 11). Interestingly, suggestion of causal relation between increased iNOS expression and markedly depressed LV contractility 24h after LPS administration in PI3K γ ^{-/-} mice has been further substantiated, because an iNOS inhibition rescued cardiac function (Fig. 17B).

These data strongly suggest and support that iNOS appears to be responsible for massive myocardial depression observed in PI3K γ ^{-/-} mice after 24h LPS. Therefore, the involvement of PI3K γ in the regulation of iNOS is clearly suggested.

3.4.2 PI3K γ and iNOS expression in cardiomyocyte

Following the previous observation, we asked for the contribution of cardiomyocyte in the expression of iNOS and furthermore the contribution of PI3K γ in this expression at cardiomyocyte level. Mechanistic experiments in cardiomyocytes were performed regarding the expression of iNOS.

We first found in cell culture investigations on primary cardiomyocytes that the expression of iNOS could be induced by LPS as well as single cytokines including TNF α and IL-1 β , but the mixture of these components induces the highest response (Fig. 18A). Next, profound and long-lasting upregulation of iNOS expression in PI3K γ ^{-/-} mice was observed, whereas wildtype cells showed just a weak induction of iNOS expression corroborating our previous observations in heart tissue and therefore indicating and confirming the sustained contribution of PI3K γ on regulation of iNOS expression at the cardiomyocyte level under inflammatory conditions (Fig. 18B). Furthermore, PI3K γ ^{KD/KD} cells displayed a weak iNOS expression compared to PI3K γ deficient mice (Fig. 18B). Therefore data revealed that the impact of PI3K γ on iNOS regulation is kinase independent (scaffold).

These findings indicate that iNOS upregulation induced by stimulation with a LPS/proinflammatory cytokine (PIC) mixture mimicking early SIRS conditions is regulated by PI3K γ 's scaffold function.

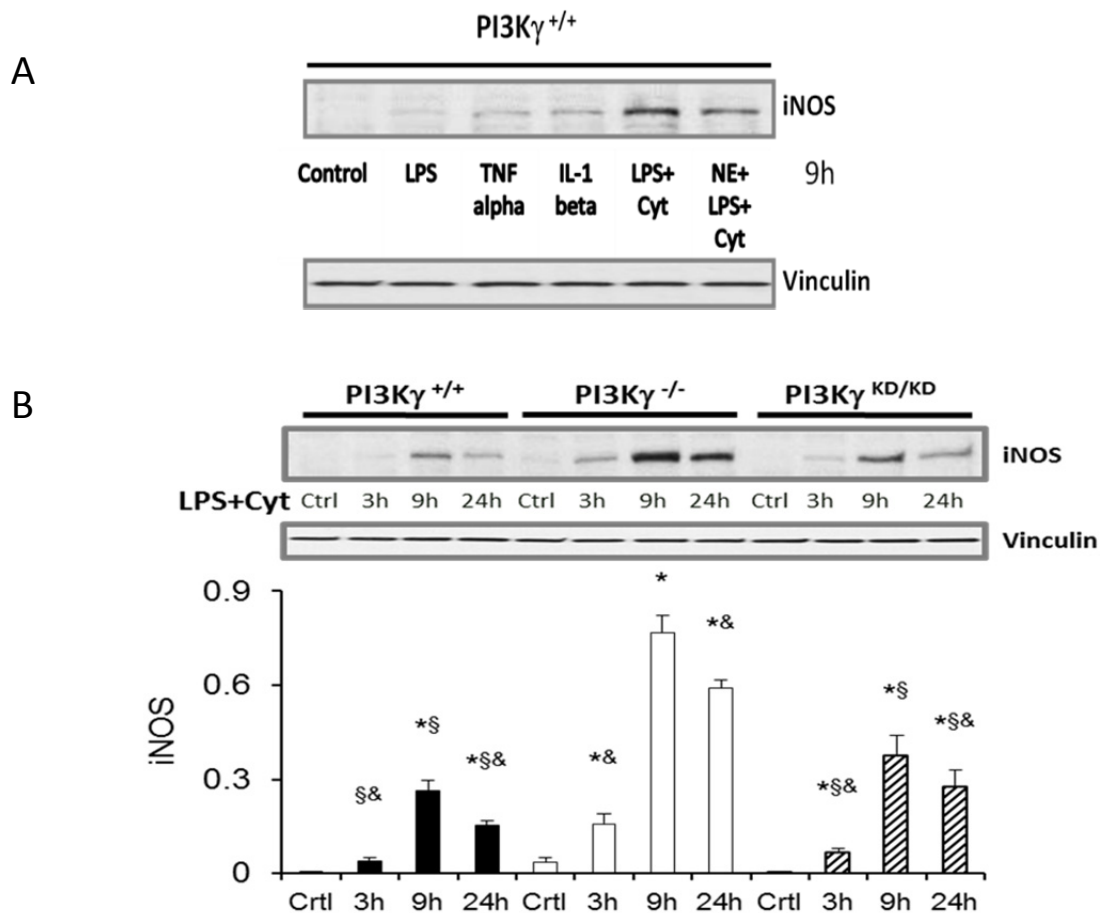


Figure 18: Loss of PI3K γ results in enhanced iNOS expression in cardiomyocytes in consequence of sustained proinflammatory stimuli and appears to be PI3K γ 's scaffold function related. (A): Representative western blot (7.5% SDS-Page) of iNOS in primary cardiomyocytes isolated from wild-type and stimulated with different stimuli showing an optimal iNOS expression using the mixture LPS+Cyt (LPS=1 μ g/ml; Cyt: TNF α =50ng/ml + IL-1 β =50ng/ml). (B): Representative western blot (7.5% SDS-Page) and densitometric quantification (normalized to vinculin) of iNOS in primary cardiomyocytes isolated from wild-type (PI3K γ ^{+/+}), PI3K γ ^{-/-} and PI3K γ ^{KD/KD} mice and stimulated with LPS+Cyt for indicated times (n=4 at each group and time point). Note that this response was markedly enhanced in cells derived from PI3K γ ^{-/-} mice. Wild-type (black columns), PI3K γ ^{-/-} (open columns) and PI3K γ ^{KD/KD} (hatched columns). Values are mean + SD. * $\&$ § $\#$ p < 0.05, * significant difference vs. control, § significant difference to PI3K γ ^{-/-} cardiomyocytes, & significant difference to "9h", (two-way ANOVA), followed by Holm-Sidak test for post hoc multiple comparisons).

3.4.3 iNOS and Ca²⁺ trafficking in PI3K γ ^{-/-} cardiomyocytes

To confirm and evaluate the causal contribution of iNOS in myocardial depression of PI3K γ ^{-/-} mice, an experimental system was established using PLB phosphorylation as an indicator for intracellular Ca²⁺ trafficking. Thus, stimulation by NE was compared to

NE/LPS/PIC to see the effect of inflammation of the Ca²⁺ trafficking and, a highly selective inhibitor of iNOS was used for confirmation.

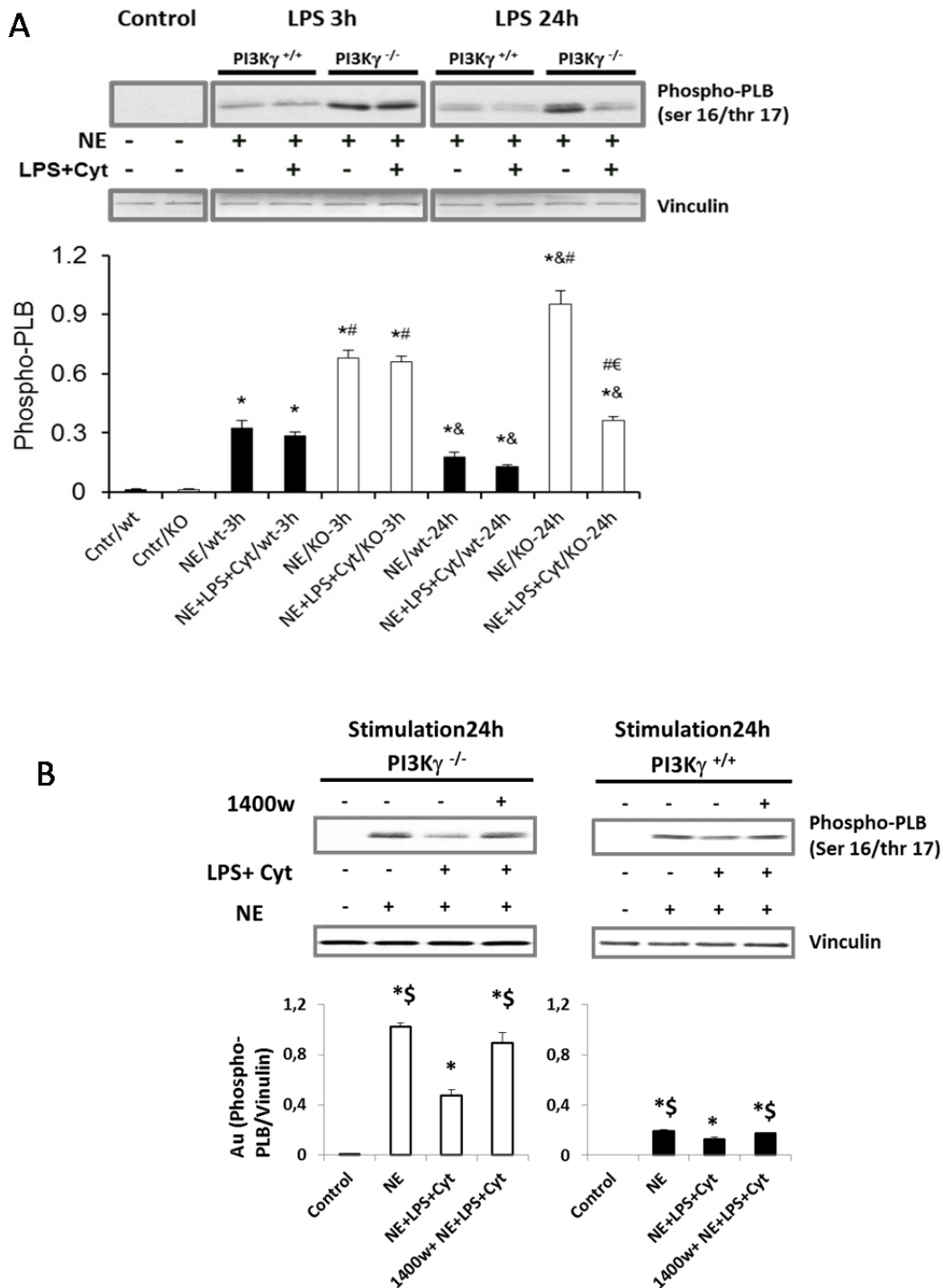


Figure 19: Enhanced iNOS expression in PI3K γ deficient cardiomyocytes in consequence of sustained proinflammatory stimuli appears to be responsible for delayed myocardial depression. (A): Inflammation-induced iNOS upregulation led to phospholamban (PLB) phosphorylation suppression (after 24h) during β -adrenergic activation (NE, 30 μ M). (Top panel: Representative western blot (10% SDS-Page) of phospholamban phosphorylation after NE (30mM) and NE + LPS+Cyt (LPS=1 μ g/ml; Cyt: TNF α =50ng/ml + IL-1 β =50ng/ml) of primary cardi-

omyocytes isolated from wild-type ($PI3K\gamma^{+/+}$) and $PI3K\gamma^{-/-}$ mice. Bottom panel: densitometric quantification of phospholamban phosphorylation normalized to vinculin (n=4 at each group and time point). (B): Pharmacological iNOS inhibition (1400w, ##) rescued suppressed PLB phosphorylation. (Top panel: Representative western blot of Phospho-PLB in primary cardiomyocytes treated with NE (30 μ M), NE + LPS+Cyt (LPS=1 μ g/ml; Cyt: TNF α =50ng/ml + IL-1 β =50ng/ml) or NE + LPS+Cyt, after pretreatment with 1400w (highly selective iNOS inhibitor, 40 μ M), respectively. Bottom panel: Densitometric quantification of iNOS (normalized to vinculin, n=3 at each group and time point)).

Values are mean + SD. *\$&# p < 0.05, * significant difference vs. control, wild-type cardiomyocytes, & significant difference to “3h” (in A), \$ significant difference to “NE+LPS+Cyt” (in B), # significant difference between wild-type and $PI3K\gamma^{-/-}$ cardiomyocytes at same treatment and time-point (two-way ANOVA, one-way ANOVA (D), followed by Holm–Sidak test for post hoc multiple comparisons).

PLB phosphorylation as an indicator for efficiency of intracellular Ca^{2+} -trafficking in cardiomyocytes was activated quite similarly by NE and a NE/LPS/PIC mixture early after application (3h), whereas the extent of stimulation up to 24h has shown markedly enhanced difference in $PI3K\gamma^{-/-}$ cardiomyocytes (Fig. 19A). Longer-lasting β -adrenergic stimulation led to a substantial Phospho-PLB downregulation in $PI3K\gamma^{+/+}$ cardiomyocytes, whereas additional LPS/PIC administration induced only a slight reduction. In contrast, NE stimulation provoked in $PI3K\gamma^{-/-}$ cardiomyocytes a further Phospho-PLB upregulation while LPS/PIC stimulation together with NE resulted in a massive downregulation of phosphorylated PLB (Fig. 19A). These observations appear to be in accordance with the pronounced iNOS upregulation in $PI3K\gamma^{-/-}$ cardiomyocytes.

In order to confirm that iNOS contribute significantly on the control of Ca^{2+} -trafficking fluxes via PLB activity, $PI3K\gamma^{-/-}$ cells were treated with a selective iNOS inhibitor (1400w) during NE/LPS/PIC stimulation. As shown in Figure 19B, iNOS inhibition rescued the previous Phospho-PLB downregulation.

Taking together, our data revealed a so far unknown but functionally important role of the $PI3K\gamma$'s scaffold function on intracellular Ca^{2+} -trafficking mediated by control of iNOS expression: Loss of $PI3K\gamma$ resulted in enhanced iNOS expression in cardiomyocytes in consequence of sustained proinflammatory stimuli after LPS administration and appears to be responsible for delayed myocardial depression in $PI3K\gamma^{-/-}$ mice.

3.5 Enhanced iNOS expression is mediated by NFAT activation in PI3K γ ^{-/-} cardiomyocytes

In order to bring more clarification for better understanding of PI3K γ 's implication on iNOS regulation, we checked in primary cardiomyocytes for transcriptional associated factors potentially regulated by PI3K γ . Therefore, activation of several transcriptional factors was evaluated using cells derived from wild type (PI3K γ ^{+/+}), PI3K γ ^{-/-} and PI3K γ ^{KD/KD} mice.

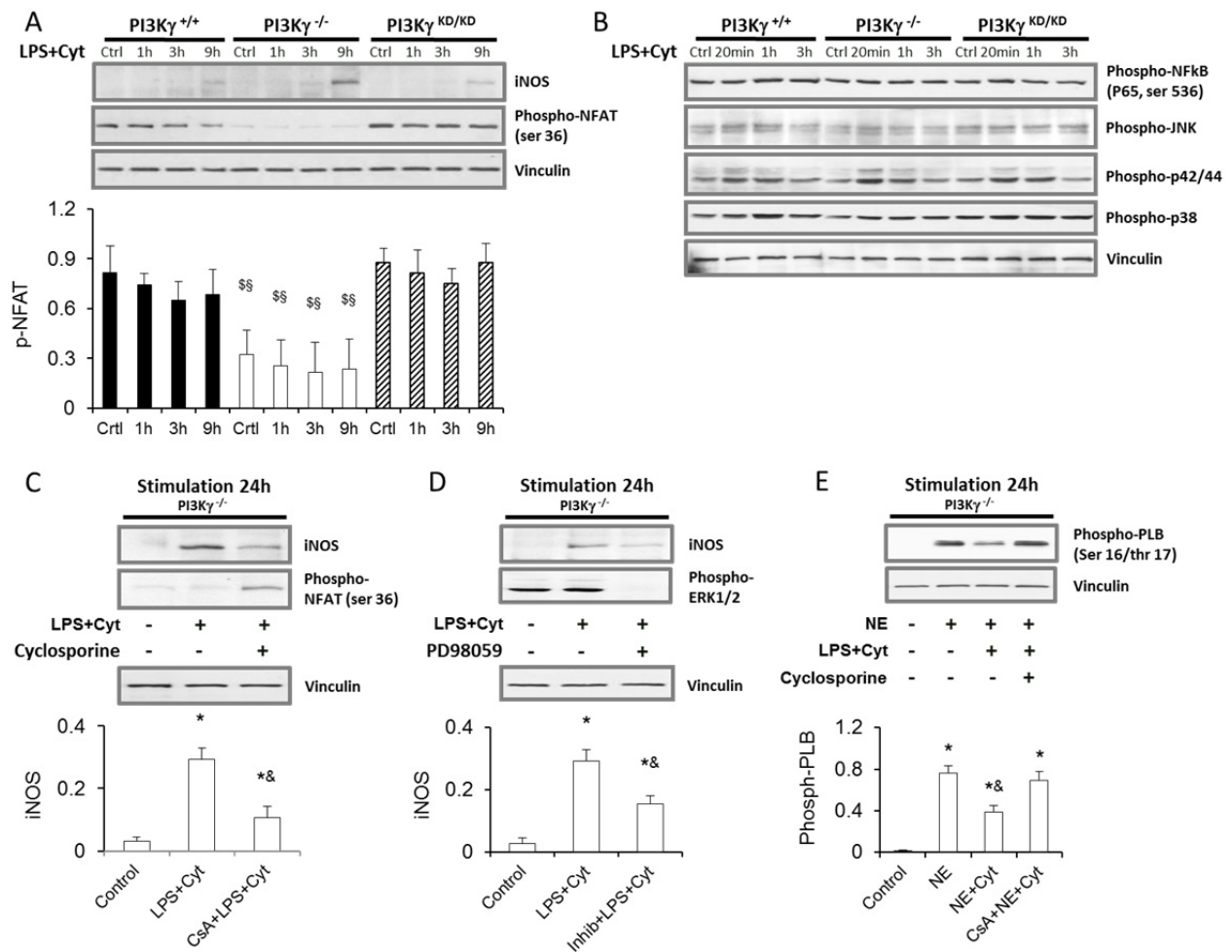


Figure 20: iNOS upregulation in PI3K γ ^{-/-} cardiomyocytes in consequence of sustained LPS/proinflammatory stimulation. (A) Primary cardiomyocytes showed a rising iNOS expression by LPS+Cyt stimulation, whereas the transcription factor NFAT displays permanent activation even under resting conditions. (A: Top panel: representative western blots (7.5% SDS-Page) of NFAT activation (dephosphorylation) in adult mice primary cardiomyocytes isolated from wild-type (PI3K γ ^{+/+}), PI3K γ ^{-/-} and PI3K γ ^{KD/KD} mice and stimulated with LPS+Cyt (LPS=1 μ g/ml; Cyt: TNF α =50ng/ml + IL-1 β =50ng/ml) for indicated times. Bottom panel: densitometric quantification of NFAT phosphorylation normalized to vinculin (n=4 at each group and time point). B: Top panel: representative western blots (7.5% SDS-Page) of

MAPKs (JNK, ERK1/2 and P38) and NFκB activation (phosphorylation) after LPS+Cyt stimulation of adult mice primary cardiomyocytes isolated from wild-type (PI3Kγ^{+/+}), PI3Kγ^{-/-} and PI3Kγ^{KD/KD} mice (n=3 at each group and time point). C: Top panel: representative western blots (7.5% SDS-Page) of iNOS and NFAT in PI3Kγ^{-/-} cardiomyocytes stimulated by LPS+Cyt (9h) without or with pretreatment (1h) with cyclosporine (NFAT inhibitor: 1μM). Bottom panel: densitometric quantification of iNOS expression intensity (n=4 at each group). D: Top panel: representative western blots (7.5% SDS-Page) of iNOS and ERK1/2 in PI3Kγ^{-/-} cardiomyocytes stimulated by LPS+Cyt (9h) without or with pretreatment (1h) with PD98059 (ERK1/2 inhibitor: 50μM). Bottom panel: densitometric quantification of iNOS expression intensity (n=4 at each group). E: Top panel: representative western blot (7.5% SDS-Page) of phosphorylated phospholamban (Phospho-PLB) in PI3Kγ^{-/-} cardiomyocytes stimulated by LPS+Cyt (24h) without or with pretreatment (1h) with cyclosporine (NFAT inhibitor: 1μM). Bottom panel: densitometric quantification of Phospho-PLB intensity (n=4 at each group). Note that iNOS upregulation requires co-operative activation of NFAT and AP-1. Values are mean + SD. *[&][&] p < 0.05, * significant difference vs. control, [&] significant difference to wild-type cardiomyocytes, [&] significant difference to PI3Kγ^{KD/KD} cardiomyocytes, & significant difference to “LPS+Cyt” (in C, D), to “NE” and to “CsA+NE+Cyt” (in E), (two-way ANOVA, one-way ANOVA (C-E), followed by Holm–Sidak test for post hoc multiple comparisons).

Whereas NFκB and MAP kinases upstream of AP-1 did not show considerable genotype-specific differences (Fig. 20B), NFAT was markedly activated by dephosphorylation in PI3Kγ^{-/-} cells compared to PI3Kγ^{+/+} and PI3Kγ^{KD/KD} cells (Fig. A). Pharmacological inhibition of NFAT with cyclosporine led to a markedly reduced iNOS expression (Fig. 20C) confirming the putative role of NFAT. Furthermore, NFAT-mediated iNOS upregulation is causally involved in LPS+Cyt-induced suppression of myocardial excitation–contraction coupling via reduced Ca²⁺ trafficking, as shown by rescued phospholamban (PLB) phosphorylation by cyclosporine (Fig. 20E). However, AP-1 via ERK1/2 inhibition (PD98059) led to iNOS downregulation (Fig. 20D) indicating the contribution of AP-1 in the mechanism leading to iNOS expression. In addition, the fact that NFAT was already activated in PI3Kγ^{-/-} cells at the basal condition strongly confirm the contribution of AP-1 for iNOS expression.

Together, these data clearly indicate that the massive increase expression of iNOS in PI3Kγ-deficient mice and cardiomyocytes required the co-operative activation of NFAT and AP-1. These findings indicate the important role of PI3Kγ in the regulation of NFAT and AP-1 cooperation via the regulation of NFAT.

3.6 Enhanced MMP9 expression in PI3Kγ deficient mice

We observed that the marked myocardial depression observed in PI3Kγ deficient mice after 24h LPS was not fully recovered at the end of the observation period (Fig. 11) suggesting

an ongoing inflammation-related alteration in cardiac tissue. In addition, a delay was observed regarding recovery in PI3K γ deficient mice at 7 days after LPS compared to wild type and PI3K γ ^{KD/KD} mice that displayed at this time point almost fully recovery contractility.

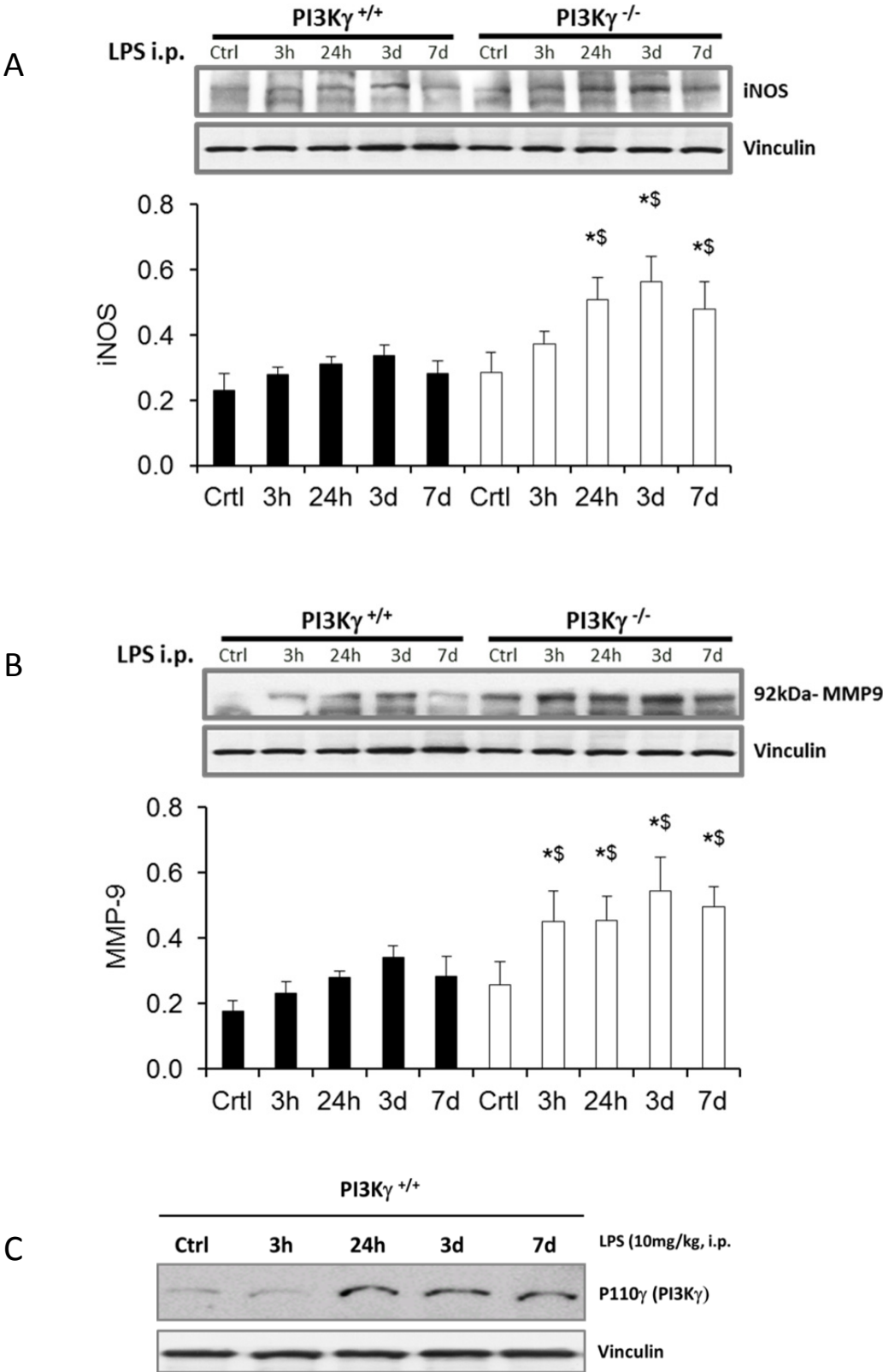


Figure 21: Long lasting iNOS expression in PI3K γ deficient mice after SIRS is associated with MMP9 expression and inflammation. Wild-type (black columns) and PI3K γ -deficient mice (PI3K γ ^{-/-}, open columns). (A): representative western blot (top panel) and quantification (bottom panel) of iNOS expression in cardiomyocytes isolated at indicated time after intraperitoneal injection of LPS (n=3 each group and time point). (B): representative western blot (top panel) and quantification (Bottom panel) of MMP9 expression in cardiomyocytes isolated at indicated time after intraperitoneal injection of LPS (n=3 each group and time point). (C): representative western blot of P110 γ (PI3K γ) at indicated time after intraperitoneal injection of LPS (n=3 each group and time point) Values are mean + SD. *[§]p < 0.05, * significant difference vs. control, § significant difference to wild-type cardiomyocytes (two-way ANOVA, followed by Holm–Sidak test for post hoc multiple comparisons).

These observations raised questions on possibly sustained negative effects for heart function due to prolonged proinflammatory activity of cardiomyocytes under PI3K γ deficiency. Therefore, we decided to investigate the long term (up to 1week) expression of iNOS as well as consecutive potential negative prognosis mediators including inflammation and MMPs. Using cardiomyocytes isolated from LPS -treated mice at indicated time, we found that the iNOS upregulation persisted in PI3K γ ^{-/-} cardiomyocytes up to 1 week with peak at 3 days (Fig. 21A). Consecutively, we found that MMP9 was similarly increased in PI3K γ ^{-/-} cells compared to wild type (Fig. 21B) suggesting a likely detrimental role of iNOS overexpression in the myocardium of PI3K γ deficient mice.

Finally, P110 γ displayed a long-lasting up-regulation in cardiomyocytes in consequence of LPS-induced SIRS (Fig 21C).

4. Discussion

In this study, we provide evidence that PI3K γ controls by its lipid kinase independent function proinflammatory disturbances of myocardial performance and the extent of inflammatory response in heart tissue in a mouse model of LPS generated SIRS. Indeed, in PI3K γ -deficient mice we found signs of myocardial overstimulation leading to an early hypercontractility state followed by an intensified proinflammatory response with sustained upregulation of iNOS and MMP expression in cardiac tissue with concomitantly depressed myocardial contractility until the third day after SIRS onset. In contrast, wildtype mice and mice expressing a catalytically inactive PI3K γ developed sustained SIMD early after LPS administration despite similarly increased catecholamine availability and a dampened cardiomyocytic inflammatory response. Therefore, scaffold function of PI3K γ appears to be crucial to preserve the heart against exaggerated immune response caused by infection/LPS induced SIRS.

Early systemic response on infection-related SIRS involves enhanced myocardial sympathetic activity, which is mainly delivered by norepinephrine released from cardiac sympathetic nerve endings as a result of increased sympathetic outflow from CNS driven by neurohumoral stimulation (Sternberg 2006). Our results revealed similarities in altered ANS response verified by HRV analysis and cardiac catecholamine release regardless whether mice displayed PI3K γ mutations or not. However, myocardial responsiveness on the increased sympathetic tone provoked strikingly reverse responses in PI3K γ deficient mice as well as wildtype mice and those containing a lipid kinase dead mutation of PI3K γ . The observed strongly enhanced increase of myocardial contractility in PI3K γ -knockout mice appears to be a state of hypercontractility caused by intensified β -AR signaling with elevated myocardial cAMP content and reinforced cardiac excitation-contraction coupling, indicated by intensified RyR and PLN phosphorylation, as a result of missing PI3K γ scaffold function (Damilano et al. 2010). Recent studies revealed that the catalytic subunit p110 γ of PI3K γ anchors protein kinase A (PKA) through a site in its N-terminal region. Anchored PKA activates PDE3B to enhance cAMP degradation and phosphorylates p110 γ to inhibit PIP3 production. This provides local feedback control of PIP3 and cAMP signaling events (Perino et al. 2011). Hence, loss of PI3K γ impedes formation of this multiprotein complex which tethers the phosphodiesterase near its activator, PKA resulting in enhanced cardiomyocytic cAMP signaling. In contrast, LPS-induced myocardial TLR4 stimulation led to marked upregulation of PI3K γ

expression (Fig. 21C) which reduces β -AR density by enhanced receptor internalization and concomitant receptor desensitization (Naga Prasad et al. 2001, Naga Prasad et al. 2005). This reported PI3K γ -related attenuation of β -AR signaling appears to be an adaptive event with rather cardioprotective consequences because of reduced cardiac energy demands. The following indications support such a perception: (i) Pharmacological blockade with short-acting β 1-AR antagonists improve hemodynamic and outcome data in different preclinical sepsis models and preliminary clinical approaches (Rudiger 2010). Our data support this notion in so far as the systemic perfusion pressure remained firm despite reduced myocardial contractility and cardiac output in wildtype and PI3K $\gamma^{KD/KD}$ mice (Table. 8). (ii) Enhanced contractility in PI3K $\gamma^{-/-}$ mice was not followed by improvements in cardiac output or heart rate reduction indicating myocardial dysregulation with enhanced cardiac energy demands. Furthermore, attenuation of contractile function affects evidently systolic functions with preserved diastolic processes indicated by maintained myocardial relaxation dynamics, suggesting merely unaltered ATP availability

For the first time, our data revealed that a single administration of LPS with adequate fluid resuscitation leading to infection-like SIRS resulted in prolonged myocardial depression indicated by reduced myocardial contractility and attenuated hemodynamic performance for a minimum of three days. LPS-induced myocardial depression was reported in several previous studies performed on different species including men (Baumgarten et al. 2006, Joulin et al. 2009, Kumar et al. 2004), but considered merely acute responses. Intriguingly, PI3K $\gamma^{-/-}$ mice displayed a progressive SIMD during this period after initial hyper-contractility, whereas wildtype and PI3K $\gamma^{KD/KD}$ mice retained their initially suppressed status.

Whereas the early myocardial suppression in wildtype and PI3K $\gamma^{KD/KD}$ mice is clearly mediated by dampened cAMP response induced by the PI3K γ -scaffold function, the reason for progressive attenuation of myocardial contractility in PI3K $\gamma^{-/-}$ mice needs further considerations. Previous experimental studies have reported that intraperitoneal LPS injection in mice delivers for at least three hours increased blood levels of LPS inducing TLR4 signaling and returned to normal values latest after twelve hours (Kadoi et al. 1996). Proinflammatory response of circulating cytokines delivered by stimulated immune cells displayed similar temporal patterns (Copeland et al. 2005). Prolonged myocardial TLR4 signaling after LPS may be caused by PI3K γ -dependent alarmin release (Xu et al. 2010). Moreover, the early enhanced myocardial catecholamine content returned to baseline values within 24 hours (Fig. 12D). Therefore, the observed sustained SIMD results evidently by long-term altered cardiomyo-

cytic manner of functioning. Considering a recent transcriptomic analysis in septic heart tissue with identified upregulation of several proinflammatory pathways and concomitant dysregulation in the β -AR/cAMP/PKA pathway suggesting causal relation between activated myocardial immune response and suppressed contractile performance (Rudiger et al. 2013), we searched for PI3K γ -related effects prone to provoke combined proinflammatory activation and attenuated contractile performance in cardiomyocytes. Our search explored a thus far unrevealed mechanism in adult cardiomyocytes, whereby PI3K γ deficit is responsible for accentuation of calcineurin/NFAT activation leading to enhanced iNOS expression with concomitantly attenuated cardiac excitation-contraction coupling by altered Ca²⁺-trafficking (Fig. 19, Fig. 20). We verified by genetic and pharmacological approaches that NFAT is activated in PI3K γ ^{-/-} cardiomyocytes under resting conditions and remained activated over time during LPS/cytokine stimulation leading to enhanced long-lasting iNOS upregulation (Fig. 20) with markedly reduced Phospho-PLB indicating attenuated cardiac excitation-contraction coupling. Together, cardiomyocytes with missing PI3K γ retrain delayed myocardial hypocontractility during LPS-induced SIRS by an alternative pathway driven by enhanced iNOS upregulation and achieve thereby a similar downregulation of cardiac performance.

Intriguingly, sustained NFAT activation in resting PI3K γ ^{-/-} cardiomyocytes indicates clearly that the intracellular Ca²⁺ content is critically elevated already under unstimulated conditions in order to drive Ca²⁺/calmodulin signaling via activated phosphatase calcineurin which we have verified by cyclosporine inhibition (Fig. 20C, Fig. 20E). This finding extends a recent report who has been shown that after β 2-adrenergic receptor activation an abnormal cAMP accumulation occurred in PI3K γ ^{-/-} cardiomyocytes with protein kinase A-mediated hyperphosphorylation of L-type calcium channel (Cav1.2) and phospholamban leading to increased Ca²⁺ spark occurrence and amplitude (Ghigo et al. 2012). Our data reveal that already under resting conditions the missing scaffold function of PI3K γ resulting in an elevated cAMP level induces a sustained activation of the Ca²⁺/calmodulin/calcineurin/NFAT transcription pathway which plays a central role in the heart's response to pathologic stressors (Heineke und Molkentin 2006). NFAT inhibition by phosphorylation appears GSK3 β -independent comforting that this phosphorylation is enhanced via the scaffold function of PI3K γ in cardiomyocytes under proinflammatory stimulation (Fig. 20A) since GSK3 β is known as an important mediator of NFAT phosphorylation (Xue et al. 2007).

Intriguingly, LPS/Cyt stimulation with concomitant Erk1/2 induced activator protein 1 (AP-1) activation was necessary to provoke enhanced iNOS expression. This observation con-

firming previous reports that in adult cardiomyocytes a cooperation of NFAT with the transcription factor AP-1 is indispensable to regulate the expression of inducible genes, like iNOS (Rao et al. 1997, Molkentin 2004). We verified that iNOS upregulation is responsible for downregulation of myocardial contractility because LPS/Cyt-induced PLB suppression is rescued either by direct iNOS blockade (Fig. 17B, Fig. 19B) or cyclosporine-induced calcineurin blockade (Fig. 20E). NO is known to signal through at least two distinct signaling pathways: cGMP-dependently and/or cGMP-independently (Ziolo et al. 2008). cGMP-dependent signaling occurs through the activation of guanylate cyclase and protein kinase G (PKG), while cGMP-independent signaling primarily occurs via direct protein modification (e.g., S-nitrosylation) (Kohr et al. 2011). A number of different cGMP-dependent effects of iNOS signaling have been observed leading to decreased myocardial contraction such as reduction in myofilament Ca^{2+} sensitivity (Yasuda und Lew 1997), likely mediated by troponin I phosphorylation via PKG (Layland et al. 2002) and reduced calcium current dependent upon the phosphorylation of the L-type Ca^{2+} channel by PKG (Ziolo et al. 2001). cGMP-independent effects of iNOS expression are causally linked to peroxynitrite formation by uncoupling leading to NO and superoxide production (Mungrue et al. 2002). Peroxynitrite is most likely the major signaling molecule of iNOS (Ferdinandy et al. 2000) capable in high concentrations to directly inactivate SERCA and exerts antiadrenergic effects by reducing cAMP-dependent PLB phosphorylation (Ziolo et al. 2008). Together, both cGMP-dependent and cGMP-independent pathways of iNOS signaling appear to be involved in mediating delayed downregulation of contractile function in $PI3K\gamma^{-/-}$ mice: (i) Reduced contractility despite elevated intracellular Ca^{2+} content in $PI3K\gamma^{-/-}$ cardiomyocytes suggests attenuated myofilament Ca^{2+} sensitivity. (ii) In $PI3K\gamma^{-/-}$ cardiomyocytes show reduced Phospho-PLB after prolonged LPS/Cyt stimulation while iNOS expression remained upregulated (Fig. 19A).

Furthermore, we demonstrate for the first time a $PI3K\gamma$ dependency of a sustained upregulation of proinflammatory molecules in cardiac tissue, like iNOS and MMP-9 (Fig. 21A, Fig. 21B) with harmful potential for functional disturbances and myocardial remodeling (Halade et al. 2013, Kohr et al. 2012) in consequence of a single administration of LPS leading to infection-like SIRS. We are unable to distinguish the cell types within cardiac tissue responsible for long-lasting proinflammatory response. Nevertheless, our findings reveal that $PI3K\gamma$ by its scaffold function attenuates myocardial proinflammatory response.

Thus, control and down-regulation of myocardial contractility under acute stressful conditions like infection-induced SIRS appears to be of substantial importance, because at least two differently regulated intracellular signaling pathways are triggered by inflammatory stimula-

tion in order to prevent and/or cope with a hyper-contractility state. Our data reveal that PI3K γ plays a coordinative role by dampening enhanced β -adrenergic signaling via its scaffold function in order to control an exaggeration of cAMP formation and prevent an enhanced iNOS expression with possible harmful side effects. PI3K γ deficiency copes with an early hyper-contractility state by enhanced iNOS upregulation via cooperative NFAT/AP-1 activation. Unexpectedly, loss of control for iNOS regulation in cardiomyocytes was lipid kinase independent, possibly a cell type-specific effect (Xue et al. 2007). Given that the consequences of enhanced and probably exaggerated iNOS activity occurs transiently and without permanent structural and functional sequels under the here used experimental setting with a strong but just singular inflammation stimulus. However, our data clearly indicate a prolonged proinflammatory state of cardiomyocytes derived from PI3K γ -deficient mice with activated pathways prone for harmful sequels.

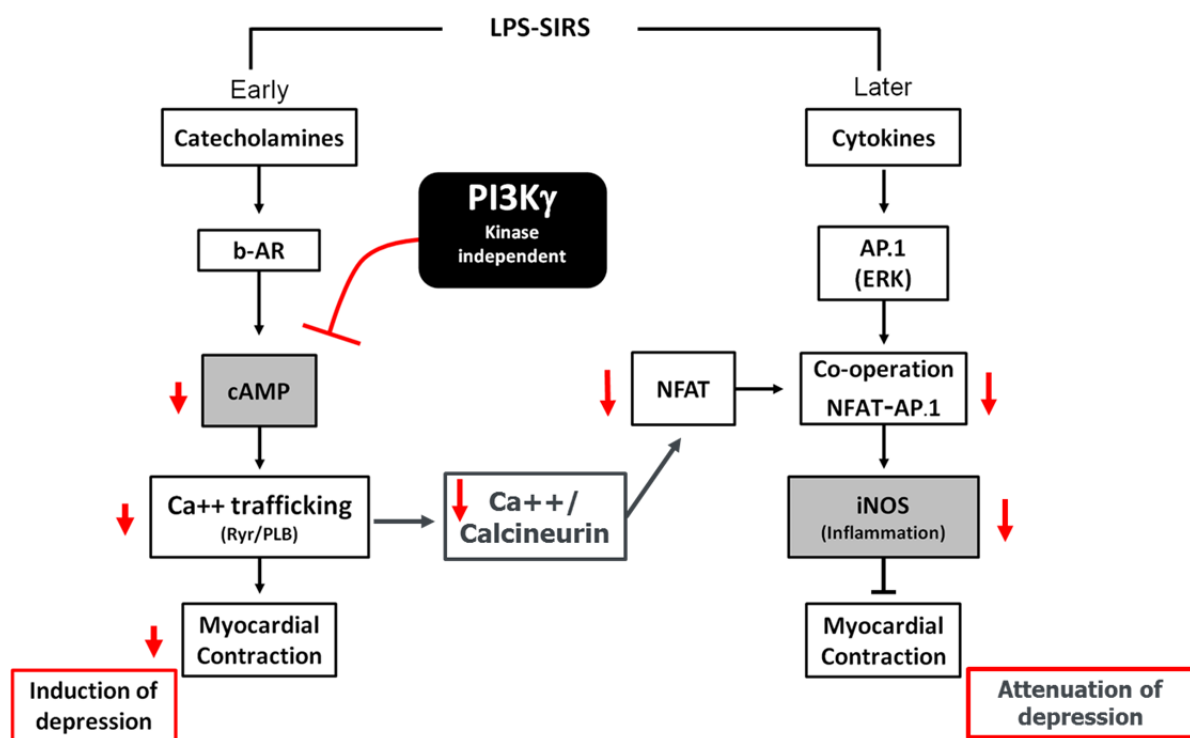


Figure 22: Model illustrating sequential and dual roles of PI3K γ 's scaffold function in the regulation of LPS/SIRS-induced myocardial depression via cAMP and iNOS.

5. Outlook

During the present study, we focused our investigations on understanding of basal mechanism involving PI3K γ in the pathogenesis of SIRS- associated myocardial depression. We could successfully established a sequential implication of PI3K γ including induction of depression via cAMP degradation, reduction of depression via iNOS suppression and likely limitation of harm via suppression of MMP-9. Nevertheless the experimental model of endotoxin (LPS) we have used and sepsis in humans differ in several key points, among others in the profile of cytokine release. Cytokine levels (TNF- α , IL-6, CXC chemokine) peaked much later and occurred at much lower levels in human patients with sepsis (Cavaillon et al. 2003, Remick et al. 2000, Gonnert et al. 2011). Therefore complementary investigations supported by timely mechanistic and physiologic involvement of PI3K γ established in the present study are necessary when considering the application of animal models to the development of sepsis therapeutics. Infection models such as polymicrobial infection are more appropriate in order to mimic sepsis in patients and prove therapy options (Gonnert et al. 2011, Rittirsch et al. 2009).

Although the hitherto unknown contribution of PI3K γ in pathogenesis of SIRS-induced myocardial depression (and revealed in present study) seems to be driven by suppression of calcium trafficking consecutive to enhanced cAMP degradation, the possibility of a direct impact of PI3K γ on suppression of NFAT activation remains open. In fact, it has been recently reported (Mohan et al. 2013) that PI3K γ could independently to its kinase function mediates the inhibition of phosphatase methyl transferase (PPMT-1) in cardiomyocyte leading to a reduced activation of Phosphatase 2a (PP2a) and reduce activation of GSK3 β . A similar mechanism can be presumed regarding the activation of NFAT because Ca²⁺ may activate more than calcineurin and also PP2a might be involve in the activation of NFAT. So, it will be promising to bring more clarification concerning this mechanism.

As a potential therapeutic perspective - the hitherto unknown and long-lasting suppression of inflammation by PI3K γ 's scaffold function during SIRS via suppression of iNOS and MMP-9 expression - seems to be concomitant to P110 γ up-regulation. Therefore, prove of principle approaches in infection models are recommended.

6. Conclusion

Our findings characterize lipid kinase-independent scaffold function of PI3K γ as a key mediator of cardiac excitation-contraction coupling early after LPS-induced SIRS. In addition, PI3K γ was shown to attenuate inflammatory myocardial response leading to only moderate iNOS expression. Loss of PI3K γ function provokes enhanced iNOS activity responsible for markedly attenuated myocardial contractility and sustained MMP-9 release in cardiac tissue. Together, the results depict a protective function of PI3K γ in cardiomyocytes and heart tissue during infection-induced SIRS.

These results confirm and expand recent data on regulatory effects of PI3K γ via lipid kinase-independent signaling in cardiomyocytes and heart tissue in infection-induced SIRS to prevent likely harmful sequels.

7. References

- Angus DC, van der Poll T. 2013. Severe sepsis and septic shock. *N Engl J Med*, 369 (9):840-851.
- Angus DC, Linde-Zwirble WT, Lidicker J, Clermont G, Carcillo J, Pinsky MR. 2001. Epidemiology of severe sepsis in the United States: analysis of incidence, outcome, and associated costs of care. *Crit Care Med*, 29 (7):1303-1310.
- Annane D, Trabold F, Sharshar T, Jarrin I, Blanc AS, Raphael JC, Gajdos P. 1999. Inappropriate sympathetic activation at onset of septic shock: a spectral analysis approach. *Am J Respir Crit Care Med*, 160 (2):458-465.
- Azimi G, Vincent JL. 1986. Ultimate survival from septic shock. *Resuscitation*, 14 (4):245-253.
- Baan J, van der Velde ET, de Bruin HG, Smeenk GJ, Koops J, van Dijk AD, Temmerman D, Senden J, Buis B. 1984. Continuous measurement of left ventricular volume in animals and humans by conductance catheter. *Circulation*, 70 (5):812-823.
- Barth E, Radermacher P, Thiemermann C, Weber S, Georgieff M, Albuszies G. 2006. Role of inducible nitric oxide synthase in the reduced responsiveness of the myocardium to catecholamines in a hyperdynamic, murine model of septic shock. *Crit Care Med*, 34 (2):307-313.
- Baumgarten G, Knuefermann P, Schuhmacher G, Vervolgyi V, von Rappard J, Dreiner U, Fink K, Djoufack C, Hoefl A, Grohe C, Knowlton AA, Meyer R. 2006. Toll-like receptor 4, nitric oxide, and myocardial depression in endotoxemia. *Shock*, 25 (1):43-49.
- Beca S, Aschars-Sobbi R, Panama BK, Backx PH. 2011. Regulation of murine cardiac function by phosphodiesterases type 3 and 4. *Curr Opin Pharmacol*, 11 (6):714-719.
- Belcher E, Mitchell J, Evans T. 2002. Myocardial dysfunction in sepsis: no role for NO? *Heart*, 87 (6):507-509.
- Bergquist J, Tarkowski A, Ekman R, Ewing A. 1994. Discovery of endogenous catecholamines in lymphocytes and evidence for catecholamine regulation of lymphocyte function via an autocrine loop. *Proc Natl Acad Sci U S A*, 91 (26):12912-12916.
- Bernardin G, Strosberg AD, Bernard A, Mattei M, Marullo S. 1998. Beta-adrenergic receptor-dependent and -independent stimulation of adenylate cyclase is impaired during severe sepsis in humans. *Intensive Care Med*, 24 (12):1315-1322.
- Bers DM. 2002. Cardiac excitation-contraction coupling. *Nature*, 415 (6868):198-205.
- Bohm M, Kirchmayr R, Gierschik P, Erdmann E. 1995. Increase of myocardial inhibitory G-proteins in catecholamine-refractory septic shock or in septic multiorgan failure. *Am J Med*, 98 (2):183-186.
- Boldt J, Menges T, Kuhn D, Diridis C, Hempelmann G. 1995. Alterations in circulating vasoactive substances in the critically ill--a comparison between survivors and non-survivors. *Intensive Care Med*, 21 (3):218-225.
- Bone RC. 1991. Sepsis syndrome. New insights into its pathogenesis and treatment. *Infect Dis Clin North Am*, 5 (4):793-805.
- Bone RC, Sibbald WJ, Sprung CL. 1992. The ACCP-SCCM consensus conference on sepsis and organ failure. *Chest*, 101 (6):1481-1483.
- Boyd JH, Mathur S, Wang Y, Bateman RM, Walley KR. 2006. Toll-like receptor stimulation in cardiomyocytes decreases contractility and initiates an NF-kappaB dependent inflammatory response. *Cardiovasc Res*, 72 (3):384-393.
- Boyd JH, Kan B, Roberts H, Wang Y, Walley KR. 2008. S100A8 and S100A9 mediate endotoxin-induced cardiomyocyte dysfunction via the receptor for advanced glycation end products. *Circ Res*, 102 (10):1239-1246.

- Boyle WA, 3rd, Parvathaneni LS, Bourlier V, Sauter C, Laubach VE, Cobb JP. 2000. iNOS gene expression modulates microvascular responsiveness in endotoxin-challenged mice. *Circ Res*, 87 (7):E18-24.
- Braunwald E. 2013. Cardiovascular science: opportunities for translating research into improved care. *J Clin Invest*, 123 (1):6-10.
- Brealey D, Karyampudi S, Jacques TS, Novelli M, Stidwill R, Taylor V, Smolenski RT, Singer M. 2004. Mitochondrial dysfunction in a long-term rodent model of sepsis and organ failure. *Am J Physiol Regul Integr Comp Physiol*, 286 (3):R491-497.
- Brealey D, Brand M, Hargreaves I, Heales S, Land J, Smolenski R, Davies NA, Cooper CE, Singer M. 2002. Association between mitochondrial dysfunction and severity and outcome of septic shock. *Lancet*, 360 (9328):219-223.
- Brinckerhoff CE, Matrisian LM. 2002. Matrix metalloproteinases: a tail of a frog that became a prince. *Nat Rev Mol Cell Biol*, 3 (3):207-214.
- Brock C, Schaefer M, Reusch HP, Czupalla C, Michalke M, Spicher K, Schultz G, Nurnberg B. 2003. Roles of G beta gamma in membrane recruitment and activation of p110 gamma/p101 phosphoinositide 3-kinase gamma. *J Cell Biol*, 160 (1):89-99.
- Buras JA, Holzmann B, Sitkovsky M. 2005. Animal models of sepsis: setting the stage. *Nat Rev Drug Discov*, 4 (10):854-865.
- Burkhoff D, Mirsky I, Suga H. 2005. Assessment of systolic and diastolic ventricular properties via pressure-volume analysis: a guide for clinical, translational, and basic researchers. *Am J Physiol Heart Circ Physiol*, 289 (2):H501-512.
- Carre JE, Orban JC, Re L, Felsmann K, Iffert W, Bauer M, Suliman HB, Piantadosi CA, Mayhew TM, Breen P, Stotz M, Singer M. 2010. Survival in critical illness is associated with early activation of mitochondrial biogenesis. *Am J Respir Crit Care Med*, 182 (6):745-751.
- Cavaillon JM, Adib-Conquy M, Fitting C, Adrie C, Payen D. 2003. Cytokine cascade in sepsis. *Scand J Infect Dis*, 35 (9):535-544.
- Cerra FB. 1985. The systemic septic response: multiple systems organ failure. *Crit Care Clin*, 1 (3):591-607.
- Chagnon F, Bentourkia M, Lecomte R, Lessard M, Lesur O. 2006. Endotoxin-induced heart dysfunction in rats: assessment of myocardial perfusion and permeability and the role of fluid resuscitation. *Crit Care Med*, 34 (1):127-133.
- Chung MK, Gulick TS, Rotondo RE, Schreiner GF, Lange LG. 1990. Mechanism of cytokine inhibition of beta-adrenergic agonist stimulation of cyclic AMP in rat cardiac myocytes. Impairment of signal transduction. *Circ Res*, 67 (3):753-763.
- Cohen RI, Shapir Y, Chen L, Scharf SM. 1998. Right ventricular overload causes the decrease in cardiac output after nitric oxide synthesis inhibition in endotoxemia. *Crit Care Med*, 26 (4):738-747.
- Conti M, Beavo J. 2007. Biochemistry and physiology of cyclic nucleotide phosphodiesterases: essential components in cyclic nucleotide signaling. *Annu Rev Biochem*, 76:481-511.
- Copeland S, Warren HS, Lowry SF, Calvano SE, Remick D, Inflammation, the Host Response to Injury I. 2005. Acute inflammatory response to endotoxin in mice and humans. *Clin Diagn Lab Immunol*, 12 (1):60-67.
- Costa M, Goldberger AL, Peng CK. 2005. Multiscale entropy analysis of biological signals. *Phys Rev E Stat Nonlin Soft Matter Phys*, 71 (2 Pt 1):021906.
- Cotton JM, Kearney MT, Shah AM. 2002. Nitric oxide and myocardial function in heart failure: friend or foe? *Heart*, 88 (6):564-566.
- Crackower MA, Oudit GY, Kozieradzki I, Sarao R, Sun H, Sasaki T, Hirsch E, Suzuki A, Shioi T, Irie-Sasaki J, Sah R, Cheng HY, Rybin VO, Lembo G, Fratta L, Oliveira-dos-Santos AJ, Benovic JL, Kahn CR, Izumo S, Steinberg SF, Wymann MP, Backx PH,

- Penninger JM. 2002. Regulation of myocardial contractility and cell size by distinct PI3K-PTEN signaling pathways. *Cell*, 110 (6):737-749.
- Cunzio RE, Schaer GL, Parker MM, Natanson C, Parrillo JE. 1986. The coronary circulation in human septic shock. *Circulation*, 73 (4):637-644.
- Damilano F, Perino A, Hirsch E. 2010. PI3K kinase and scaffold functions in heart. *Ann N Y Acad Sci*, 1188:39-45.
- Dellinger RP, Levy MM, Rhodes A, Annane D, Gerlach H, Opal SM, Sevransky JE, Sprung CL, Douglas IS, Jaeschke R, Osborn TM, Nunnally ME, Townsend SR, Reinhart K, Kleinpell RM, Angus DC, Deutschman CS, Machado FR, Rubenfeld GD, Webb S, Beale RJ, Vincent JL, Moreno R, Surviving Sepsis Campaign Guidelines Committee including The Pediatric S. 2013. Surviving Sepsis Campaign: international guidelines for management of severe sepsis and septic shock, 2012. *Intensive Care Med*, 39 (2):165-228.
- Dong LW, Wu LL, Ji Y, Liu MS. 2001. Impairment of the ryanodine-sensitive calcium release channels in the cardiac sarcoplasmic reticulum and its underlying mechanism during the hypodynamic phase of sepsis. *Shock*, 16 (1):33-39.
- Dyson A, Singer M. 2009. Animal models of sepsis: why does preclinical efficacy fail to translate to the clinical setting? *Crit Care Med*, 37 (1 Suppl):S30-37.
- Dyson A, Rudiger A, Singer M. 2011. Temporal changes in tissue cardiorespiratory function during faecal peritonitis. *Intensive Care Med*, 37 (7):1192-1200.
- Engelman JA, Luo J, Cantley LC. 2006. The evolution of phosphatidylinositol 3-kinases as regulators of growth and metabolism. *Nat Rev Genet*, 7 (8):606-619.
- Etchecopar-Chevreuril C, Francois B, Clavel M, Pichon N, Gastinne H, Vignon P. 2008. Cardiac morphological and functional changes during early septic shock: a transesophageal echocardiographic study. *Intensive Care Med*, 34 (2):250-256.
- Fallach R, Shainberg A, Avlas O, Fainblut M, Chepurko Y, Porat E, Hochhauser E. 2010. Cardiomyocyte Toll-like receptor 4 is involved in heart dysfunction following septic shock or myocardial ischemia. *J Mol Cell Cardiol*, 48 (6):1236-1244.
- Ferdinandy P, Danial H, Ambrus I, Rothery RA, Schulz R. 2000. Peroxynitrite is a major contributor to cytokine-induced myocardial contractile failure. *Circ Res*, 87 (3):241-247.
- Flierl MA, Rittirsch D, Huber-Lang MS, Sarma JV, Ward PA. 2008. Molecular events in the cardiomyopathy of sepsis. *Mol Med*, 14 (5-6):327-336.
- Flierl MA, Rittirsch D, Nadeau BA, Chen AJ, Sarma JV, Zetoune FS, McGuire SR, List RP, Day DE, Hoesel LM, Gao H, Van Rooijen N, Huber-Lang MS, Neubig RR, Ward PA. 2007. Phagocyte-derived catecholamines enhance acute inflammatory injury. *Nature*, 449 (7163):721-725.
- Friedman G, Silva E, Vincent JL. 1998. Has the mortality of septic shock changed with time. *Crit Care Med*, 26 (12):2078-2086.
- Funk DJ, Parrillo JE, Kumar A. 2009. Sepsis and septic shock: a history. *Crit Care Clin*, 25 (1):83-101, viii.
- Ghigo A, Morello F, Perino A, Damilano F, Hirsch E. 2011. Specific PI3K isoform modulation in heart failure: lessons from transgenic mice. *Curr Heart Fail Rep*, 8 (3):168-175.
- Ghigo A, Perino A, Mehel H, Zahradnikova A, Jr., Morello F, Leroy J, Nikolaev VO, Damilano F, Cimino J, De Luca E, Richter W, Westenbroek R, Catterall WA, Zhang J, Yan C, Conti M, Gomez AM, Vandecasteele G, Hirsch E, Fischmeister R. 2012. Phosphoinositide 3-kinase gamma protects against catecholamine-induced ventricular arrhythmia through protein kinase A-mediated regulation of distinct phosphodiesterases. *Circulation*, 126 (17):2073-2083.

- Gonnert FA, Recknagel P, Seidel M, Jbeily N, Dahlke K, Bockmeyer CL, Winning J, Losche W, Claus RA, Bauer M. 2011. Characteristics of clinical sepsis reflected in a reliable and reproducible rodent sepsis model. *J Surg Res*, 170 (1):e123-134.
- Gulick T, Chung MK, Pieper SJ, Lange LG, Schreiner GF. 1989. Interleukin 1 and tumor necrosis factor inhibit cardiac myocyte beta-adrenergic responsiveness. *Proc Natl Acad Sci U S A*, 86 (17):6753-6757.
- Gustot T. 2011. Multiple organ failure in sepsis: prognosis and role of systemic inflammatory response. *Curr Opin Crit Care*, 17 (2):153-159.
- Hahn PY, Wang P, Tait SM, Ba ZF, Reich SS, Chaudry IH. 1995. Sustained elevation in circulating catecholamine levels during polymicrobial sepsis. *Shock*, 4 (4):269-273.
- Halade GV, Jin YF, Lindsey ML. 2013. Matrix metalloproteinase (MMP)-9: a proximal biomarker for cardiac remodeling and a distal biomarker for inflammation. *Pharmacol Ther*, 139 (1):32-40.
- Hall RA, Lefkowitz RJ. 2002. Regulation of G protein-coupled receptor signaling by scaffold proteins. *Circ Res*, 91 (8):672-680.
- Hausdorff WP, Lohse MJ, Bouvier M, Liggett SB, Caron MG, Lefkowitz RJ. 1990. Two kinases mediate agonist-dependent phosphorylation and desensitization of the beta 2-adrenergic receptor. *Symp Soc Exp Biol*, 44:225-240.
- Hawkins PT, Anderson KE, Davidson K, Stephens LR. 2006. Signalling through Class I PI3Ks in mammalian cells. *Biochem Soc Trans*, 34 (Pt 5):647-662.
- Heineke J, Molkentin JD. 2006. Regulation of cardiac hypertrophy by intracellular signalling pathways. *Nat Rev Mol Cell Biol*, 7 (8):589-600.
- Heublein S, Hartmann M, Hagel S, Hutagalung R, Brunkhorst FM. 2013. Epidemiology of sepsis in German hospitals derived from administrative databases. *Infection* 41:S71.
- Hiles ID, Otsu M, Volinia S, Fry MJ, Gout I, Dhand R, Panayotou G, Ruiz-Larrea F, Thompson A, Totty NF, et al. 1992. Phosphatidylinositol 3-kinase: structure and expression of the 110 kd catalytic subunit. *Cell*, 70 (3):419-429.
- Hirsch E, Braccini L, Ciralo E, Morello F, Perino A. 2009. Twice upon a time: PI3K's secret double life exposed. *Trends Biochem Sci*, 34 (5):244-248.
- Hirsch E, Katanaev VL, Garlanda C, Azzolino O, Pirola L, Silengo L, Sozzani S, Mantovani A, Altruda F, Wymann MP. 2000. Central role for G protein-coupled phosphoinositide 3-kinase gamma in inflammation. *Science*, 287 (5455):1049-1053.
- Hoffmann JN, Werdan K, Hartl WH, Jochum M, Faist E, Inthorn D. 1999. Hemofiltrate from patients with severe sepsis and depressed left ventricular contractility contains cardiotoxic compounds. *Shock*, 12 (3):174-180.
- Hoffmann U, Bertsch T, Dvortsak E, Liebetau C, Lang S, Liebe V, Huhle G, Borggrefe M, Brueckmann M. 2006. Matrix-metalloproteinases and their inhibitors are elevated in severe sepsis: prognostic value of TIMP-1 in severe sepsis. *Scand J Infect Dis*, 38 (10):867-872.
- Hotchkiss RS, Karl IE. 1992. Reevaluation of the role of cellular hypoxia and bioenergetic failure in sepsis. *JAMA*, 267 (11):1503-1510.
- Hotchkiss RS, Karl IE. 2003. The pathophysiology and treatment of sepsis. *N Engl J Med*, 348 (2):138-150.
- Hotchkiss RS, Rust RS, Dence CS, Wasserman TH, Song SK, Hwang DR, Karl IE, Welch MJ. 1991. Evaluation of the role of cellular hypoxia in sepsis by the hypoxic marker [¹⁸F]fluoromisonidazole. *Am J Physiol*, 261 (4 Pt 2):R965-972.
- Hotchkiss RS, Swanson PE, Freeman BD, Tinsley KW, Cobb JP, Matuschak GM, Buchman TG, Karl IE. 1999. Apoptotic cell death in patients with sepsis, shock, and multiple organ dysfunction. *Crit Care Med*, 27 (7):1230-1251.

- Houser SR, Margulies KB, Murphy AM, Spinale FG, Francis GS, Prabhu SD, Rockman HA, Kass DA, Molckentin JD, Sussman MA, Koch WJ, American Heart Association Council on Basic Cardiovascular Sciences CoCC, Council on Functional G, Translational B. 2012. Animal models of heart failure: a scientific statement from the American Heart Association. *Circ Res*, 111 (1):131-150.
- Hoyer D, Nowack S, Bauer S, Tetschke F, Rudolph A, Wallwitz U, Jaenicke F, Heinicke E, Gotz T, Huonker R, Witte OW, Schleussner E, Schneider U. 2013. Fetal development of complex autonomic control evaluated from multiscale heart rate patterns. *Am J Physiol Regul Integr Comp Physiol*, 304 (5):R383-392.
- Hu P, Mondino A, Skolnik EY, Schlessinger J. 1993. Cloning of a novel, ubiquitously expressed human phosphatidylinositol 3-kinase and identification of its binding site on p85. *Mol Cell Biol*, 13 (12):7677-7688.
- Huber M, Helgason CD, Scheid MP, Duronio V, Humphries RK, Krystal G. 1998. Targeted disruption of SHIP leads to Steel factor-induced degranulation of mast cells. *EMBO J*, 17 (24):7311-7319.
- Hurley JH, Misra S. 2000. Signaling and subcellular targeting by membrane-binding domains. *Annu Rev Biophys Biomol Struct*, 29:49-79.
- Ichinose F, Hataishi R, Wu JC, Kawai N, Rodrigues AC, Mallari C, Post JM, Parkinson JF, Picard MH, Bloch KD, Zapol WM. 2003. A selective inducible NOS dimerization inhibitor prevents systemic, cardiac, and pulmonary hemodynamic dysfunction in endotoxemic mice. *Am J Physiol Heart Circ Physiol*, 285 (6):H2524-2530.
- Ishida H, Ichimori K, Hirota Y, Fukahori M, Nakazawa H. 1996. Peroxynitrite-induced cardiac myocyte injury. *Free Radic Biol Med*, 20 (3):343-350.
- Iwase M, Yokota M, Kitaichi K, Wang L, Takagi K, Nagasaka T, Izawa H, Hasegawa T. 2001. Cardiac functional and structural alterations induced by endotoxin in rats: importance of platelet-activating factor. *Crit Care Med*, 29 (3):609-617.
- Jardin F, Fourme T, Page B, Loubieres Y, Vieillard-Baron A, Beauchet A, Bourdarias JP. 1999. Persistent preload defect in severe sepsis despite fluid loading: A longitudinal echocardiographic study in patients with septic shock. *Chest*, 116 (5):1354-1359.
- Jones AE, Craddock PA, Tayal VS, Kline JA. 2005. Diagnostic accuracy of left ventricular function for identifying sepsis among emergency department patients with nontraumatic symptomatic undifferentiated hypotension. *Shock*, 24 (6):513-517.
- Joulin O, Marechaux S, Hassoun S, Moutaigne D, Lancel S, Neviere R. 2009. Cardiac force-frequency relationship and frequency-dependent acceleration of relaxation are impaired in LPS-treated rats. *Crit Care*, 13 (1):R14.
- Kadoi Y, Saito S, Kunimoto F, Imai T, Fujita T. 1996. Impairment of the brain beta-adrenergic system during experimental endotoxemia. *J Surg Res*, 61 (2):496-502.
- Kass DA, Yamazaki T, Burkhoff D, Maughan WL, Sagawa K. 1986. Determination of left ventricular end-systolic pressure-volume relationships by the conductance (volume) catheter technique. *Circulation*, 73 (3):586-595.
- Kass DA, Beyar R, Lankford E, Heard M, Maughan WL, Sagawa K. 1989. Influence of contractile state on curvilinearity of in situ end-systolic pressure-volume relations. *Circulation*, 79 (1):167-178.
- Katz AM, Lorell BH. 2000. Regulation of Cardiac Contraction and Relaxation. *Circulation*, 102 (Supplement 4):IV-69-IV-74.
- Kelm M, Schafer S, Dahmann R, Dolu B, Perings S, Decking UK, Schrader J, Strauer BE. 1997. Nitric oxide induced contractile dysfunction is related to a reduction in myocardial energy generation. *Cardiovasc Res*, 36 (2):185-194.
- Kerfant BG, Rose RA, Sun H, Backx PH. 2006. Phosphoinositide 3-kinase gamma regulates cardiac contractility by locally controlling cyclic adenosine monophosphate levels. *Trends Cardiovasc Med*, 16 (7):250-256.

- Kerfant BG, Zhao D, Lorenzen-Schmidt I, Wilson LS, Cai S, Chen SR, Maurice DH, Backx PH. 2007. PI3Kgamma is required for PDE4, not PDE3, activity in subcellular microdomains containing the sarcoplasmic reticular calcium ATPase in cardiomyocytes. *Circ Res*, 101 (4):400-408.
- Khadour FH, Panas D, Ferdinandy P, Schulze C, Csont T, Lalu MM, Wildhirt SM, Schulz R. 2002. Enhanced NO and superoxide generation in dysfunctional hearts from endotoxemic rats. *Am J Physiol Heart Circ Physiol*, 283 (3):H1108-1115.
- Klippel A, Escobedo JA, Hu Q, Williams LT. 1993. A region of the 85-kilodalton (kDa) subunit of phosphatidylinositol 3-kinase binds the 110-kDa catalytic subunit in vivo. *Mol Cell Biol*, 13 (9):5560-5566.
- Kohr MJ, Roof SR, Zweier JL, Ziolo MT. 2012. Modulation of myocardial contraction by peroxynitrite. *Front Physiol*, 3:468.
- Kohr MJ, Aponte AM, Sun J, Wang G, Murphy E, Gucek M, Steenbergen C. 2011. Characterization of potential S-nitrosylation sites in the myocardium. *Am J Physiol Heart Circ Physiol*, 300 (4):H1327-1335.
- Konig C, Gavrilova-Ruch O, von Banchet GS, Bauer R, Grun M, Hirsch E, Rubio I, Schulz S, Heinemann SH, Schaible HG, Wetzker R. 2010. Modulation of mu opioid receptor desensitization in peripheral sensory neurons by phosphoinositide 3-kinase gamma. *Neuroscience*, 169 (1):449-454.
- Konstantinidis K, Whelan RS, Kitsis RN. 2012. Mechanisms of cell death in heart disease. *Arterioscler Thromb Vasc Biol*, 32 (7):1552-1562.
- Koyasu S. 2003. The role of PI3K in immune cells. *Nat Immunol*, 4 (4):313-319.
- Krishnagopalan S, Kumar A, Parrillo JE, Kumar A. 2002. Myocardial dysfunction in the patient with sepsis. *Curr Opin Crit Care*, 8 (5):376-388.
- Krystal G. 2000. Lipid phosphatases in the immune system. *Semin Immunol*, 12 (4):397-403.
- Kumar A, Bunnell E, Lynn M, Anel R, Habet K, Neumann A, Parrillo JE. 2004. Experimental human endotoxemia is associated with depression of load-independent contractility indices: prevention by the lipid analogue E5531. *Chest*, 126 (3):860-867.
- Kumar A, Brar R, Wang P, Dee L, Skorupa G, Khadour F, Schulz R, Parrillo JE. 1999. Role of nitric oxide and cGMP in human septic serum-induced depression of cardiac myocyte contractility. *Am J Physiol*, 276 (1 Pt 2):R265-276.
- Lalu MM, Gao CQ, Schulz R. 2003. Matrix metalloproteinase inhibitors attenuate endotoxemia induced cardiac dysfunction: a potential role for MMP-9. *Mol Cell Biochem*, 251 (1-2):61-66.
- Lalu MM, Csont T, Schulz R. 2004. Matrix metalloproteinase activities are altered in the heart and plasma during endotoxemia. *Crit Care Med*, 32 (6):1332-1337.
- Lamia B, Chemla D, Richard C, Teboul JL. 2005. Clinical review: interpretation of arterial pressure wave in shock states. *Crit Care*, 9 (6):601-606.
- Lancel S, Tissier S, Mordon S, Marechal X, Depontieu F, Scherpereel A, Chopin C, Neviere R. 2004. Peroxynitrite decomposition catalysts prevent myocardial dysfunction and inflammation in endotoxemic rats. *J Am Coll Cardiol*, 43 (12):2348-2358.
- Landesberg G, Gilon D, Meroz Y, Georgieva M, Levin PD, Goodman S, Avidan A, Beeri R, Weissman C, Jaffe AS, Sprung CL. 2012. Diastolic dysfunction and mortality in severe sepsis and septic shock. *Eur Heart J*, 33 (7):895-903.
- Layland J, Li JM, Shah AM. 2002. Role of cyclic GMP-dependent protein kinase in the contractile response to exogenous nitric oxide in rat cardiac myocytes. *J Physiol*, 540 (Pt 2):457-467.
- Lefler AM. 1970. Role of a myocardial depressant factor in the pathogenesis of circulatory shock. *Fed Proc*, 29 (6):1836-1847.
- Lemmon MA. 2004. Pleckstrin homology domains: not just for phosphoinositides. *Biochem Soc Trans*, 32 (Pt 5):707-711.

- Leslie NR, Downes CP. 2002. PTEN: The down side of PI 3-kinase signalling. *Cell Signal*, 14 (4):285-295.
- Levy MM, Fink MP, Marshall JC, Abraham E, Angus D, Cook D, Cohen J, Opal SM, Vincent JL, Ramsay G, Scm/Esicm/Accp/Ats/Sis. 2003. 2001 SCCM/ESICM/ACCP/ATS/SIS International Sepsis Definitions Conference. *Crit Care Med*, 31 (4):1250-1256.
- Levy RJ, Piel DA, Acton PD, Zhou R, Ferrari VA, Karp JS, Deutschman CS. 2005. Evidence of myocardial hibernation in the septic heart. *Crit Care Med*, 33 (12):2752-2756.
- Li Z, Jiang H, Xie W, Zhang Z, Smrcka AV, Wu D. 2000. Roles of PLC-beta2 and -beta3 and PI3Kgamma in chemoattractant-mediated signal transduction. *Science*, 287 (5455):1046-1049.
- Lindmo K, Stenmark H. 2006. Regulation of membrane traffic by phosphoinositide 3-kinases. *J Cell Sci*, 119 (Pt 4):605-614.
- Liu S, Schreuer KD. 1995. G protein-mediated suppression of L-type Ca²⁺ current by interleukin-1 beta in cultured rat ventricular myocytes. *Am J Physiol*, 268 (2 Pt 1):C339-349.
- Lorente L, Martin MM, Labarta L, Diaz C, Sole-Violan J, Blanquer J, Orbe J, Rodriguez JA, Jimenez A, Borreguero-Leon JM, Belmonte F, Medina JC, Lliminana MC, Ferrer-Aguero JM, Ferreres J, Mora ML, Lubillo S, Sanchez M, Barrios Y, Sierra A, Paramo JA. 2009. Matrix metalloproteinase-9, -10, and tissue inhibitor of matrix metalloproteinases-1 blood levels as biomarkers of severity and mortality in sepsis. *Crit Care*, 13 (5):R158.
- Louch WE, Sheehan KA, Wolska BM. 2011. Methods in cardiomyocyte isolation, culture, and gene transfer. *J Mol Cell Cardiol*, 51 (3):288-298.
- Macarthur H, Westfall TC, Riley DP, Misko TP, Salvemini D. 2000. Inactivation of catecholamines by superoxide gives new insights on the pathogenesis of septic shock. *Proc Natl Acad Sci U S A*, 97 (17):9753-9758.
- Majno G. 1991. The ancient riddle of sigma eta psi iota sigma (sepsis). *J Infect Dis*, 163 (5):937-945.
- Matsuda N, Hattori Y, Akaishi Y, Suzuki Y, Kemmotsu O, Gando S. 2000. Impairment of cardiac beta-adrenoceptor cellular signaling by decreased expression of G(s alpha) in septic rabbits. *Anesthesiology*, 93 (6):1465-1473.
- Mayr FB, Yende S, Linde-Zwirble WT, Peck-Palmer OM, Barnato AE, Weissfeld LA, Angus DC. 2010. Infection rate and acute organ dysfunction risk as explanations for racial differences in severe sepsis. *JAMA*, 303 (24):2495-2503.
- Merx MW, Weber C. 2007. Sepsis and the heart. *Circulation*, 116 (7):793-802.
- Mohan ML, Jha BK, Gupta MK, Vasudevan NT, Martelli EE, Mosinski JD, Naga Prasad SV. 2013. Phosphoinositide 3-kinase gamma inhibits cardiac GSK-3 independently of Akt. *Sci Signal*, 6 (259):ra4.
- Molkentin JD. 2004. Calcineurin-NFAT signaling regulates the cardiac hypertrophic response in coordination with the MAPKs. *Cardiovasc Res*, 63 (3):467-475.
- Moore TD, Frenneaux MP, Sas R, Atherton JJ, Morris-Thurgood JA, Smith ER, Tyberg JV, Belenkie I. 2001. Ventricular interaction and external constraint account for decreased stroke work during volume loading in CHF. *Am J Physiol Heart Circ Physiol*, 281 (6):H2385-2391.
- Mungrue IN, Gros R, You X, Pirani A, Azad A, Csont T, Schulz R, Butany J, Stewart DJ, Husain M. 2002. Cardiomyocyte overexpression of iNOS in mice results in peroxynitrite generation, heart block, and sudden death. *J Clin Invest*, 109 (6):735-743.
- Naga Prasad SV, Perrino C, Rockman HA. 2003. Role of phosphoinositide 3-kinase in cardiac function and heart failure. *Trends Cardiovasc Med*, 13 (5):206-212.

- Naga Prasad SV, Jayatileke A, Madamanchi A, Rockman HA. 2005. Protein kinase activity of phosphoinositide 3-kinase regulates beta-adrenergic receptor endocytosis. *Nat Cell Biol*, 7 (8):785-796.
- Naga Prasad SV, Barak LS, Rapacciuolo A, Caron MG, Rockman HA. 2001. Agonist-dependent recruitment of phosphoinositide 3-kinase to the membrane by beta-adrenergic receptor kinase 1. A role in receptor sequestration. *J Biol Chem*, 276 (22):18953-18959.
- Nienaber JJ, Tachibana H, Naga Prasad SV, Esposito G, Wu D, Mao L, Rockman HA. 2003. Inhibition of receptor-localized PI3K preserves cardiac beta-adrenergic receptor function and ameliorates pressure overload heart failure. *J Clin Invest*, 112 (7):1067-1079.
- O'Connell TD, Swigart PM, Rodrigo MC, Ishizaka S, Joho S, Turnbull L, Tecott LH, Baker AJ, Foster E, Grossman W, Simpson PC. 2006. Alpha1-adrenergic receptors prevent a maladaptive cardiac response to pressure overload. *J Clin Invest*, 116 (4):1005-1015.
- Opie LH. 2004. Receptors and signal transduction. In: Opie LH, Hrsg. *Heart Physiology: From Cell to*
- Circulation*. Aufl. London: Lippincott Williams & Wilkins, 186-220.
- Pacher P, Beckman JS, Liaudet L. 2007. Nitric oxide and peroxynitrite in health and disease. *Physiol Rev*, 87 (1):315-424.
- Pacher P, Nagayama T, Mukhopadhyay P, Batkai S, Kass DA. 2008. Measurement of cardiac function using pressure-volume conductance catheter technique in mice and rats. *Nat Protoc*, 3 (9):1422-1434.
- Pacold ME, Suire S, Perisic O, Lara-Gonzalez S, Davis CT, Walker EH, Hawkins PT, Stephens L, Eccleston JF, Williams RL. 2000. Crystal structure and functional analysis of Ras binding to its effector phosphoinositide 3-kinase gamma. *Cell*, 103 (6):931-943.
- Parker MM, Shelhamer JH, Bacharach SL, Green MV, Natanson C, Frederick TM, Damske BA, Parrillo JE. 1984. Profound but reversible myocardial depression in patients with septic shock. *Ann Intern Med*, 100 (4):483-490.
- Parrillo JE. 1989. The cardiovascular pathophysiology of sepsis. *Annu Rev Med*, 40:469-485.
- Parrillo JE, Burch C, Shelhamer JH, Parker MM, Natanson C, Schuette W. 1985. A circulating myocardial depressant substance in humans with septic shock. Septic shock patients with a reduced ejection fraction have a circulating factor that depresses in vitro myocardial cell performance. *J Clin Invest*, 76 (4):1539-1553.
- Parrillo JE, Parker MM, Natanson C, Suffredini AF, Danner RL, Cunnion RE, Ognibene FP. 1990. Septic shock in humans. Advances in the understanding of pathogenesis, cardiovascular dysfunction, and therapy. *Ann Intern Med*, 113 (3):227-242.
- Patrucco E, Notte A, Barberis L, Selvetella G, Maffei A, Brancaccio M, Marengo S, Russo G, Azzolino O, Rybalkin SD, Silengo L, Altruda F, Wetzker R, Wymann MP, Lembo G, Hirsch E. 2004. PI3Kgamma modulates the cardiac response to chronic pressure overload by distinct kinase-dependent and -independent effects. *Cell*, 118 (3):375-387.
- Perino A, Ghigo A, Ferrero E, Morello F, Santulli G, Baillie GS, Damilano F, Dunlop AJ, Pawson C, Walser R, Levi R, Altruda F, Silengo L, Langeberg LK, Neubauer G, Heymans S, Lembo G, Wymann MP, Wetzker R, Houslay MD, Iaccarino G, Scott JD, Hirsch E. 2011. Integrating cardiac PIP3 and cAMP signaling through a PKA anchoring function of p110gamma. *Mol Cell*, 42 (1):84-95.
- Rabuel C, Mebazaa A. 2006. Septic shock: a heart story since the 1960s. *Intensive Care Med*, 32 (6):799-807.
- Rao A, Luo C, Hogan PG. 1997. Transcription factors of the NFAT family: regulation and function. *Annu Rev Immunol*, 15:707-747.

- Rassaf T, Poll LW, Brouzos P, Lauer T, Totzeck M, Kleinbongard P, Gharini P, Andersen K, Schulz R, Heusch G, Modder U, Kelm M. 2006. Positive effects of nitric oxide on left ventricular function in humans. *Eur Heart J*, 27 (14):1699-1705.
- Recknagel P, Gonnert FA, Westermann M, Lambeck S, Lupp A, Rudiger A, Dyson A, Carre JE, Kortgen A, Krafft C, Popp J, Sponholz C, Fuhrmann V, Hilger I, Claus RA, Riedemann NC, Wetzker R, Singer M, Trauner M, Bauer M. 2012. Liver dysfunction and phosphatidylinositol-3-kinase signalling in early sepsis: experimental studies in rodent models of peritonitis. *PLoS Med*, 9 (11):e1001338.
- Reithmann C, Hallstrom S, Pilz G, Kapsner T, Schlag G, Werdan K. 1993. Desensitization of rat cardiomyocyte adenylyl cyclase stimulation by plasma of noradrenaline-treated patients with septic shock. *Circ Shock*, 41 (1):48-59.
- Remick DG, Newcomb DE, Bolgos GL, Call DR. 2000. Comparison of the mortality and inflammatory response of two models of sepsis: lipopolysaccharide vs. cecal ligation and puncture. *Shock*, 13 (2):110-116.
- Remick DG, Strieter RM, Eskandari MK, Nguyen DT, Genord MA, Raiford CL, Kunkel SL. 1990. Role of tumor necrosis factor-alpha in lipopolysaccharide-induced pathologic alterations. *Am J Pathol*, 136 (1):49-60.
- Rittirsch D, Hoesel LM, Ward PA. 2007. The disconnect between animal models of sepsis and human sepsis. *J Leukoc Biol*, 81 (1):137-143.
- Rittirsch D, Huber-Lang MS, Flierl MA, Ward PA. 2009. Immunodesign of experimental sepsis by cecal ligation and puncture. *Nat Protoc*, 4 (1):31-36.
- Rivers E, Nguyen B, Havstad S, Ressler J, Muzzin A, Knoblich B, Peterson E, Tomlanovich M, Early Goal-Directed Therapy Collaborative G. 2001. Early goal-directed therapy in the treatment of severe sepsis and septic shock. *N Engl J Med*, 345 (19):1368-1377.
- Rohrschneider LR, Fuller JF, Wolf I, Liu Y, Lucas DM. 2000. Structure, function, and biology of SHIP proteins. *Genes Dev*, 14 (5):505-520.
- Rossi MA, Celes MR, Prado CM, Saggioro FP. 2007. Myocardial structural changes in long-term human severe sepsis/septic shock may be responsible for cardiac dysfunction. *Shock*, 27 (1):10-18.
- Ruckle T, Schwarz MK, Rommel C. 2006. PI3Kgamma inhibition: towards an 'aspirin of the 21st century'? *Nat Rev Drug Discov*, 5 (11):903-918.
- Rudiger A. 2010. Beta-block the septic heart. *Crit Care Med*, 38 (10 Suppl):S608-612.
- Rudiger A, Singer M. 2007. Mechanisms of sepsis-induced cardiac dysfunction. *Crit Care Med*, 35 (6):1599-1608.
- Rudiger A, Singer M. 2013. The heart in sepsis: from basic mechanisms to clinical management. *Curr Vasc Pharmacol*, 11 (2):187-195.
- Rudiger A, Stotz M, Singer M. 2008a. Cellular processes in sepsis. *Swiss Med Wkly*, 138 (43-44):629-634.
- Rudiger A, Fischler M, Harpes P, Gasser S, Hornemann T, von Eckardstein A, Maggiorini M. 2008b. In critically ill patients, B-type natriuretic peptide (BNP) and N-terminal pro-BNP levels correlate with C-reactive protein values and leukocyte counts. *Int J Cardiol*, 126 (1):28-31.
- Rudiger A, Dyson A, Felsmann K, Carre JE, Taylor V, Hughes S, Clatworthy I, Protti A, Pellerin D, Lemm J, Claus RA, Bauer M, Singer M. 2013. Early functional and transcriptomic changes in the myocardium predict outcome in a long-term rat model of sepsis. *Clin Sci (Lond)*, 124 (6):391-401.
- Sasaki T, Irie-Sasaki J, Jones RG, Oliveira-dos-Santos AJ, Stanford WL, Bolon B, Wakeham A, Itie A, Bouchard D, Kozieradzki I, Joza N, Mak TW, Ohashi PS, Suzuki A, Penninger JM. 2000. Function of PI3Kgamma in thymocyte development, T cell activation, and neutrophil migration. *Science*, 287 (5455):1040-1046.

- Schmidt H, Muller-Werdan U, Hoffmann T, Francis DP, Piepoli MF, Rauchhaus M, Prondzinsky R, Loppnow H, Buerke M, Hoyer D, Werdan K. 2005. Autonomic dysfunction predicts mortality in patients with multiple organ dysfunction syndrome of different age groups. *Crit Care Med*, 33 (9):1994-2002.
- Schmidt HB, Werdan K, Muller-Werdan U. 2001. Autonomic dysfunction in the ICU patient. *Curr Opin Crit Care*, 7 (5):314-322.
- Schulz R, Rassaf T, Massion PB, Kelm M, Balligand JL. 2005. Recent advances in the understanding of the role of nitric oxide in cardiovascular homeostasis. *Pharmacol Ther*, 108 (3):225-256.
- Shan J, Kushnir A, Betzenhauser MJ, Reiken S, Li J, Lehnart SE, Lindegger N, Mongillo M, Mohler PJ, Marks AR. 2010. Phosphorylation of the ryanodine receptor mediates the cardiac fight or flight response in mice. *J Clin Invest*, 120 (12):4388-4398.
- Sharshar T, Gray F, Lorin de la Grandmaison G, Hopkinson NS, Ross E, Dorandeu A, Orlikowski D, Raphael JC, Gajdos P, Annane D. 2003. Apoptosis of neurons in cardiovascular autonomic centres triggered by inducible nitric oxide synthase after death from septic shock. *Lancet*, 362 (9398):1799-1805.
- Shoelson SE, Sivaraja M, Williams KP, Hu P, Schlessinger J, Weiss MA. 1993. Specific phosphopeptide binding regulates a conformational change in the PI 3-kinase SH2 domain associated with enzyme activation. *EMBO J*, 12 (2):795-802.
- Singer M. 2005. Metabolic failure. *Crit Care Med*, 33 (12 Suppl):S539-542.
- Singer M, De Santis V, Vitale D, Jeffcoate W. 2004. Multiorgan failure is an adaptive, endocrine-mediated, metabolic response to overwhelming systemic inflammation. *Lancet*, 364 (9433):545-548.
- Sleeman MW, Wortley KE, Lai KM, Gowen LC, Kintner J, Kline WO, Garcia K, Stitt TN, Yancopoulos GD, Wiegand SJ, Glass DJ. 2005. Absence of the lipid phosphatase SHIP2 confers resistance to dietary obesity. *Nat Med*, 11 (2):199-205.
- Steendijk P, Baan J. 2000. Comparison of intravenous and pulmonary artery injections of hypertonic saline for the assessment of conductance catheter parallel conductance. *Cardiovasc Res*, 46 (1):82-89.
- Stengl M, Bartak F, Sykora R, Chvojka J, Benes J, Krouzecky A, Novak I, Svirglerova J, Kuncova J, Matejovic M. 2010. Reduced L-type calcium current in ventricular myocytes from pigs with hyperdynamic septic shock. *Crit Care Med*, 38 (2):579-587.
- Stephens LR, Eguinoa A, Erdjument-Bromage H, Lui M, Cooke F, Coadwell J, Smrcka AS, Thelen M, Cadwallader K, Tempst P, Hawkins PT. 1997. The G beta gamma sensitivity of a PI3K is dependent upon a tightly associated adaptor, p101. *Cell*, 89 (1):105-114.
- Sternberg EM. 2006. Neural regulation of innate immunity: a coordinated nonspecific host response to pathogens. *Nat Rev Immunol*, 6 (4):318-328.
- Stoyanov B, Volinia S, Hanck T, Rubio I, Loubtchenkov M, Malek D, Stoyanova S, Vanhaesebroeck B, Dhand R, Nurnberg B, et al. 1995. Cloning and characterization of a G protein-activated human phosphoinositide-3 kinase. *Science*, 269 (5224):690-693.
- Suire S, Hawkins P, Stephens L. 2002. Activation of phosphoinositide 3-kinase gamma by Ras. *Curr Biol*, 12 (13):1068-1075.
- Suire S, Coadwell J, Ferguson GJ, Davidson K, Hawkins P, Stephens L. 2005. p84, a new Gbetagamma-activated regulatory subunit of the type IB phosphoinositide 3-kinase p110gamma. *Curr Biol*, 15 (6):566-570.
- Suliman HB, Welty-Wolf KE, Carraway M, Tatro L, Piantadosi CA. 2004. Lipopolysaccharide induces oxidative cardiac mitochondrial damage and biogenesis. *Cardiovasc Res*, 64 (2):279-288.

- Takeuchi K, del Nido PJ, Ibrahim AE, Poutias DN, Glynn P, Cao-Danh H, Cowan DB, McGowan FX, Jr. 1999. Increased myocardial calcium cycling and reduced myofilament calcium sensitivity in early endotoxemia. *Surgery*, 126 (2):231-238.
- Tang C, Liu MS. 1996. Initial externalization followed by internalization of beta-adrenergic receptors in rat heart during sepsis. *Am J Physiol*, 270 (1 Pt 2):R254-263.
- Tang C, Yang J, Wu LL, Dong LW, Liu MS. 1998. Phosphorylation of beta-adrenergic receptor leads to its redistribution in rat heart during sepsis. *Am J Physiol*, 274 (4 Pt 2):R1078-1086.
- Tavernier B, Mebazaa A, Mateo P, Sys S, Ventura-Clapier R, Veksler V. 2001. Phosphorylation-dependent alteration in myofilament Ca^{2+} sensitivity but normal mitochondrial function in septic heart. *Am J Respir Crit Care Med*, 163 (2):362-367.
- Teng L, Yu M, Li JM, Tang H, Yu J, Mo LH, Jin J, Liu XZ. 2012. Matrix metalloproteinase-9 as new biomarkers of severity in multiple organ dysfunction syndrome caused by trauma and infection. *Mol Cell Biochem*, 360 (1-2):271-277.
- Ullrich R, Scherrer-Crosbie M, Bloch KD, Ichinose F, Nakajima H, Picard MH, Zapol WM, Quezado ZM. 2000. Congenital deficiency of nitric oxide synthase 2 protects against endotoxin-induced myocardial dysfunction in mice. *Circulation*, 102 (12):1440-1446.
- van der Poll T, Opal SM. 2008. Host-pathogen interactions in sepsis. *Lancet Infect Dis*, 8 (1):32-43.
- Vanhaesebroeck B, Leervers SJ, Ahmadi K, Timms J, Katso R, Driscoll PC, Woscholski R, Parker PJ, Waterfield MD. 2001. Synthesis and function of 3-phosphorylated inositol lipids. *Annu Rev Biochem*, 70:535-602.
- Vanhaesebroeck B, Welham MJ, Kotani K, Stein R, Warne PH, Zvelebil MJ, Higashi K, Volinia S, Downward J, Waterfield MD. 1997. P110delta, a novel phosphoinositide 3-kinase in leukocytes. *Proc Natl Acad Sci U S A*, 94 (9):4330-4335.
- Vaughan DJ, Millman EE, Godines V, Friedman J, Tran TM, Dai W, Knoll BJ, Clark RB, Moore RH. 2006. Role of the G protein-coupled receptor kinase site serine cluster in beta2-adrenergic receptor internalization, desensitization, and beta-arrestin translocation. *J Biol Chem*, 281 (11):7684-7692.
- Vieillard-Baron A, Caille V, Charron C, Belliard G, Page B, Jardin F. 2008. Actual incidence of global left ventricular hypokinesia in adult septic shock. *Crit Care Med*, 36 (6):1701-1706.
- Vieillard Baron A, Schmitt JM, Beauchet A, Augarde R, Prin S, Page B, Jardin F. 2001. Early preload adaptation in septic shock? A transesophageal echocardiographic study. *Anesthesiology*, 94 (3):400-406.
- Vincent JL, Rello J, Marshall J, Silva E, Anzueto A, Martin CD, Moreno R, Lipman J, Gomersall C, Sakr Y, Reinhart K, Investigators EICo. 2009. International study of the prevalence and outcomes of infection in intensive care units. *JAMA*, 302 (21):2323-2329.
- Voigt P, Dorner MB, Schaefer M. 2006. Characterization of p87PIKAP, a novel regulatory subunit of phosphoinositide 3-kinase gamma that is highly expressed in heart and interacts with PDE3B. *J Biol Chem*, 281 (15):9977-9986.
- Voigt P, Brock C, Nurnberg B, Schaefer M. 2005. Assigning functional domains within the p101 regulatory subunit of phosphoinositide 3-kinase gamma. *J Biol Chem*, 280 (6):5121-5127.
- Waage A, Halstensen A, Espevik T. 1987. Association between tumour necrosis factor in serum and fatal outcome in patients with meningococcal disease. *Lancet*, 1 (8529):355-357.
- Waisbren BA. 1951. Bacteremia due to gram-negative bacilli other than the Salmonella; a clinical and therapeutic study. *AMA Arch Intern Med*, 88 (4):467-488.

- Werdan K, Schmidt H, Ebelt H, Zorn-Pauly K, Koidl B, Hoke RS, Heinroth K, Muller-Werdan U. 2009. Impaired regulation of cardiac function in sepsis, SIRS, and MODS. *Can J Physiol Pharmacol*, 87 (4):266-274.
- Werdan K, Oelke A, Hettwer S, Nuding S, Bubel S, Hoke R, Russ M, Lautenschlager C, Mueller-Werdan U, Ebelt H. 2011. Septic cardiomyopathy: hemodynamic quantification, occurrence, and prognostic implications. *Clin Res Cardiol*, 100 (8):661-668.
- Wu LL, Liu MS. 1992. Altered ryanodine receptor of canine cardiac sarcoplasmic reticulum and its underlying mechanism in endotoxin shock. *J Surg Res*, 53 (1):82-90.
- Wu LL, Tang C, Liu MS. 2001. Altered phosphorylation and calcium sensitivity of cardiac myofibrillar proteins during sepsis. *Am J Physiol Regul Integr Comp Physiol*, 281 (2):R408-416.
- Wu LL, Tang C, Dong LW, Liu MS. 2002. Altered phospholamban-calcium ATPase interaction in cardiac sarcoplasmic reticulum during the progression of sepsis. *Shock*, 17 (5):389-393.
- Wu LL, Yang SL, Yang RC, Hsu HK, Hsu C, Dong LW, Liu MS. 2003. G protein and adenylate cyclase complex-mediated signal transduction in the rat heart during sepsis. *Shock*, 19 (6):533-537.
- Xiang Y, Kobilka BK. 2003. Myocyte adrenoceptor signaling pathways. *Science*, 300 (5625):1530-1532.
- Xie YW, Kaminski PM, Wolin MS. 1998. Inhibition of rat cardiac muscle contraction and mitochondrial respiration by endogenous peroxynitrite formation during posthypoxic reoxygenation. *Circ Res*, 82 (8):891-897.
- Xu H, Su Z, Wu J, Yang M, Penninger JM, Martin CM, Kvietys PR, Rui T. 2010. The alarmin cytokine, high mobility group box 1, is produced by viable cardiomyocytes and mediates the lipopolysaccharide-induced myocardial dysfunction via a TLR4/phosphatidylinositol 3-kinase gamma pathway. *J Immunol*, 184 (3):1492-1498.
- Xue L, Gyles SL, Barrow A, Pettipher R. 2007. Inhibition of PI3K and calcineurin suppresses chemoattractant receptor-homologous molecule expressed on Th2 cells (CRTH2)-dependent responses of Th2 lymphocytes to prostaglandin D(2). *Biochem Pharmacol*, 73 (6):843-853.
- Yasuda S, Lew WY. 1997. Lipopolysaccharide depresses cardiac contractility and beta-adrenergic contractile response by decreasing myofilament response to Ca²⁺ in cardiac myocytes. *Circ Res*, 81 (6):1011-1020.
- Yu P, Boughner DR, Sibbald WJ, keys J, Dunmore J, Martin CM. 1997. Myocardial collagen changes and edema in rats with hyperdynamic sepsis. *Crit Care Med*, 25 (4):657-662.
- Zaky A, Deem S, Bendjelid K, Treggiari MM. 2014. Characterization of cardiac dysfunction in sepsis: an ongoing challenge. *Shock*, 41 (1):12-24.
- Ziolo MT, Kohr MJ, Wang H. 2008. Nitric oxide signaling and the regulation of myocardial function. *J Mol Cell Cardiol*, 45 (5):625-632.
- Ziolo MT, Harshbarger CH, Roycroft KE, Smith JM, Romano FD, Sondgeroth KL, Wahler GM. 2001. Myocytes isolated from rejecting transplanted rat hearts exhibit a nitric oxide-mediated reduction in the calcium current. *J Mol Cell Cardiol*, 33 (9):1691-1699.
- Zuurbier CJ, Emons VM, Ince C. 2002. Hemodynamics of anesthetized ventilated mouse models: aspects of anesthetics, fluid support, and strain. *Am J Physiol Heart Circ Physiol*, 282 (6):H2099-2105.

Curriculum Vitae

Personal details:

Name: Bernadin, Ndongson Dongmo

Adresse: Tal-straße – 26a, 07743-Jena

Date of birth: 15.05.1977

Place of birth: Dschang (Cameroon)

Nationality: Cameroonian

Email: bernadin-NDONGSON_DONGMO@med.uni-jena.de

Telephone: 00 49176 70708714 /00 4936419 395605

Education:

May 2011-October 2014: PhD thesis; Phosphoinositide 3-kinase γ controls LPS-induced myocardial depression via sequential cAMP- and iNOS- signaling. Institute of Molecular Cell Biology, Center for Molecular Biomedicine, University Hospital Jena.

January 2010-April 2011: Research activities in PhD project; Impact of hydroxynonenal (HNE) in the pathogenesis of malaria-associated acute respiratory distress. Department of Genetics, Biology and Biochemistry, Molecular Medicine School, University of Turin, Italy - **not achieved**

January 2008- December 2009: Research activities in PhD project; potential anti-inflammatory, antimicrobial and anti-oxidants activities of 4 African species of *Aeolanthus*. ENSAI, University of Ngaoundere, Cameroon - **not achieved**

2008: Master science: Food Science and Nutrition; Chemical characteristics, antiradical, anti-inflammatory and antifungal activity of essential oils of some Cameroon *Myrtaceae*. ENSAI, University of Ngaoundere, Cameroon.

2005: Master's Degree: Biochemistry; Extraction and analysis of the essential oil of seeds of *Monodora Myristica*. University of Douala, Cameroon.

2003: Bachelor's Degree in Biochemistry (University of Douala, Cameroon)

1998: Higher secondary school certificate (BACC)

1994: Secondary school certificate (BEPC)

Others academic activities:

- 2007-2009: Volunteer Assistant-teacher in microbiology and biochemistry laboratory at ENSAI University of Ngaoundere, Cameroon.

-2012-2014: Practical assistance of student including bachelor's student, Master's student and MD's student at the institute of molecular cell biology (university hospital of Jena, Germany)

Publications:

Chemical composition, antiradical and antifungal activities of Essential oils of the leaves of *Cinnamomum zeylanicum* Blume from Cameroon; P.M. Jazet Dongmo, L. Tatsadjieu Ngouné, F. Tchoumboungang, M.L. Sameza, **B. Ndongson Dongmo**, P H Amvam Zollo et C Menut, *Natural Products Communications*, 2(12):1287-1290, 2007.

Antifungal potential of *Eucalyptus saligna* and *Eucalyptus camaldulensis* essential oils from Cameroon against *Phaeoramularia angolensis*, P M Jazet Dongmo, L Tatsadjieu Ngoune, **B Ndongson Dongmo**, J Kuate, P H Amvam Zollo et C Menut, *European Journal of Scientific Research*, 24(3), 348-357. 2008.

Correlation between chemical composition and antifungal properties of essential oils of *Calistemon rigidus* and *Callistemon citrinus* of Cameroon against *Phaeoramularia angolensis*, Pierre M.D Jazet, Léopold N Tatsadjieu, **Bernadin D Ndongson**, Jean Kuate, Paul H Amvam Zollo and Chantal Menut, *Journal of Medicinal Plants Research*, 3 (1), 2009.

SIRS-related cardiomyopathy is mediated via lipid Kinase-independent control of cAMP by phosphoinositide 3-kinase γ . **Bernadin Ndongson-Dongmo**, Regine Heller, Falk A. Gonnert, Michael Bauer, Reinhard Wetzker, Reinhard Bauer. *Weimar sepsis update-Congress (Abstract)*, 2013.

PI3K γ mediates LPS-induced myocardial depression via sequential cAMP- and iNOS- signalling. **Bernadin Ndongson-Dongmo**, Regine Heller, Michael Bauer, Emilio Hirsch, Reinhard Wetzker, and Reinhard Bauer. *39th European Symposium on Hormones and Cell Regulation (Abstract)*, 2014.

Cardiomyocyte-specific inactivation of the sodium proton exchanger NHE1 does not protect from hypertensive heart hypertrophy. J. Christopher Hennings, Katharina Völker, Theresa Heinrich, **Bernadin Ndongson-Dongmo**, Marco Abesser, Antje K. Hübner, Anne Sinning, Regine Heller, Hideo A. Baba, Kai Schuh, Stefan Frantz, Michaela Kuhn, Christian A. Hübner. *Basical research in cardiology (revision)*, February 2015.

Phosphoinositide 3-kinase gamma controls LPS-induced myocardial depression via sequential cAMP- and iNOS- signaling and dampened cardiomyocytic inflammatory response. **Bernadin Ndongson-Dongmo**, Regine Heller, Dirk Hoyer, Michael Brodhun, Michael Bauer, Falk A. Gonnert, Johannes Winning, Emilio Hirsch, Reinhard Wetzker, and Reinhard Bauer. *Cardiovascular research (revision)*, March 2015.

Prizes:

- 39th Symposium on Hormones and Cell Regulation, 2014: **short talk travel grant winner**
- Weimar Sepsis Update (International congress), 2013: **first Poster Prize winner**
- DAAD prize for international students, 2012: **year's nominee**

Extra-academic activities:

- Volunteer of PIPAD (Integrated Project for Promotion of Self-Development), a non-governmental organization involved in health, environment and socio-economic status of vulnerable populations in Cameroon (2005-2009).

-Volunteer in several Fund raising events for charity project supported by “Ein Welt Hause” organisation members in Jena, Germany (2011-2015)

Acknowledgements

Prof. Dr. Reinhard Bauer, you charge everything you fashion with the deep breath of your passion and respect for science. Thank you for guiding me in every single step toward the achievement of this project. You provided me not only necessities and determinants knowledge, supports, trainings and advices, but also the extraordinary working environment and conditions. It's definitely a trill working under your supervision.

I would like to thank my professors, Prof. Dr. Regine Heller and Prof. Dr. Reinhard Wetzker for providing me suitable and remarkable working conditions. Your availability, support and continuous interest to the success of this project was at the same time inspiring and motivating.

I am very much thankful to my working colleagues as well as all professors of our institute for their continuous cooperation and help. Your kindness and collaborative nature make it a pleasure to work with you.

I would like to dedicate this thesis to my late brother, Ndongson Teinkala Jean Claude who unaccountably gave me. Life didn't allow you to live these moments despite the sharing of this dream with me, but you are definitely a part of me and there is no doubt in my spirit that we are living all of this together.

To my late parents (Djoulifack Anastasie and Ndongson Rene), I salute at this special occasion your spirits that I'm sure are constantly guiding mine. I still believe and will always believe to the power and rewarding of the devotion to hard work, to the authentic being and to the focus on my path along the path of anyone else. Thank you for planted those seeds on me.

Finally, I would like to thank my entire family and especially, Barthelemy, Alain, Solange and Theodore. The reason I always find the way to fight to win even in the very desperate situation is because I know I can unconditionally count on you. "I am because you are".

Ehrenwörtliche Erklärung

Hiermit erkläre ich, dass mir die Promotionsordnung der Medizinischen Fakultät der Friedrich-Schiller-Universität bekannt ist,

ich die Dissertation selbst angefertigt habe und alle von mir benutzten Hilfsmittel, persönlichen Mitteilungen und Quellen in meiner Arbeit angegeben sind,

mich folgende Personen bei der Auswahl und Auswertung des Materials sowie bei der Herstellung des Manuskripts unterstützt haben:

Dr. Michael Brodhun: Auswertung der Herzmuskel-Histologien;

Prof. Dr. Reinhard Bauer: Unterstützung bei der Einführung der *in vivo*-Experimente, Diskussion und Interpretation, Redigieren der Dissertation;

Frau Prof. Dr. Regine Heller: Unterstützung bei der Einführung zellbiologischer Methoden, Diskussion und Interpretation der Ergebnisse;

Prof. Dr. Reinhard Wetzker, Prof. Dr. Emilio Hirsch: Diskussion und Interpretation der Ergebnisse;

die Hilfe eines Promotionsberaters nicht in Anspruch genommen wurde und dass Dritte weder unmittelbar noch mittelbar geldwerte Leistungen von mir für Arbeiten erhalten haben, die im Zusammenhang mit dem Inhalt der vorgelegten Dissertation stehen,

dass ich die Dissertation noch nicht als Prüfungsarbeit für eine staatliche oder andere wissenschaftliche Prüfung eingereicht habe und dass ich die gleiche, eine in wesentlichen Teilen ähnliche oder eine andere Abhandlung nicht bei einer anderen Hochschule als Dissertation eingereicht habe.

Jena, den 17.03.2015

Unterschrift des Verfassers